

University of Alberta

An Analysis of Mandibular Asymmetry Using Digital Panoramic Imaging - A Skull
Study Measuring Jaw Dimensions of Artificially Induced Mandibular Asymmetry

by

Shawn Joseph Russett



A thesis submitted to the Faculty of Graduate Studies and Research in partial
fulfillment of the
requirements for the degree of Master of Science

in

Medical Sciences - Orthodontics

Edmonton, Alberta
Fall 2006



Library and
Archives Canada

Bibliothèque et
Archives Canada

Published Heritage
Branch

Direction du
Patrimoine de l'édition

395 Wellington Street
Ottawa ON K1A 0N4
Canada

395, rue Wellington
Ottawa ON K1A 0N4
Canada

Your file *Votre référence*
ISBN: 978-0-494-22362-8
Our file *Notre référence*
ISBN: 978-0-494-22362-8

NOTICE:

The author has granted a non-exclusive license allowing Library and Archives Canada to reproduce, publish, archive, preserve, conserve, communicate to the public by telecommunication or on the Internet, loan, distribute and sell theses worldwide, for commercial or non-commercial purposes, in microform, paper, electronic and/or any other formats.

The author retains copyright ownership and moral rights in this thesis. Neither the thesis nor substantial extracts from it may be printed or otherwise reproduced without the author's permission.

AVIS:

L'auteur a accordé une licence non exclusive permettant à la Bibliothèque et Archives Canada de reproduire, publier, archiver, sauvegarder, conserver, transmettre au public par télécommunication ou par l'Internet, prêter, distribuer et vendre des thèses partout dans le monde, à des fins commerciales ou autres, sur support microforme, papier, électronique et/ou autres formats.

L'auteur conserve la propriété du droit d'auteur et des droits moraux qui protègent cette thèse. Ni la thèse ni des extraits substantiels de celle-ci ne doivent être imprimés ou autrement reproduits sans son autorisation.

In compliance with the Canadian Privacy Act some supporting forms may have been removed from this thesis.

Conformément à la loi canadienne sur la protection de la vie privée, quelques formulaires secondaires ont été enlevés de cette thèse.

While these forms may be included in the document page count, their removal does not represent any loss of content from the thesis.

Bien que ces formulaires aient inclus dans la pagination, il n'y aura aucun contenu manquant.


Canada

Abstract

Objective: The aims of this study were to 1) determine if shape analysis of digital panoramic radiographs is a useful method for assessing known asymmetries of the mandible, 2) determine if a linear measurements of digital panoramic radiographs are useful in assessing the known asymmetries of the mandible, 3) determine if angular measurements of digital panoramic radiographs are useful in assessing the known asymmetries of the mandible.

Methods: Digital panoramic radiographs were obtained on experimental models of a human dry skull base coupled with a series of synthetic mandibles with known amounts of asymmetry. The images were used to measure the shape, linear and angular variables.

Results: Shape analysis did not detect significant differences between ranges of asymmetries but size analysis did. Specific linear and angular measurements revealed clinical asymmetries on digital panoramic radiographs.

Conclusion: Various sizes, linear and angular measurements have been proven to be useful in describing clinical asymmetries from digital panoramic radiographs.

Table of Contents

Chapter 1 - Introduction and Literature Review	1
1.1 Introduction.....	2
1.2 Literature Review.....	4
1.2.1 Facial Esthetics Attractiveness and Craniofacial Symmetry	5
1.2.2 Mandibular Asymmetry- Development, Classification and Treatment.....	10
1.2.3 Measuring Asymmetry.....	17
1.3 Conclusion	28
1.4 Research Objectives.....	29
1.5 Research Hypothesis and Questions	30
Chapter 2 - An Experimental Method for Stereolithic Mandible Fabrication and Preparation (Paper 1)	38
2.1 Abstract	39
2.2 Introduction.....	40
2.3 Methodology	42
2.3.1 Concept of Design.....	42
2.3.2 Methodology for construction of the Synthetic Mandibles	42
2.3.2.1 Scanning Skull Mandible	42
2.3.2.2 Generating Virtual Mandible and Asymmetries	44
2.3.2.3 Fabrication of the Mandibles	52
2.3.2.4 Coating and Landmarking the Synthetic Mandibles.....	53
2.3.2.5 Experimental Model.....	54
2.3.2.6 Imaging the Experimental Model	55
2.4 Discussion	57
2.5 Conclusion	58
Chapter 3 - The Accuracy of Digital Panoramic Unit for Detection of Mandibular Asymmetry Using Coordinate Derived Size and Shape Analysis (Paper 2)	61
3.1 Abstract	62
3.2 Introduction.....	63
3.3 Materials and Methods.....	65
3.4 Results.....	73
3.5 Discussion	74
3.6 Conclusion	78
Chapter 4 - The Accuracy of Digital Panoramic Unit for Linear Measurements (Paper 3)	81
4.1 Abstract	82
4.2 Introduction.....	83
4.3 Materials and Methods.....	86
4.3.1 Data Acquisition	86
4.3.2 Panoramic Image to True Length (CBCT) Comparison.....	92
4.3.3 Panoramic Image Left to Right Comparison	94
4.4 Results.....	94
4.4.1 Panoramic Image to True Length (CBCT) Comparison.....	94
4.4.2 Panoramic Image Left to Right Comparison	98
4.5 Discussion	100

4.5.1 Panoramic Length to True Length Measurements.....	101
4.5.2 Panoramic Image Left to Right Comparison	104
4.6 Conclusion	108
Chapter 5 - The Accuracy of Digital Panoramic Unit for Mandibular Angular Measurements (Paper 4)	112
5.1 Abstract	113
5.2 Introduction.....	114
5.3 Materials and Methods.....	115
5.3.1 Data Acquisition	115
5.3.2 Panoramic to True Angular Comparison (CBCT).....	122
5.3.3 Panoramic Image Left to Right Side Comparison	123
5.4 Results.....	124
5.4.1 Panoramic Image to True Angular (Newtom [®] and Amira [™]) Comparison.....	124
5.4.2 Panoramic Image Left to Right Comparison	128
5.5 Discussion	135
5.5.1 Panoramic to True Length Measurements	136
5.5.2 Panoramic Image Left to Right Comparison	138
5.6 Conclusion	140
Chapter 6 – General Discussion	143
6.1 Introduction.....	144
6.2 Using Panoramic Radiography to Assess and Measuring Mandibular Asymmetry.	145
6.3 Techniques used for Measuring Mandibular Asymmetries and clinical relevance ..	147
6.4 Limitations of the current study	152
6.5 Recommendation for future studies	153
Appendices	158
Appendices for Chapter Four.....	159
Appendices for Chapter Five	164

List of Tables

Table 2-1: Anatomic landmark descriptions.....	47
Table 3-1: Description of location and amount of asymmetries.....	66
Table 3-2: Landmark descriptions.....	67
Table 3-3: Average right (unaltered) X and Y coordinate for all models (std. dev.).....	70
Table 3-4: Average left (altered) X and Y coordinates for all models (std. dev.).....	71
Table 3-5: Models and landmarks where symmetry and asymmetry were expected.....	72
Table 3-6: P-values for shape analysis per model.....	73
Table 3-7: P-values for size analysis per model.....	74
Table 4-1: Landmark anatomical description.....	88
Table 4-2: True linear measurements in millimeters (std. dev.) from CBCT (n=3).....	90
Table 4-3: Average linear measurements in millimeters (std. dev.) for models from panoramic images (n=35).....	91
Table 4-4: Magnification (std. dev.) and length differences (mm) for model A between panoramic and true by side (n=35).....	95
Table 4-5: Magnification (std. dev.) and length differences (mm) for models B through F between panoramic and true left side (n=35).....	96
Table 4-6: Mean disagreement in percent (std. dev.) between panoramic and true lengths.....	97
Table 4-7: Left to right percent and millimeter (std. dev.) differences (n=35).....	99
Table 5-1: Landmark description for the points used for angular measurements.....	117
Table 5-2: True angular measurements in degrees (std. dev.) from CBCT (n=3).....	120
Table 5-3: Average angular measurements (°) for synthetic mandible models. (n=35).	121
Table 5-4: Magnification and degree difference (std. dev.) for model A (n=35).....	125
Table 5-5: Panoramic to true magnification and ° differences (std. dev.) (n=35).....	126
Table 5-6: Mean disagreement in percent (std. dev.) between panoramic and true angles.....	127
Table 5-7: Left to right percent and degree (std. dev) differences (n=35).....	129

List of figures

Figure 2-1: Original skull mandible.....	43
Figure 2-2: Three-dimensional scan of original mandible.....	44
Figure 2-3: Pro/ENGINEER triangulated STL file.....	45
Figure 2-4: Image of virtual mandible split in half.....	46
Figure 2-5: Remaining half of mandible with landmark concavities designed	46
Figure 2-6: Labeled virtual symmetric mandible as Model A.....	47
Figure 2-7: Mandible indicating the cuts for asymmetry.....	49
Figure 2-8: Location of condyle asymmetries	50
Figure 2-9: Model B with a 9mm vertical condyle asymmetry	50
Figure 2-10: Model C with a complex 9mm vertical and 6mm horizontal lateral condyle asymmetry	50
Figure 2-11: Location and design of the body asymmetry	51
Figure 2-12: Model D with a 9mm anteroposterior body asymmetry	51
Figure 2-13: Location of the ramus asymmetries	51
Figure 2-14: Model E with a 9mm vertical ramus asymmetry	52
Figure 2-15: Model F with a complex 9mm vertical and 6mm horizontal lateral ramus asymmetry	52
Figure 2-16: Experimental model positioned in panoramic unit	56
Figure 2-17: An example of a TIFF image	57
Figure 3-1: Locations of the asymmetries in the synthetic mandibles.....	66
Figure 3-2: Landmark location for synthetic mandibles.....	67
Figure 3-3: Experimental model in the panoramic unit.....	69
Figure 3-4: Tagged image file format (TIFF) obtained from panoramic unit	69
Figure 3-5: Representation of “virtual” perimeter created using R statistics program...	72
Figure 3-6: Shape superimpositions for mean shapes of left and right all models	76
Figure 3-7: Example of how adding landmarks changes the outcome of shape analysis	77
Figure 3-8: Depiction of centroids used by statistics program R.....	78
Figure 4-1: Example of Asymmetric Synthetic Mandible from Fused Deposition Modeling (FDM) Process	87
Figure 4-2: Landmark locations and description for Synthetic mandibles	87
Figure 4-3: Experimental model positioned into the panoramic unit for imaging	89
Figure 4-4: Example of tagged image file format (TIFF) obtained from the panoramic unit	89
Figure 5-1: Mandible F with a 9mm horizontal body asymmetry	116
Figure 5-2: Landmark locations and description for Synthetic mandibles	117
Figure 5-3: Experimental model positioned into the panoramic unit for imaging	118
Figure 5-4: Example of tagged image file format (TIFF) obtained for angular measurements from digital panoramic.....	119
Figure 5-5: Model B with angle Sn-Cs-Ag traced left and right	131
Figure 5-6: Model C with angle Sn-Cs-Ag traced left and right	132
Figure 5-7: Model D with angles Ag-Sn-Mf and Ag-Cs-Mf traced left and right	133
Figure 5-8: Model E with angle Cs-Mf-Ag traced on left and right sides.....	134

List of Equations

Equation 3-1: Repeatability (K).....	73
Equation 4-1: Magnification Left	92
Equation 4-2: Magnification Right	92
Equation 4-3: Magnification Left	93
Equation 4-4: Mean Disagreement	93
Equation 4-5: Pan Left to Pan Right % Difference.....	94
Equation 5-1: Magnification Left	122
Equation 5-2: Magnification Right	122
Equation 5-3: Magnification Left	123
Equation 5-4: Mean Disagreement	123
Equation 5-5: Pan Left to Pan Right Percent Difference	124

Chapter 1 - Introduction and Literature Review

1.1 Introduction

Facial esthetics has a major role in self esteem and success in life. Judging esthetics of a face is far more involved than simply assessing the texture or tone of a person's skin but also includes gauging pigmentation, quality, contour and proportion. It is imperative that orthodontists, plastic surgeons as well as oral and maxillofacial surgeons adequately diagnose and thereby treat significant asymmetries in the oro-facial complex. Less than ideal diagnosis may lead to compromised treatment for the patient, which may translate to patient dissatisfaction, not to mention frustration for the doctor or doctors. Asymmetry in the oro-facial complex may present as incongruence in the vertical, horizontal or posteroanterior dimensions of the maxilla, mandible, or any multitude of other combinations. It has been estimated that facial asymmetry in a US population ranges from 6%-12%.¹

Mandibular asymmetry, not unlike other clinical anomalies, presents in varying degrees of severity. To further complicate matters, occlusal canting, attrition, anterior and posterior cross-bites, midline shifting and temporomandibular joint remodeling and/or trauma are often commonly reported in concurrence with mandibular asymmetry, posing the question: which is the cause and which is the effect? More specifically, clinical indications of mandibular asymmetry may present simply as deviations of facial features such as deflection of the tip of the nose giving the perception of a deviated mandible. The chin itself may also possess a slight hard or soft tissue deflection leading to the illusion of a significant underlying skeletal asymmetry. It has been estimated that chin deviations comprise 4% and nose deviations contribute to 3% of facial

asymmetries.¹ Other indications may be an obvious increase in mandibular facial mass or, in contrast, a relative lack of facial mass in one facial hemisphere. As expected, the soft tissue draping of the face will often disguise a significant mandibular deviation or asymmetry. Conversely, an inconsistent soft tissue draping may also exaggerate an insignificant or non-existing asymmetry. The diagnosing clinician must afford a keen eye to the intra-oral and extra-oral signs that present on examination to ensure that these findings or indications are not overlooked.

Unfortunately there is currently no clearly defined way to facilitate the clinical decisions as to when an asymmetric patient should be treated with orthodontics, orthopedics, orthognathic surgery, plastic surgery or some combination of the above. Considerable time and thought regarding treatment planning must be dedicated to ensure that appropriate measures are taken to diagnose and treat the affected individual accordingly. To date the methods commonly used for detecting and measuring mandibular asymmetry remain limited in their abundance and usefulness. Protocols using posteroanterior (PA) cephalometric radiographs, 45° PA cephalometric radiographs, Submentovertex (SMV) radiographs, SMV with PA cephalometric radiographs, anthropometric measurements, 3-D imaging such as photogrammetry, photographic superposition and/or comparison, are all reported methods to assess asymmetry but no one particular method has been universally accepted as a clinical standard. As with many new technologies, new diagnostic systems continue to be introduced, often without significant data as to how the images produced relate and compare to contemporary systems not to mention the traditional ones.

Panoramic images are routinely prescribed and obtained for virtually every orthodontic patient in North America as a component of diagnosis and treatment planning. It is well documented that conventional panoramic images produce significant, and often unknown, levels of distortion.²⁻⁹ To further complicate matters, the current trend toward digital radiography as a means to decrease radiation dosage and increase office technology and efficiency has led to yet another new form of image collection. It is evermore important to be aware of the limitations as well as the advantages as new tools continue to be developed and introduced to the profession to ensure errors of use and interpretation are realized.

This research topic evaluates mandibular asymmetry as a subcomponent of the much more widely discussed topic of facial asymmetries and, further, a methodology to measure asymmetry in the posteroanterior, and vertical dimensions. More specifically, the purpose of this paper is to assess asymmetric mandibular shapes in addition to linear and angular measurements obtained from multiple images exposed on a series of six synthetically produced experimental models (skull base and synthetic asymmetric mandible) using a single digital panoramic machine.

1.2 Literature Review

There are three sections of reference that have been explored in this literature review. Firstly, an overview of the work that has been conducted on facial esthetics attractiveness and craniofacial symmetry, secondly, a review of the literature to discuss mandibular asymmetry regarding development classification and treatment, thirdly, the various modalities and methods used to measure mandibular asymmetry.

1.2.1 Facial Esthetics Attractiveness and Craniofacial Symmetry

Many studies have appeared in the literature that aimed to discuss facial attractiveness and isolate esthetic or attractive facial features. It is evident that describing the feature or features that make one attractive is a very difficult task to undertake. Is perception of beauty a skill passed down by our ancient ancestors or do we possess an innate ability to decipher unattractive and pretty? One set of authors conducted a study to determine if preference of attractive faces was a learned or inherent behavioral characteristic by looking into the minds of infants. As part of their study, the authors presented images of unattractive faces and attractive faces to a group of infants. The authors surmised that infants preferred to look at attractive faces as they noted that the infants gazed at photos of attractive faces for longer periods of time than the unattractive faces.¹⁰ In a notable paper by Peck and Peck, the authors illustrate the importance of beauty and esthetics from a historic perspective. Through the eyes of the Egyptians and Greeks, dating from the Renaissance to Present times, the authors describe attributes that each society found esthetically pleasing for their era. The writings discussed the sociologic and psychological considerations of facial esthetic and facial preference by analyzing historic societal figures. The researchers noted that the figures immortalized in carvings, busts and paintings rarely met current standards of “ideal” proportions yet were revered as exceptional beauties in their time.¹¹ Perhaps, not unlike today, the Egyptians and Greeks revered the uniqueness of the individual and assigned a value of attractiveness to the character based on their accomplishments or social rank rather than their physical features. In a more current study, the authors looked at a sample of fifty-two (52) young adult subjects of models, beauty contest

winners and performing stars who were considered to be beauties in their own right. Among the sample, each individual was considered to have facial qualities that were considered to be exceptionally attractive. The investigators concluded that the observers preferred a fuller dentofacial pattern with more overall protrusion than would be considered normal from today's cephalometric standard.¹² It was surmised that this would indicate that esthetic beauty may not be in harmony with accepted cephalometric norms and that perceived beauty is not necessarily coincident with perfect orthodontic treatment objectives.¹²

Physical beauty is a critically vital component of an individual's self perception and a fundamental measure of social acceptance. The age old adage that "beauty is in the eye of the beholder" may present some exceptional challenges to practitioners as they attempt to positively alter the physical appearance of a patient as is the case in orthodontics and dentofacial orthopedics. Edler suggests that a high level of agreement between practitioners when determining characteristics that indicate higher levels of facial attractiveness may be difficult to achieve. He feels that sexual selection favors averageness, especially in the human female and enhanced secondary sex characteristics, especially in the human male.¹³ He further suggests that a patient's facial appearance, following treatment, should be brought closer to the mean of the population. The author feels that it is more desirable to treat to a more symmetric face.¹³ It would seem that the gravitation toward averageness would indeed increase the persons overall attractiveness, however, the uniqueness that is prescribed to a beautiful face may be lost. It would initially seem intuitive that one would perceive beauty to be limited to those facial features that appear most symmetric. In fact, one research group

found quite the opposite to be the case in their 1995 study. The authors set out to manipulate facial features by altering characteristics without changing sizes. They employed 32 black and white photographs of 17-19 year old subjects of equal gender distribution that represented a full spectrum of attractiveness. The authors used software to manipulate the photographs to create new images that ranged from perfectly symmetric to very asymmetric throughout a range of asymmetries. The photographs were then viewed by 37 male and 45 female university students who assigned the image a score of attractiveness. The results indicated that decreased facial asymmetry is not preferred over natural levels of asymmetry that existed in un-manipulated faces. They also found that as asymmetry of the faces decreases the perceived attractiveness also decreased. The researchers surmised there was a positive relationship between perceived attractiveness and facial asymmetry.¹⁴ In an alternative study, a collection of authors explored facial esthetics by altering facial symmetry and inter-ocular distance through a series of photographs. The research group presented thirty six facial photographs of patients to 50 undergraduate dental and law students. They conducted an experiment whereby the observers were shown either an unaltered photograph, an image with inter-ocular distance increased by 20% or a mirrored symmetrical photograph. The authors noted that all modifications had an undesirable effect on perceived facial esthetics and that inter-ocular distance increases and formation of symmetry were considered to have a negative effect on facial esthetics.¹⁵

A study looking into asymmetry as it relates to attractiveness from a biologic developmental perspective consisted of four separate experiments on aging faces. The writers conducted one study to examine attractiveness of expressionless faces as it

relates to symmetry. The second study was designed to examine symmetry with respect to attractiveness in aging faces. The third study looked at symmetrical emotional expressions and the last study tested whether symmetric smiles looked less natural than asymmetric ones. The authors concluded that a low degree of facial asymmetry found in normal people does not affect attractiveness ratings.¹⁶ A supplemental article compiled 36 face-on photographs of professional models for observation of attractiveness and symmetry. The models were not considered to be famous as they did not regularly appear in the media. The photographs were halved down the racial midline and mirror imaged to construct left-left and right-right pairs of images for a group of observers to evaluate. The evaluators were assessing the original plus each mirror image for attractiveness and symmetry. The authors concluded that subjects were able to detect asymmetry and further reported that beautiful faces can be functionally asymmetric.¹⁷ In a separate study, Zaidel also looked into the correlation between symmetry and beauty. In this study, the author included a component on subjective observation of overall health. The author used 128 black and white photographs of expressionless male and female faces for the experiment. The observers were instructed to rate the degree of attractiveness, the level of health and the amount of asymmetry from each picture. The results revealed that there was not a significant difference between health judgments and symmetry but there was a significant difference between attractiveness and symmetry with symmetry being valued higher.¹⁸ In an Australian study, a group of authors studied monozygotic twins as a part of a study looking at perception of facial attractiveness and its relation for facial symmetry. The study used black and white photographs of 16 male and 18 female monozygotic twin

pairs. The researchers compiled left-left and right-right mirror image composites. The composites were examined by a group of observers for symmetry. A second set of observers were employed to assess the original photographs for attractiveness. The scientists determined that the more symmetric twin was more consistently perceived as attractive. Interestingly, the investigators also determined that attractiveness was calibrated by the magnitude of difference from symmetry.¹⁹ There was no reported difference for gender. In a paper penned by Penton-Voak et al in 2001, the authors agreed the symmetric faces were more attractive but qualified by stating that symmetric faces possess characteristics that are attractive independent of symmetry.²⁰ A fault with this paper was that the details as to how that claim was made were unclear. An additional study consisting of photographs of 62 young adult females described three characteristics of female faces including size of individual features, averageness and facial symmetry. The authors noted that the observations made by the 8 male viewers determined female faces to be more attractive when symmetry was present. Based on anthropometric measurements, the authors determined there was a tendency toward averageness among those selected.²¹

From an orthodontic perspective, it is interesting to examine the copious amounts of literature arguing that symmetry is desired as a prerequisite to facial attractiveness when it is commonly taught that every individual has some degree of normal facial asymmetry.²² From a strictly observational perspective perhaps it would be better stated that, while symmetry is a desirable objective to achieve averageness or normality, a portion of what society reveres as a uniquely attractive individual is arguably small amounts of asymmetry in facial features. A glance through some of the

more popular entertainment magazines reveals most photographed faces of our contemporary celebrities and super models are fraught with asymmetries yet are considered to be the benchmark for determining beauty.

1.2.2 Mandibular Asymmetry- Development, Classification and Treatment

Mandibular asymmetry and subsequent correction has been the subject of interest for a wide spectrum of professionals. Efforts have been made to detect and measure, quantify and correct asymmetry. Oral health care professionals are interested in the impact on the dentition, support structures and temporomandibular joint (TMJ) of those afflicted with significant asymmetries. Orthodontists are concerned with diagnosing and treatment planning for the orthopedic/orthodontic correction of the asymmetry. Oral surgeons and plastic surgeons are in tune with advancing techniques and improving surgical procedures to correct the asymmetries. Much attention has been paid to the development, measurement techniques, attempts at classification and correction of mandibular asymmetries.

Some of the earlier work looking into mandibular asymmetry has dealt with efforts to determine the etiology of development. As expected, one author suggested a link between genetics and mandibular asymmetry. The author studied a total of 8 patients including six women and two men from two non-related families. Dental casts and cephalometric radiographs were obtained for each individual. The author reported a mirror image asymmetry in two sisters from one of the families and further elaborated that both families possessed asymmetry across two generations. The author felt that there was significant observational data to link the mandibular asymmetry to a familial

trait.²³ Other authors have associated specific genetic conditions or aberrations to mandibular asymmetries. Some authors have reported birth and genetic anomalies in association with mandibular asymmetries. In a contemporary study, Polley et al looked mandibular asymmetry as a component of hemifacial microsomia. The authors studied longitudinal records including PA cephalometric radiographs of 26 untreated patients afflicted with hemifacial microsomia. Initial records were gathered at roughly 3 years of age and the final records were collected at about 16½ years of age. The authors were interested in determining the stability of the asymmetry throughout growth. They were able to establish that growth of the affected side, when compared to the non-affected side, was parallel. The group further indicated that mandibular asymmetry in hemifacial microsomia was non progressive.²⁴

Another association of researchers conducted a pair of studies relating cleft lip and palate defects to asymmetry. In the first study, the group looked at PA cephalograms of unilateral cleft lip and palate patients in retrospect. The authors were attempting to analyze mandibular asymmetry to lower face asymmetry among the cleft patients. The investigation of 34 unilateral cleft lip and palate patients compared with 142 non-cleft controls revealed that there was no significant between mandibular asymmetry of the cleft patients and the control group. In addition, the authors noted that lower face asymmetry and mandibular asymmetry were not related among the cleft group.²⁵ In the second study, authors assessed the amount of asymmetries from PA cephalograms from postoperative unilateral cleft lip and palate patients over time. Using the records of 40 cleft patients and the 142 control group, the authors determined that mandibular asymmetry in the cleft group increased with age, peaking at post-

pubertal growth-spurt stages.²⁶ They also indicated that maxillary asymmetry matched mandibular in the study group. Another study assessed mandibular asymmetry with congenital muscular torticollis in a case report. The authors described a significant amount of mandibular asymmetry associated with the condition as well as the surgical intervention taken to correct the problem.²⁷

Genetic and developmental TMJ conditions have also been implicated with mandibular asymmetry. Some authors have focused on the effects of juvenile rheumatoid (RA) arthritis^{28,29} as it relates to mandibular asymmetry. As part of their 1988 study, Stabrun et al analyzed and compared PA cephalograms of 103 patients consisting of three distinct types of RA. The group of researchers determined that mandibular asymmetry increased as the grade of joint abnormality increased.²⁹ Other authors have discussed degenerative joint disease under the same context with respect to mandibular asymmetry.³⁰⁻³² Mandibular asymmetries among a group of adult patients with unilateral degenerative joint disease was assessed against a control group. The authors obtained PA radiographs and mandibular laminagraphs of the 20 patients and 20 controls for comparison. The PA radiograph was used to assess lower face asymmetry among both groups by tracing and comparing cephalometric landmarks. The authors found that there was likely an association between the joint disease and mandibular asymmetry.³⁰ A separate group of authors conducted two studies looking into TMJ correlations with mandibular asymmetry. In the first study, conducted in 2004, the group of authors retrospectively researched articular disc displacement of 31 asymmetric patients. The authors gathered their sample group by identifying articular disc displacement from MRI. All subjects also possessed mandibular asymmetry. The

authors traced pre-treatment PA cephalometric radiographs and categorized the mandibular asymmetries into three grades (mild, moderate and severe) based on mandibular plane. The authors established that the amount of vertical asymmetry from the measurement was related to the degree to which the disc was displaced.³² In the second study, the same group of researchers discussed internal joint derangement in patients presenting with mandibular asymmetry. Using the same method, the authors assessed the PA cephalograms of 187 adult patients with asymmetry in the lower jaw. A self administered TMJ history indicated that 142 of the subjects had some form of degenerative joint disease. The results of the TMJ history exam were compared to the asymmetry measurements to reveal that there was a significant correlation between them.³¹ Two separate studies attempting to correlate untreated posterior unilateral posterior crossbites with mandibular asymmetry have been conducted. One study considered children with crossbites³³ while the other study analyzed adults.³⁴ The results of both studies indicate that there was no significant correlation between unilateral posterior crossbites and mandibular asymmetry.

Other factors contributing to asymmetry of the lower jaw include trauma and pathologic disease. Skolnick et al explored asymmetry and trauma among 109 orthodontic and 52 orthognathic surgery patients. From the sample groups studied, six orthognathic and 20 orthodontic patients had reported a history of facial trauma. The authors measured and compared frontal photos and PA radiographs of all subjects. The results of the statistical analysis indicated that there was a significant association between mandibular asymmetry and history of facial trauma.³⁵ One author presented a case report discussing excessive mandibular growth caused by multiple

neurofibromatosis. The autosomal dominant disease presented as a generalized swelling over the body of the mandible on a 25 year old female and appeared as a bony growth and subsequent mandibular asymmetry. The surgically correctable condition presents with skeletal manifestations 50% of the time, however, the patient refused corrective treatment.³⁶ Another researcher discussed two cases of mandibular hypoplasia due to hemangiomas. In the paper, the author implicates a rare vascular anomaly with the mandibular dysplasia. The author describes the radiographic and clinical asymmetries and relates the findings to the disorder as well as the subsequent surgical treatment. The surgeon concluded that perimandibular hemangiomas could be responsible for mandibular hypoplasia and dysplasia.³⁷

Classification of mandibular asymmetry is one area that has not been well established in the literature. There are only a few dated studies available that discuss a possible classification of asymmetry. In the most notable paper, although not recently published, states that there are really only two types of asymmetry that occurred due to underdevelopment or overgrowth. The author further established that either condition can be derived from two basic etiologies. The causes were determined as Inherent (genetic) or Acquired and suggested the following classification scheme: 1) Inherent consisting of either a) Deviation prognathism or b) Condylar recession or absence (Hypoplasia). 2) Acquired comprising a) Developmental with subcategories of i) Hyperplasia and ii) Hypoplasia (infection or trauma) and b) Mechanical including tumor trauma and surgery.³⁸ The remaining papers limit their discussions specifically to condylar or hemimandibular hyperplasia.^{39, 40} Cheney looked at the entire face to determine type and amount of facial asymmetry. He then attempted to classify facial

asymmetry by dividing them into four categories. 1) Unilateral Antero-posterior displacements. He felt that these asymmetries resulted from a range of horizontal anteroposterior differences in size, shape, and/or position of components of the two sides of the face. 2) Vertical displacements. These displacements were variations which result from height differences in size, shape, and/or form between dentofacial components on the two sides of the face. 3) Lateral displacements. In this category, there are asymmetrical variations which result when there are horizontal lateral differences in size, shape, and/or position of dentofacial components on one side of the face as compared to similar components on the opposite side of the face. 4) Rotary displacements. These are variations which result from a displacement of the whole body of the maxilla or the whole body of the ramus. Unilateral size variations may or may not be present.⁴¹

Treatment of mandibular asymmetry relies essentially on surgical correction, orthodontic correction or often through a combined approach. It has been reported that surgical correction of mandibular asymmetry through bone augmentation using autogenous iliac crest bone grafts⁴² or by synthetic implants⁴³ can be successfully employed to treat an underdevelopment in the mandibular body. Techniques for correcting mandibular asymmetry including inferior body osteotomies to increase or reduce length have also been reported.⁴⁴⁻⁴⁶ Many procedures described in the historic literature, although very unique at the time, have fallen from text as they have become common place surgical techniques of today. More contemporary discussions surrounding surgical correction of mandibular asymmetries involve methods that integrate distraction osteogenesis.^{45 47} The first author described case reports of four

patients that underwent surgical procedures to deliver distraction devices to provide lengthening of the mandibular ramus and body. The surgical distraction was performed coincidentally with orthodontic appliance therapy to maximize the correction of the asymmetry. The author reported that all patients achieved lengthening of their jaws and substantial improvement in facial symmetry.⁴⁵ The remaining author reported two cases requiring lengthening mandibular condyles on patients presenting with asymmetry due to temporomandibular joint ankylosis. Both patients had undergone previous surgeries of more traditional nature. In both instances, the surgeries had not provided the desired results for correcting the asymmetric mandible. After two years of follow-up, the surgeon reported distraction osteogenesis proved successful for both patients for correcting the asymmetry.⁴⁷ As is the case with most orthognathic surgery cases, asymmetry correction is often best treated by a combined orthodontic-orthognathic surgery approach. Many authors have recently discussed complex combined treatment approaches for treating mandibular asymmetries⁴⁸⁻⁵¹ to continue to provide optimum and current options to the patient. There have been fewer reports describing correction of asymmetry through non-surgical approaches with functional appliance therapy.^{52,53} One author proposed the use of functional appliance, namely an anterior repositioning splint, for the correction of asymmetric mandibles. The author selected 18 asymmetric Class II patients (9-14 years old) and matched them against 20 symmetric Class II controls. The investigator assessed nine patients to have ramus asymmetry from PA radiographs and nine patients to possess corpus asymmetry from SMV images. Treatment for all groups to treat the Class II as well as the asymmetries was provided over roughly 7 months using a “ligated” anterior repositioning splint. The author found

that a reduction in mandibular asymmetry was possible by this method claiming that vertical correction was due to vertical condylar growth.⁵⁴ The drawback with this article was that no long term follow-up regarding correction and relapse was discussed.

It has been discussed that mandibular asymmetry presents with a variety of etiologic circumstances from genetic disposition to pathologic onset. Some rudimentary research attempted to classify various types of asymmetries and treatment was discussed. Although most forms of treatment include an orthognathic approach, some less invasive approaches were argued.

1.2.3 Measuring Asymmetry

Measurement of asymmetry has taken many forms as various techniques for imaging and assessment have been developed. Methods range from simple craniometric measurements to complex three dimensional analysis. This section reviews some of the literature for techniques available.

Possibly the earliest form of measuring craniofacial features is through anthropometry. Anthropometric techniques are conducted by directly measuring skeletal or soft tissue components on the subject of interest. One of the pioneering studies was conducted by Woo in 1931. Woo conducted anthropometric measurements on roughly 53,000 dimensions from nearly 800 Egyptian skulls. The purpose was to study various aspects of craniofacial asymmetry using basic craniometric techniques. He concluded that nearly all skulls exhibited some form of asymmetry, and more specifically, determined that nearly all the asymmetry noted was attributed to a larger right side unit. Woo attributed this larger right side to a cerebral hemisphere dominance and described an increased size in the majority of bones that structure the cranial vault. There was no

mention specifically of mandibular asymmetry assessments throughout the content of his works.⁵⁵ In a more recent report, a group of scientists measured 18 mandibular dimensions from a collection of 10th to 12th century European skulls. The measurements were primarily made using sliding gauges and calipers. The results of the anthropometric study indicated that roughly 40% of the study sample exhibited some kind of left to right asymmetry.⁵⁶ Rossi et al demonstrated the use for anthropometric measurement techniques in a study attempting to determine whether asymmetries exist prior to the development of occlusion. Measurements, using a caliper, were obtained from a collection of skulls from the Federal University of Sao Paulo. It was determined that the presence of cranial asymmetry was statistically significant throughout the whole sample. The group of infants presented a higher degree of asymmetry on distance from spinous foramen to the zygomatic arch, followed by the groups of fetuses, children, and adults. Therefore, the group concluded that that craniofacial asymmetry does not only appear after establishment of the chewing habit.⁵⁷ Also in 2003 Kim et al set out to evaluate the asymmetry of the sphenoid bone and to determine its suitability as a reference for analyzing asymmetry of the skull. Thirty-seven dry skulls from India were divided into group two groups based on a right-left discrepancy of greater than or less than 2 mm discrepancy for both the external acoustic meatus-frontozygomatic suture and external acoustic meatus-subspinale distances. The skulls were then examined with regard to the percentage of asymmetry of the sphenoid bone, the angles between the cranial base and the facial axis, and the distance between reference surfaces of the sphenoid bone and facial landmarks. They found that asymmetry of the sphenoid bone was found in both groups and there was no significant difference between the groups.

They also found that the external acoustic meatus was the most suitable reference for analysis of craniofacial asymmetry.⁵⁸ A final example of anthropometric measurements was demonstrated by St. John et al in 2002 through a prospective study to assess mandibular asymmetry as a segment of a larger project researching deformational posterior plagiocephaly in infants. The authors conducted anthropometric measurements of 27 infants afflicted with deformational posterior plagiocephaly using calipers to measure mandibular dimensions such as ramal height, mandibular body length, and condylion-gnation length. They found that “mandibular asymmetry secondary to rotation of the cranial base was found in 27 patients in this study... who [had] lower facial asymmetry”.⁵⁹

Anthropometric measurements have proven to be a useful system for obtaining measurements from hard tissue such as skulls and long bones but present some technical difficulties when involving soft tissue quantities. Depending on the suppleness of the soft tissue, considerable measurement error can occur. Some authors have derived a method of obtaining anthropometric-like measurement of soft tissue while overcoming the shortfalls of tissue deflection during measurement. A group of clinical scientists designed a study surveying clinicians and their ability to assess mandibular asymmetry from 12 standard facial photographs ranging in asymmetry. The authors then assessed a computer program for analyzing lower facial asymmetry based on the same facial photographs. Computer analysis comparing right and left differences in area, compactness, perimeter and center of area ratios were compared to the results of the clinician’s observations. The results indicated, in this preliminary study, the left to right differences determined from the computer program showed high sensitivity and

specificity to the clinicians' assessment. The authors felt that the program may be a useful aid in determining the need for treatment of asymmetries.⁶⁰ The authors then studied 66 patients which they divided into three subject groups ranging from no noticeable mandibular asymmetry to visible asymmetry to mandibular asymmetry requiring orthognathic surgery for correction. The group of researchers set out to test the same four methods of measurement for usefulness in discerning mandibular asymmetries from digital photographs of the subject's faces. Three of the methods were specifically used to evaluate left to right mandibular asymmetry (area, compactness and perimeter) while one method was based on an overall percentage using moment ratio. The authors found that three methods comparing left to right were sensitive at distinguishing mandibular asymmetry while the moment ratio variable was not.⁶¹ In a further study using the same four variables, the authors compared before and after photographs of 16 patients that had undergone corrective orthognathic surgery for mandibular asymmetry. The authors found that all four parameters were useful in comparing original and post-surgical mandibular asymmetry correction. The authors also indicated that they felt their technique for measuring frontal photographs could be used as a noninvasive means of quantifying treatment outcome.⁶² In their most recent study involving some of the same researchers, the group looked at 66 orthodontic patients ranging from 8 to 19 years of age to assess skeletal discrepancy as it relates to mandibular outline asymmetry. The authors used the same four variables previously described and compared the results of asymmetry from the frontal photographs to cephalometric values obtained from the patients lateral radiographs. The members found that there was a significant relationship between a reduced ANB to mandibular

asymmetry. The group also surmised that as lower face height increased so did mandibular outline asymmetry.⁶³

Many authors have outlined techniques for measuring asymmetry by enlisting the use of PA cephalometric radiographs. Vig and Hewitt's 1975 study attempted to establish a method for the analysis of standardized posteroanterior cephalometric radiographs to investigate facial asymmetry in terms of components. Their study consisted of a wide age range of children from 9-18 years of age. The midline of the upper and lower face was established using anatomic landmarks and then a method utilizing triangles was employed to determine asymmetry between left and right halves of the face. Specifically, the lower face assessment used points for triangulation drawn between the condyle points, gonion and menton. The findings indicated an overall asymmetry with the larger side being the left from their study of 63 subjects.^{64,65} Peck and Peck observed 52 exceptionally well balanced Caucasian adult faces to "quantify the morphogenic intensity and variability of sub clinical craniofacial asymmetry".¹² From posteroanterior cephalograms the authors measured distances between landmark points. To be more specific, the study used a midface reference line and three bilateral landmarks to determine asymmetry. The following landmarks were used: The lateral orbit (LO), the zygomatic prominence (Zyg) and the lateral prominence of the gonial angle (Go). All faces were deemed to be clinically symmetric but had an underlying sub-clinical skeletal asymmetry. The results indicated that the least amount of asymmetry was noted in the lateral orbit dimension and increased as the anatomic landmarks moved inferiorly with the highest level of asymmetry being noted in the mandibular region in the gonial landmark regions.¹² More recently Inui et al studied

posteroanterior cephalometric radiographs of 34 adult female and 15 matched control subjects to analyze facial asymmetry on patients possessing temporomandibular dysfunction and internal derangement (TMD ID). The group was interested in the relationship between TMD ID with respect to facial occlusal plane (FOP) and Facial mandibular plane (FMP). They determined that facial asymmetry due to mandibular lateral deviation is an important characteristic in the etiology of internal derangement of TMJ. The authors concluded that any investigation of occlusal factors as they relate to the TMJ, the inclination of the frontal occlusal plane appears to be of significance.⁶⁶ A 2003 study conducted by Trpkova et al was designed to test the accuracy of vertical, horizontal and best-fit lines in an attempt to determine asymmetries from a series of PA cephalometric radiographs. The group obtained PA radiographs of 30 dry human skulls imaged in a variety of asymmetric position, measured horizontal and vertical reference lines from each and compared the measurements to the true skeletal positions. Among several conclusions made, the authors indicated that all horizontal lines connecting bilateral cranial landmarks can adequately serve as reference lines in the analysis of vertical asymmetry from PA cephalograms.⁶⁷ As a follow-up to their earlier studies, Edler *et al* compared PA radiographic images to photographic images on 29 human subjects. The study outlined to assess the potential for PA radiographs for use with their computer program for asymmetry assessment. The authors digitized the mandibular outline of the photographs as well as the PA cephalometric radiographs of the 29 subjects and applied the same four parameters as defined in their earlier studies. The authors were able to state that PA cephalometric radiographs could also be used in a similar manner as the previously established methodology for photographic assessment

of mandibular asymmetry, however area, compactness and moment were more sensitive but in this case perimeter was not.⁶⁸

Other authors have used oblique cephalometric views and submentovertex films for the purpose of measuring asymmetry. In a retrospective Burlington study that compared 45° serial Cephalometric radiographs of roughly 200 children at ages 6, 9, 12, 14 and 16. The researcher measured the right- and left-sided mandibular lengths and the gonial angles and to determine the difference from the normal population of growing individuals. The author also wanted to present ranges and limits of normal mandibular asymmetry. Landmarks and measurements of symphysis point, condyilion, length of mandible and gonial angle were compared. Regarding asymmetries, the author noted there were varying degrees of mandibular asymmetries present at all ages and in both sexes. Among the conclusions, the author noted the left side was longer than right on average, for boys, at 6 and 9 years but by 16 the right side was longer. For girls, the same shift occurs, but at earlier ages and the right side was longer by age 12.⁶⁹ In another study, the authors used oblique cephalometric radiographs as well as PA cephalograms of asymmetric patients to assess predictors of asymmetry. The retrospective longitudinal study of 24 patients with unilateral cleft lip and palate compared asymmetry with an equivalent non-cleft control group through measuring depth of antigonial notching. The measures of antigonial notching on both sides of the mandible for both panoramic and oblique cephalometric radiographs were recorded and compared to form a correlation with the images. It was noted that the degree of antigonial notching noted on panoramic radiographs could be used as an indicator of developing mandibular asymmetry.⁷⁰

Panoramic images have occasionally appeared in the literature as additional means to assess for asymmetry. In a landmark study conducted by Habets et al., the researchers determined that panoramic radiography was an efficient tool for screening for arthropathy of craniomandibular disorders. Through an experiment using a study model, the research group determined that as long as the position of the subject being imaged had less than 10 mm variation from original position that vertical differences between the left and right sides less than 6% were likely due to technical errors.⁷¹ In 1988, Habets et al. then looked at vertical condylar and ramal measurements on panoramic images of 152 patients. The symmetry between the right (R) and the left (L) side was calculated with the formula: $[(R-L)/(R + L)]$. The results were recorded as a percentage. The researchers found that a statistically significant difference between condylar height of each side.⁷² This percentage formula has been used in the literature by several researchers⁷²⁻⁷⁷ and has largely become the common method for comparing vertical ramal and condylar asymmetries. The use of this formula has been mostly applied to posterior vertical height assessments in ramal, condylar and overall posterior mandibular vertical height. In a subsequent study, Habets et al. set out to compare two types of images for their ability to assess asymmetries. The investigator compared lateral tomography and panoramic images of thirty-one female craniomandibular disorder (CMD) patients. The researchers deduced that, from comparison to the lateral tomograms, the Orthopantogram[®] provided sufficient view of pathology in patients with CMD but further stated that the relationship of condylar asymmetry with the radiological findings of an Orthopantogram[®] needed to be further evaluated in studies progressing of a larger patient group.⁷⁸ In an attempt to refine vertical measurements

derived from panoramic radiographs, a group of researchers developed a study looking specifically at condyle vertical height, the authors indicated that, when looking at the relative size of the condyle in relation to the ramus height, good validity was observed.⁷⁹ Mattila et al further attempted to develop and refine a method to quantitatively establish ramus and condyle heights using forty-five psoriatic arthritis patients with matched control patients. The method incorporated tangential lines of the condylar head, sigmoid notch and lower border of the mandible to establish condyle and ramal heights for posterior vertical measurement. Using the developed method in addition to the application of Habets et al. (1987) formula $|(R-L)/(R+L)| \times 100$ to calculate asymmetry, the authors felt they were able to successfully evaluate asymmetries.⁷⁴ Miller and Bodner also used the Habets et al. formula as part of their study Titled “Condylar asymmetry measurements in patients with Angle’s Class III malocclusion”. The authors determined that condylar asymmetry from the panoramic radiographs had no correlation to patients age, but condylar asymmetry was successfully determined.⁷⁶ Another study using skeletal pattern as a variable attempted to determine the affects of skeletal pattern on measurement of condylar asymmetry of panoramic radiographs. A study of 72 human subjects compared condylar and ramus ratio measurements on subjects with ranges of ANB⁸⁰. The author concluded that individual condylar and ramal measurements were unaffected by varying ANB, but combined condylar plus ramal was affected. Some authors refute the idea that symmetry measurements can routinely be conducted on panoramic radiographs. Larheim states that horizontal variables are clearly more unreliable.⁷ Boratto et al conducted a study in 2002 using 100 human dry skulls to assess condylar and mandibular asymmetry through examining panoramic

radiographs. Using a similar technique and Habets et al. formula, the researchers compared panoramic radiographs of the 100 skulls to the actual skull dimensions. The authors concluded that there was a lack of correlation between the anatomically measured and radiological measurement of asymmetry. The authors did however feel that the lack of correlation was likely due to change in head position between actual and radiographic measurement techniques.⁷³ In an additional project, also employing the previously stated Habets et al. formula, the authors found low correlation between left and right condyles and rami heights when comparing measurements of panoramic images to 25 macerated skulls.⁷⁵ In a more contemporary study, there was an attempt to determine error in linear measurements from panoramic radiographs. Laster et al. conducted the study using panoramic radiographs of 30 dry human skulls whereby the examiners measured horizontal lengths as well as vertical posterior lengths on the radiographed mandible. The authors measured the lengths from the subsequent radiographs that were achieved while the skulls were positioned in “ideal, shifted and rotated positions” within the panoramic unit. They noted the greatest differences were in horizontal and shifted skull positions from the measurements. The authors noted that accuracy for detecting asymmetry from panoramic images was 67%, 70% and 47% for ideal, rotated and shifted skull positions respectively and further concluded that panoramic radiographs should be used with caution when making absolute measurements or relative comparisons.⁸¹ In a recent study Kambylafkas et al were able to establish that panoramic radiographs may be useful in determining ramal height asymmetry with some under diagnosis of the asymmetry. Generally, the authors found that less than a 6% difference between the left and right sides may not be diagnosed

with panoramic radiography. The authors also felt that condylar height was not reliably assessed from panoramic images.⁷⁷ Despite the abundant use of panoramic radiology in clinical orthodontic practice, there are a few studies that involve the use of angular measurement to attempt to describe asymmetry. From the literature collected, it has been noted by one author that panoramic film angles were almost identical to those measured on the dry mandible when assessing the gonial angle.⁷ Another author noted that there was no difference in accuracy of angular measurements of teeth when observed on panoramic images when compared to lateral oblique projections.⁸² Kubota et al further support the use of panoramic images for determining asymmetries.⁸³ Akcam et al investigated the possibility of using panoramic radiography as a prediction tool for cephalometric measurements by looking at various linear and angular measurements on panoramic radiographs. The authors felt, from a clinical standpoint, that panoramic radiology is not reliable enough to provide additional information compared with that obtained from lateral cephalograms.⁸⁴ An interesting study described the use of panoramic images to compare left and right sides of two angular measurements following distraction osteogenesis. Padwa et al. used linear and angular measurements taken from panoramic radiographs to determine the result of the distraction prescribed. The angles described originated from a vertical reference line passing from the nasal septum through the midline between the central incisors ending at the symphysis of the mandible. The first angle was formed with the vertical reference line originating at the point which the reference line and the symphysis of the mandible meet and extends to condylion. The second angle is formed from the vertical reference line, at a point on the incisal edge of the maxillary dentition, and extends to condylion.

The angles were examined bilaterally to assess the amount of condylar position change gained from the distraction osteogenesis.⁸⁵

1.3 Conclusion

Among the reviewed articles there have been a variety of measurement techniques for both craniofacial and mandibular measurements that have been utilized throughout the decades. This review summarized a sampling of the varieties available however the focus was primarily on those methods used to determine mandibular measurements or at very least those concerned with lower face measurements. It can be stated that considerable advancement in technology and availability of diagnosing equipment has become available within the past decade. Determining which equipment to use as well as testing the equipment can be time consuming and expensive not to mention making it unavailable for all practitioners. Exploring the ability for use of panoramic images as a screening or measurement tool for assessing asymmetries would be an attractive asset to clinicians due to the availability and ease from which they are obtained. The ability to use the images for such a purpose adds another tool for diagnosis and appropriate treatment planning. The purpose of this paper is to determine if and how panoramic images may be used to evaluate overall shape changes in the mandible. In addition, this paper will look at various linear and angular measurements of panoramic images to determine their usefulness in evaluating known amounts of asymmetry.

1.4 Research Objectives

The primary objective of this study is to examine overall shape differences between left and right sides of panoramic images of experimental models consisting of synthetic mandibles of known asymmetries. It is hoped that shape analysis will explore the location and severity of the asymmetries within each mandible and that a relationship between the type of asymmetry and the shape obtained will be established. Shape differences between left and right sides may be a good tool for clinicians to use as a screening modality to determine whether or not further investigation is needed.

The secondary objective is to conduct linear and angular measurements to evaluate the known asymmetries and determine if they could also be used as a simple screening technique.

1.5 Research Hypothesis and Questions

The aim of this thesis is to determine if an association between known amounts of mandibular asymmetry and shape analysis, linear and angular measurements exists. Coordinate points for shape analysis as well as linear and angular measurements made on digital panoramic images will be utilized to test the following hypothesis:

- 1. No association can be made between coordinate derived shape changes gathered from digital panoramic images and known amounts of mandibular asymmetry.**
- 2. No association can be made between linear measurements conducted on digital panoramic images and known amounts of mandibular asymmetry.**
- 3. No association can be made between angular measurements obtained from digital panoramic images and known amounts of mandibular asymmetry.**

From the hypotheses the following research questions arose:

- 1. Are certain shapes obtained from coordinate points on digital panoramic images predictive of specific mandibular asymmetries?**
- 2. Can linear measurements derived from digital panoramic radiographs predict known amounts of vertical and anteroposterior asymmetries?**
- 3. Can angular measurements taken from digital panoramic radiographs serve to indicate known amounts of mandibular asymmetry?**

References:

1. Sheats RD, McGorray SP, Musmar Q, Wheeler TT, King GJ. Prevalence of orthodontic asymmetries. *Semin Orthod* 1998;4:138-145.
2. Goaz PW, White, S.C. *Oral Radiology: Principles and Interpretations*. Text 1987:314-338.
3. Updegrave WJ. The role of panoramic radiography in diagnosis. *Oral Surg Oral Med Oral Pathol* 1966;22:49-57.
4. McVaney TP, Kalkwarf KL. Misdiagnosis of an impacted supernumerary tooth from a panoramic radiograph. *Oral Surg Oral Med Oral Pathol* 1976;41:678-681.
5. Tronje G, Welander, U. McDavid, W.D., Morris, C.R. The image layer. In: McDavid WD, Tronje G, Welander U, Morris CR, Nummikoski P. Image characteristics of seven panoramic x-ray units. *Dentomaxillofac Radiol* 1985;8 (suppl):29-34.
6. Friedland B. Clinical radiological issues in orthodontic practice. *Semin Orthod* 1998;4:64-78.
7. Larheim TA, Svanaes DB. Reproducibility of rotational panoramic radiography: mandibular linear dimensions and angles. *Am J Orthod Dentofacial Orthop* 1986;90:45-51.
8. Tronje G, Eliasson S, Julin P, Welander U. Image distortion in rotational panoramic radiography. II. Vertical distances. *Acta Radiol Diagn (Stockh)* 1981;22:449-455.
9. Scarfe WC, Eraso FE, Farman AG. Characteristics of the Orthopantomograph OP 100. *Dentomaxillofac Radiol* 1998;27:51-57.
10. Rubenstein AJ, Kalakanis L, Langlois JH. Infant preferences for attractive faces: a cognitive explanation. *Dev Psychol* 1999;35:848-855.
11. Peck H, Peck S. A concept of facial esthetics. *Angle Orthod* 1970;40:284-318.
12. Peck S, Peck L, Kataja M. Skeletal asymmetry in esthetically pleasing faces. *Angle Orthod* 1991;61:43-48.
13. Edler RJ. Background considerations to facial aesthetics. *J Orthod* 2001;28:159-168.
14. Swaddle JP, Cuthill IC. Asymmetry and human facial attractiveness: symmetry may not always be beautiful. *Proc Biol Sci* 1995;261:111-116.
15. Faure JC, Rieffe C, Maltha JC. The influence of different facial components on facial aesthetics. *Eur J Orthod* 2002;24:1-7.

16. Kowner R. Facial asymmetry and attractiveness judgment in developmental perspective. *J Exp Psychol Hum Percept Perform* 1996;22:662-675.
17. Zaidel DW, Cohen JA. The face, beauty, and symmetry: perceiving asymmetry in beautiful faces. *Int J Neurosci* 2005;115:1165-1173.
18. Zaidel DW, Aarde SM, Baig K. Appearance of symmetry, beauty, and health in human faces. *Brain Cogn* 2005;57:261-263.
19. Mealey L, Bridgstock R, Townsend GC. Symmetry and perceived facial attractiveness: a monozygotic co-twin comparison. *J Pers Soc Psychol* 1999;76:151-158.
20. Penton-Voak IS, Jones BC, Little AC, Baker S, Tiddeman B, Burt DM et al. Symmetry, sexual dimorphism in facial proportions and male facial attractiveness. *Proc Biol Sci* 2001;268:1617-1623.
21. Baudouin JY, Tiberghien G. Symmetry, averageness, and feature size in the facial attractiveness of women. *Acta Psychol (Amst)* 2004;117:313-332.
22. Proffit. *Contemporary Orthodontics*. Mosby; 2000.
23. Persson M. Mandibular asymmetry of hereditary origin. *Am J Orthod* 1973;63:1-11.
24. Polley JW, Figueroa AA, Liou EJ, Cohen M. Longitudinal analysis of mandibular asymmetry in hemifacial microsomia. *Plast Reconstr Surg* 1997;99:328-339.
25. Laspos CP, Kyrkanides S, Tallents RH, Moss ME, Subtelny JD. Mandibular asymmetry in noncleft and unilateral cleft lip and palate individuals. *Cleft Palate Craniofac J* 1997;34:410-416.
26. Laspos CP, Kyrkanides S, Tallents RH, Moss ME, Subtelny JD. Mandibular and maxillary asymmetry in individuals with unilateral cleft lip and palate. *Cleft Palate Craniofac J* 1997;34:232-239.
27. Keller EE, Jackson IT, Marsh WR, Triplett WW. Mandibular asymmetry associated with congenital muscular torticollis. *Oral Surg Oral Med Oral Pathol* 1986;61:216-220.
28. Hu YS, Schneiderman ED, Harper RP. The temporomandibular joint in juvenile rheumatoid arthritis: Part II. Relationship between computed tomographic and clinical findings. *Pediatr Dent* 1996;18:312-319.
29. Stabrun AE, Larheim TA, Hoyeraal HM, Rosler M. Reduced mandibular dimensions and asymmetry in juvenile rheumatoid arthritis. Pathogenetic factors. *Arthritis Rheum* 1988;31:602-611.

30. Kambylaffkas P, Kyrkanides S, Tallents RH. Mandibular asymmetry in adult patients with unilateral degenerative joint disease. *Angle Orthod* 2005;75:305-310.
31. Buranastidporn B, Hisano M, Soma K. Temporomandibular joint internal derangement in mandibular asymmetry. What is the relationship? *Eur J Orthod* 2006;28:83-88.
32. Buranastidporn B, Hisano M, Soma K. Articular disc displacement in mandibular asymmetry patients. *J Med Dent Sci* 2004;51:75-81.
33. Lam PH, Sadowsky C, Omerza F. Mandibular asymmetry and condylar position in children with unilateral posterior crossbite. *Am J Orthod Dentofacial Orthop* 1999;115:569-575.
34. O'Byrn BL, Sadowsky C, Schneider B, BeGole EA. An evaluation of mandibular asymmetry in adults with unilateral posterior crossbite. *Am J Orthod Dentofacial Orthop* 1995;107:394-400.
35. Skolnick J, Iranpour B, Westesson PL, Adair S. Prepubertal trauma and mandibular asymmetry in orthognathic surgery and orthodontic patients. *Am J Orthod Dentofacial Orthop* 1994;105:73-77.
36. Tsiklakis K, Nikopoulou-Karayianni A. Multiple neurofibromatosis associated with mandibular growth and facial asymmetry. *Ann Dent* 1990;49:14-17.
37. Sailer HF. Mandibular asymmetry associated with perimandibular hemangiomas. *J Maxillofac Surg* 1973;1:104-109.
38. Hinds EC, Reid LC, Burch RJ. Classification and management of mandibular asymmetry. *Am J Surg* 1960;100:825-834.
39. Bruce RA, Hayward JR. Condylar hyperplasia and mandibular asymmetry: a review. *J Oral Surg* 1968;26:281-290.
40. Obwegeser HL, Makek MS. Hemimandibular hyperplasia--hemimandibular elongation. *J Maxillofac Surg* 1986;14:183-208.
41. Cheney EA. Dentofacial asymmetries and their clinical significance. *Am. J. Orthodontics* 1961;17:814-829.
42. Marano PD, Kolodny SC, Smart EA. Augmentation bone graft for correction of mandibular asymmetry. *Oral Surg Oral Med Oral Pathol* 1970;30:759-765.
43. Tuinzing DB, Swart JG. Correction of mandibular asymmetry with porous calciumphosphate implants. *J Maxillofac Surg* 1981;9:45-49.

44. Weinstein IR. Surgical treatment of mandibular asymmetry: report of a case. *J Oral Surg* 1972;30:303-306.
45. Tehranchi A, Behnia H. Treatment of mandibular asymmetry by distraction osteogenesis and orthodontics: a report of four cases. *Angle Orthod* 2000;70:165-174.
46. Blair AE, Schneider EK. Intraoral inferior border osteotomy for correction of mandibular asymmetry. *J Oral Surg* 1977;35:493-496.
47. Yoon HJ, Kim HG. Intraoral mandibular distraction osteogenesis in facial asymmetry patients with unilateral temporomandibular joint bony ankylosis. *Int J Oral Maxillofac Surg* 2002;31:544-548.
48. Decker JD. Asymmetric mandibular prognathism: a 30-year retrospective case report. *Am J Orthod Dentofacial Orthop* 2006;129:436-443.
49. Enacar A, Keser EI, Mavili E, Giray B. Facial asymmetry case with multiple missing teeth treated by molar autotransplantation and orthognathic surgery. *Angle Orthod* 2004;74:137-144.
50. Tellez Rodriguez J, Carvalho Tosin D, Belmont Laguna F. Osteogenic distraction and orthognathic surgery to correct sequelae of ankylosis of the temporomandibular joint: a case report. *Int J Adult Orthodon Orthognath Surg* 2002;17:291-296.
51. Keles A, Pamukcu B, Isik F, Gemalmaz D, Guzel MZ. Improving quality of life with a team approach: a case report. *Int J Adult Orthodon Orthognath Surg* 2001;16:293-299.
52. Gandini P, Mancini M, Grampi B. Functional treatment of mild skeletal asymmetry. *J Clin Orthod* 2004;38:607-611.
53. Kondo E, Aoba TJ. Nonsurgical and nonextraction treatment of skeletal Class III open bite: its long-term stability. *Am J Orthod Dentofacial Orthop* 2000;117:267-287.
54. Williamson EH, Varela JG. Correction of mandibular asymmetry with the ligated anterior repositioning splint. *Cranio* 1990;8:30-34.
55. Woo TL. On the asymmetry of the human skull. *Biometrika* 1931;22:324-340.
56. Ponyi S, Szabo G, Nyilasi J. Asymmetry of mandibular dimensions in European skulls. *Proc Finn Dent Soc* 1991;87:321-327.
57. Rossi M, Ribeiro E, Smith R. Craniofacial asymmetry in development: an anatomical study. *Angle Orthod* 2003;73:381-385.
58. Kim YH, Sato K, Mitani H, Shimizu Y, Kikuchi M. Asymmetry of the sphenoid

bone and its suitability as a reference for analyzing craniofacial asymmetry. *Am J Orthod Dentofacial Orthop* 2003;124:656-662.

59. St John D, Mulliken JB, Kaban LB, Padwa BL. Anthropometric analysis of mandibular asymmetry in infants with deformational posterior plagiocephaly. *J Oral Maxillofac Surg* 2002;60:873-877.

60. Edler R, Wertheim D, Greenhill D. Clinical and computerized assessment of mandibular asymmetry. *Eur J Orthod* 2001;23:485-494.

61. Edler R, Wertheim D, Greenhill D. Mandibular outline assessment in three groups of orthodontic patients. *Eur J Orthod* 2002;24:605-614.

62. Edler R, Wertheim D, Greenhill D. Outcome measurement in the correction of mandibular asymmetry. *Am J Orthod Dentofacial Orthop* 2004;125:435-443.

63. Good S, Edler R, Wertheim D, Greenhill D. A computerized photographic assessment of the relationship between skeletal discrepancy and mandibular outline asymmetry. *Eur J Orthod* 2006.

64. Hewitt AB. A radiographic study of facial asymmetry. *Br J Orthod* 1975;2:37-40.

65. Vig PS, Hewitt AB. Asymmetry of the human facial skeleton. *Angle Orthod* 1975;45:125-129.

66. Inui M, Fushima K, Sato S. Facial asymmetry in temporomandibular joint disorders. *J Oral Rehabil* 1999;26:402-406.

67. Trpkova B, Prasad NG, Lam EW, Raboud D, Glover KE, Major PW. Assessment of facial asymmetries from posteroanterior cephalograms: validity of reference lines. *Am J Orthod Dentofacial Orthop* 2003;123:512-520.

68. Edler R, Wertheim D, Greenhill D. Comparison of radiographic and photographic measurement of mandibular asymmetry. *Am J Orthod Dentofacial Orthop* 2003;123:167-174.

69. Melnik AK. A cephalometric study of mandibular asymmetry in a longitudinally followed sample of growing children. *Am J Orthod Dentofacial Orthop* 1992;101:355-366.

70. Kyrkanides S, Richter L. Mandibular asymmetry and antgonial notching in individuals with unilateral cleft lip and palate. *Cleft Palate Craniofac J* 2002;39:30-35.

71. Habets LL, Bezuur JN, van Ooij CP, Hansson TL. The orthopantomogram, an aid in diagnosis of temporomandibular joint problems. I. The factor of vertical magnification. *J Oral Rehabil* 1987;14:475-480.

72. Habets LL, Bezuur JN, Naeiji M, Hansson TL. The Orthopantomogram, an aid in diagnosis of temporomandibular joint problems. II. The vertical symmetry. *J Oral Rehabil* 1988;15:465-471.
73. Boratto R, Gambardella U, Micheletti P, Pagliani L, Preda L, Hansson TL. Condylar-mandibular asymmetry, a reality. *Bull Group Int Rech Sci Stomatol Odontol* 2002;44:52-56.
74. Mattila M, Kononen M, Mattila K. Vertical asymmetry of the mandibular ramus and condylar heights measured with a new method from dental panoramic radiographs in patients with psoriatic arthritis. *J Oral Rehabil* 1995;22:741-745.
75. Turp JC, Vach W, Harbich K, Alt KW, Strub JR. Determining mandibular condyle and ramus height with the help of an Orthopantomogram--a valid method? *J Oral Rehabil* 1996;23:395-400.
76. Miller VJ, Bodner L. Condylar asymmetry measurements in patients with an Angle's Class III malocclusion. *J Oral Rehabil* 1997;24:247-249.
77. Kambylafkas P, Murdoch K, Gilda E, Tallents R, Kyrkanides S. Validity of Panoramic Radiographs for Measuring Mandibular Asymmetry. *Angle Orthod*. 2006;76:388-393.
78. Habets LL, Bezuur JN, Jimenez Lopez V, Hansson TL. The OPG: an aid in TMJ diagnostics. III. A comparison between lateral tomography and dental rotational panoramic radiography (Orthopantomography). *J Oral Rehabil* 1989;16:401-406.
79. Kjellberg H, Ekestubbe A, Kiliaridis S, Thilander B. Condylar height on panoramic radiographs. A methodologic study with a clinical application. *Acta Odontol Scand* 1994;52:43-50.
80. Saglam AM. The condylar asymmetry measurements in different skeletal patterns. *J Oral Rehabil* 2003;30:738-742.
81. Laster WS, Ludlow JB, Bailey LJ, Hershey HG. Accuracy of measurements of mandibular anatomy and prediction of asymmetry in panoramic radiographic images. *Dentomaxillofac Radiol* 2005;34:343-349.
82. Wyatt DL, Farman AG, Orbell GM, Silveira AM, Scarfe WC. Accuracy of dimensional and angular measurements from panoramic and lateral oblique radiographs. *Dentomaxillofac Radiol* 1995;24:225-231.
83. Kubota Y, Takenoshita Y, Takamori K, Kanamoto M, Shirasuna K. Levandoski panoramic analysis in the diagnosis of hyperplasia of the coronoid process. *Br J Oral Maxillofac Surg* 1999;37:409-411.

84. Akcam MO, Altioek T, Ozdiler E. Panoramic radiographs: a tool for investigating skeletal pattern. *Am J Orthod Dentofacial Orthop* 2003;123:175-181.

85. Padwa BL, Zaragoza SM, Sonis AL. Proximal segment displacement in mandibular distraction osteogenesis. *J Craniofac Surg* 2002;13:293-296; discussion 297.

Chapter 2 - An Experimental Method for Stereolithic Mandible Fabrication and Preparation (Paper 1)

2.1 Abstract

Background: Reproduction of anatomical structures by rapid prototyping has proven to be a valid adjunct for craniofacial surgery, providing alternative methods to produce prostheses and development of surgical guides. The aim of this study is to introduce a methodology to fabricate asymmetric human mandibles by rapid prototyping to be used in future studies evaluating mandibular symmetries. **Methods:** Stereolithic models of human mandibles were produced with varying amounts of asymmetry in the condylar neck, ramus and body of the mandible by means of rapid prototyping. A method for production of the synthetic mandibles was defined. Model preparation, landmark description and development of the experimental model were described. **Results:** A series of synthetic mandibles ranging in asymmetry were produced from a scanned human mandible. A method for creating the asymmetries, fabricating, coating and landmarking the synthetic mandibles was described. A description for designing a reproducible experimental model for image acquisition was also outlined. **Conclusion:** Production of synthetic mandibles by stereolithic modeling is a viable method for creating skeletal experimental models with known amounts of asymmetry.

2.2 Introduction

Fabrication of a prototype model is a staple of engineering research and design as an intermediate step for developing inventions and bringing new ideas to fruition. Often small scale models are produced to provide a relatively inexpensive visual connection to aid in the exploration of new ideas. In addition, prototypes are used to assess the feasibility of the design as well as its intricacies and subtleties while avoiding excessive costs and unexpected fabrication flaws in the final product. Rapid prototyping (RP) by means of fused deposition modeling (FDM) is an example of such prototype development. This process of rapid prototyping generates a plastic model from a stereolithic (STL) computer file of the conceptualized object through computer guided plastic extrusion. A heated plastic filament is extruded through the nozzle and deposited onto a platform in layers building a three-dimensional (3-D) plastic model from the bottom up as each layer of plastic cools. The level of intricacy and amount of detail is driven by the information within the original stereolithic computer file as well as the software and hardware settings of the system. When applying this process to model human and animal tissue as a means to replicate biological structures, it can simply be referred to as biomodeling. Biomodeling is a relatively new concept that is quickly gaining momentum for research as a topic of interest over the past decade.

In this short period of time, there have been few areas of research within the medical field that have been explored. Some of the more interesting uses for biomodeling in medicine include the reproduction of anatomical structures and anomalies for the purpose of educating patients and guiding surgery.^{1,2} In these examples, the authors were able to produce models of tumors and other anomalies to

help describe the anatomical areas of interest and the proposed surgical procedures to their patients. In one study, displaying versatility of use, the authors produced RP plastic models of fetal faces that were derived from three-dimensional (3-D) ultrasound images.³ In yet another study, a group of researchers were able to produce a replica model of an ear for the purpose of producing a prosthesis⁴. Much of the research has focused on craniofacial surgery and reconstructive surgical planning procedures.⁵⁻⁸ RP modeling has also been demonstrated as a useful tool for design and implementation of distracters for the purpose of distraction osteogenesis procedures.⁹ From a dental perspective, production of dental splints, by means of STL modeling, as a surgical guide for implant placement has also been explored.¹⁰

The accuracy of the models produced has been a topic of exploration more recently as it is of little use to have a method to reproduce anatomical structures if they are not dimensionally accurate. Barker et al developed a study to compare the dimensional accuracy of a rapid prototyping technique using stereolithography (SLA) to a dry human skull. The authors found that there was a dimensional accuracy of 97.7-99.12%.¹¹ In a study published in 1988, Santler et al found that 80% of the STL models they produced were within ± 1 mm.¹² An additional group of researchers conducted a study that compared 16 linear measurements made on a dry human skull to the same 16 linear measurements of a rapid prototype replica of the skull. The results indicated that the absolute mean deviation was 0.62 \pm 0.35 mm (0.56 \pm 0.39%).¹³

In an attempt to critically evaluate the usefulness for measuring asymmetric mandibular shapes as well as linear and angular measurements from digital panoramic

radiographs, a technique for producing STL mandibles with known amounts of asymmetry was the primary purpose for developing this methodology.

2.3 Methodology

2.3.1 Concept of Design

The experiment was designed using a three-dimensional model consisting of a dry human skull base, complete with an intact nasio-maxillary complex and a series of thirty synthetically produced mandibles each of a known asymmetry. The original skull maxilla and mandible were free of visible damage and appeared intact with full upper and lower dentition including second molars. In addition, the maxillary arch included the upper right third molar. The mandibular asymmetries were designed with the intent of representing relevant asymmetries that may be encountered in clinical situations. From a series of thirty synthetically produced mandibles, six samples of asymmetric mandibles were selected for use in this study. The synthetic mandibles were prepared, coated and landmarked for optimal digital imaging. An experimental model was assembled consisting of the original skull base, a synthetic mandible and a camera tripod. The experimental model was imaged with a digital panoramic unit and the subsequent images were measured and statistically analyzed.

2.3.2 Methodology for construction of the Synthetic Mandibles

2.3.2.1 Scanning Skull Mandible

The preliminary information required to generate the synthetic mandibles was obtained by scanning the original skull mandible as seen in Figure 2-1 using a Zephyr[®] 3-D non-touch laser scanner (Kreon model KZ 50, Limoges, France). The Zephyr[®] KZ

50 was mounted on a Faro® arm, Titanium series (Kreon, Limoges, France). The Zephyr® laser scanner registers up to 28,800 points per second with a resolution of up to 10 um and a measurement frequency of 60 images per second with 480 points per image. The Faro® arm, Titanium series, is a six axis mounting arm with an accuracy of 12 um. The arm assembly allowed for a fast and efficient method of capturing the surface images of the skull mandible with a high resolution and accuracy given the combined specifications.

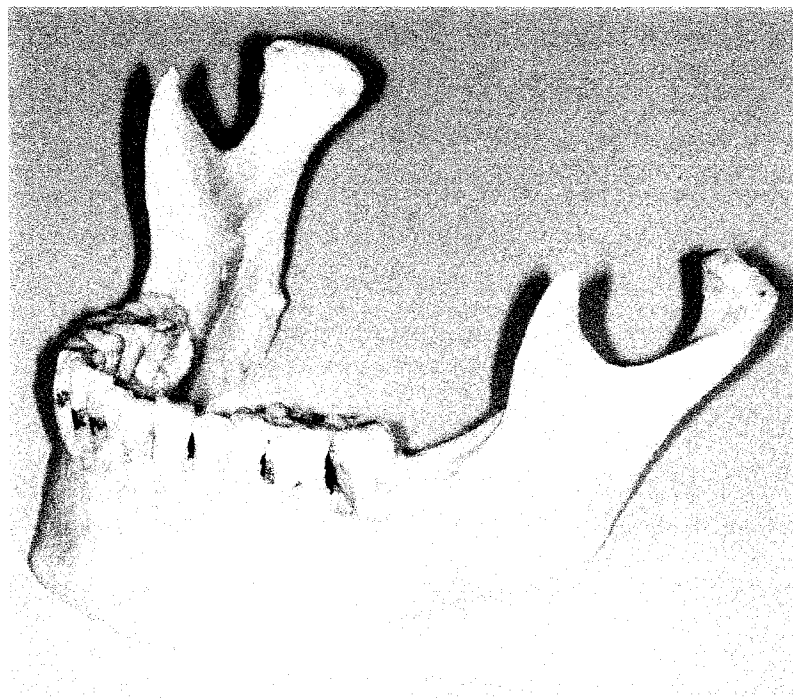


Figure 2-1: Original skull mandible

As per the manufacturer's description, the laser scanner consists of two components: the laser and a video camera. The laser projects a red line onto the surface of the object of interest to define the surface topography over its length and the video camera records the field of view and reflected light intensity as it passes by. The recording is digitized in real time over the entire surface of the object, which results in data that is a three-dimensional point cloud data set. Through the surface sweeping

process and collection of multiple three-dimensional point sets, a three-dimensional model is obtained. Figure 2-2 is a representation of the scanned three-dimensional model. The laser image was captured on the proprietary software Polygonia[®] (Kreon, Limoges, France). The software, Polygonia[®], is capable of generating multiple files including Initial Graphics Exchange Specification (IGES) and, as in this experiment, stereolithographic (STL) files. The original mandible was subsequently stored safely until completion of the project.



Figure 2-2: Three-dimensional scan of original mandible

2.3.2.2 Generating Virtual Mandible and Asymmetries

The STL files generated by the Polygonia[®] software program were then transferred into Pro/ENGINEER Wildfire 2.0 (PTC, Needham, USA) software program for detailed manipulation and further generation of the mandibular asymmetries. Figure 2-3 is Pro/ENGINEER triangulated raw data image of the STL file imported from the scanned mandible.

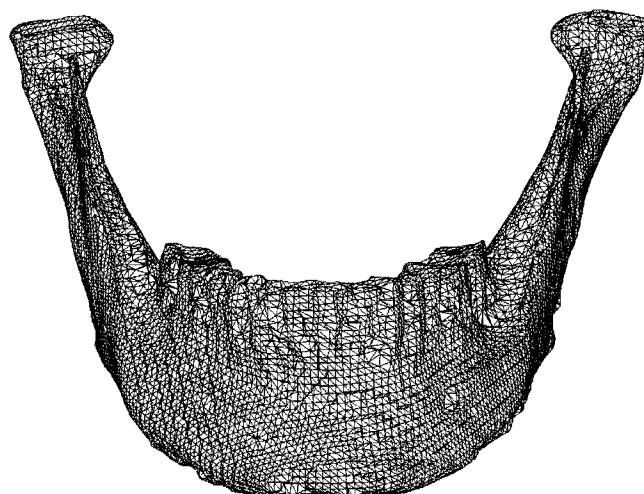


Figure 2-3: Pro/ENGINEER triangulated STL file

Using the Pro/ENGINEER software, the original STL file was subsequently exported as a solid form using a shrink wrap function in Pro/ENGINEER. This feature essentially converts the virtual mandible from a triangulated surface meshwork into a solid by filling in voids and imperfections by blending the data that was delivered from the Polygonia[®] software program. The shrink-wrapped model, now a solid file, was imported back into Pro/ENGINEER where normal functions for manipulating solid models could be utilized. The solid model was then sectioned in half. The section was constructed through the dental midline extending through the chin prominence producing a separate left and right mandibular section Figure 2-4 represents an image of the virtual mandible divided into left and right halves.

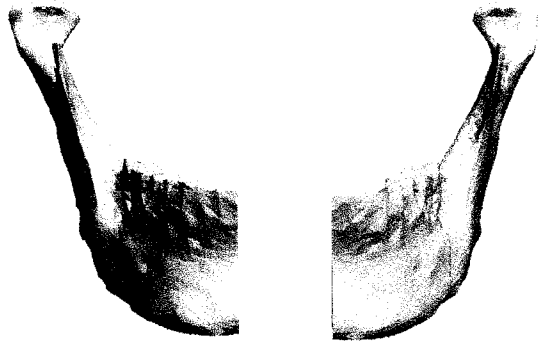


Figure 2-4: Image of virtual mandible split in half

The left half of the model was removed from the file. The corresponding right half of the mandible was used for the remainder of the project. Semi-spherical concavities were designed into the remaining right half of the virtual model as future landmark locations. Figure 2-5 represents the remaining half (right) of the virtual mandible with concavities for future landmark balls to be inserted. The concavities were designed to accept and securely seat 1.588mm steel balls for landmarks.

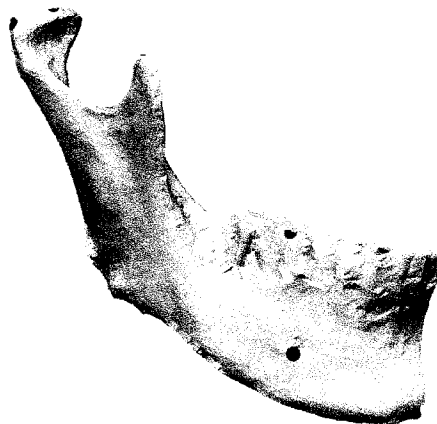


Figure 2-5: Remaining half of mandible with landmark concavities designed

The remaining virtual half-mandible was then mirror imaged and re-attached to deliver a perfectly symmetric precisely landmarked synthetic mandible and stored as an

STL file for fabrication as Model A. Labeled virtual mandible (Model A) and landmark description are shown in Figure 2-6 and Table 2-1 respectively.

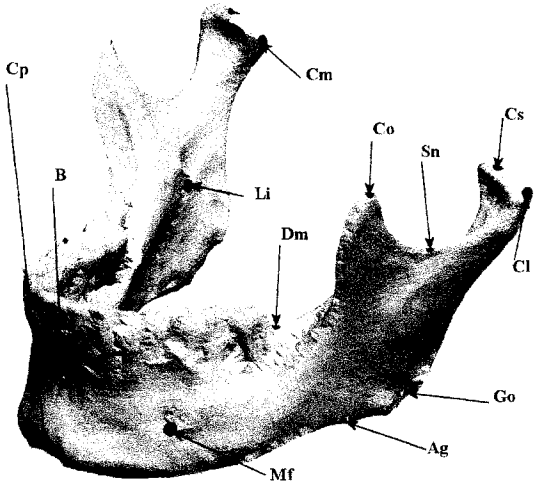


Figure 2-6: Labeled virtual symmetric mandible as Model A

Table 2-1: Anatomic landmark descriptions

Mandibular Landmarks	Description
Ag	Antigonial Notch
B	B-point
Cl	Lateral pole of Condyle head
Cm	Medial pole of Condyle head
Co	Superior point of Coronoid process
Cp	Chin Point
Cs	Superior position on Condyle head
Dm	Distal-gingival border of lower last molar
Go	Anthropometric Gonion
Li	Lingula
Mf	Mental Foramina
Sn	Sigmoid notch

The mandible halves were then re-separated and manipulated to create the remaining ranges of asymmetries. The left half of the mandible was sectioned in three

areas to which the asymmetries were assigned. Figure 2-7 shows the locations of the cuts made to the condyle, ramus and the body of the mandible. The Condyle section was located half way between the condylar head and the depth of the sigmoid notch. The location for the cut was determined by constructing a plane half way between the most superior point on the condyle head (Cs) and the depth of the sigmoid notch (Sn). The plane was perpendicular to the Cs-Sn line and was made straight through the neck of the condyle. Figure 2-8 depicts the location in the condylar neck for the sections made to generate the condyle asymmetries. From this section vertical and complex asymmetries were constructed in the condylar region. The vertical manipulation studied was a 9mm asymmetry and the complex condylar asymmetry was 9mm vertical and 6mm horizontal lateral asymmetry. Figure 2-9 and Figure 2-10 represent images of Model B with the 9mm vertical condylar asymmetry and Model C with the complex 9mm vertical and 6mm horizontal lateral condylar asymmetry respectively.

The Body section was located 43mm anterior to Cs as a plane perpendicular to the occlusal plane. The cut extended 8mm into the body before extending 10mm anterior at a 90° angle. The cut then continued vertically at 90° through the remaining body of the mandible forming a “Z” type cut. Figure 2-11 outlines the location and pattern of the section made to the body of the mandible to create the body asymmetry. From this section an anteroposterior asymmetry of 9mm was constructed in the body region. Figure 2-12 represents Model D with a 9mm anteroposterior body asymmetry.

The Ramus section was located half way between the superior aspect of the condylar head and the depth of the antgonial notch. The location for the cut was determined by constructing a point half way between the most superior point on the

condyle head (Cs) and the depth of the antgonial notch (Ag). A plane was perpendicular to this and plane MD and was constructed through the neck of the condyle parallel to the occlusal plane. Figure 2-13 represents the location in the ramus of the mandible for the sections made to generate the ramus asymmetries. From this section vertical and complex asymmetries were constructed in the ramal region. The vertical manipulation studied was a 9mm asymmetry and the complex ramal asymmetry was 9mm vertical and 6mm horizontal lateral asymmetries Figure 2-14 and Figure 2-15 represent images of Model E with the 9mm vertical ramal asymmetry and Model F with the complex 9mm vertical and 6mm horizontal lateral ramal asymmetry respectively.

The remaining twenty four of the thirty total asymmetric mandibles were fabricated in the same manner with various quantities and types of asymmetries in the condyle, ramus and body. The remaining asymmetric mandibles were subsequently stored for use on future projects.

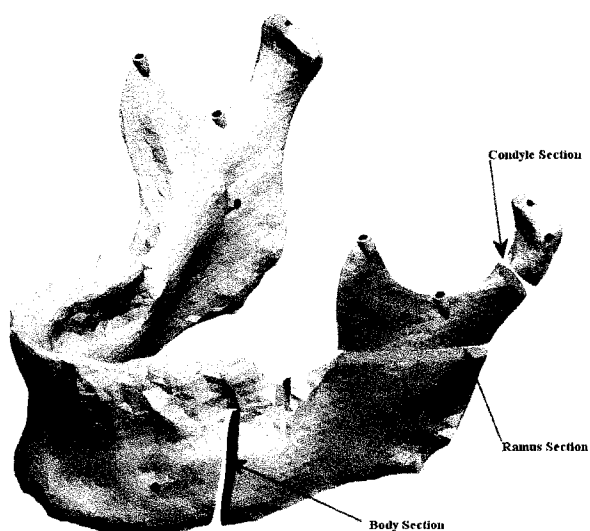


Figure 2-7: Mandible indicating the cuts for asymmetry

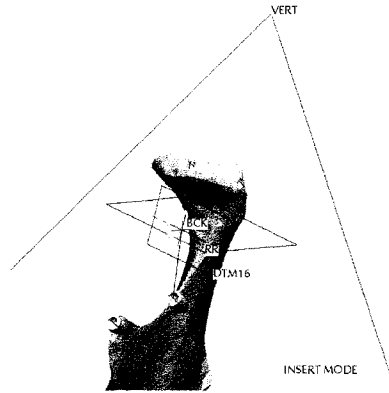


Figure 2-8: Location of condyle asymmetries

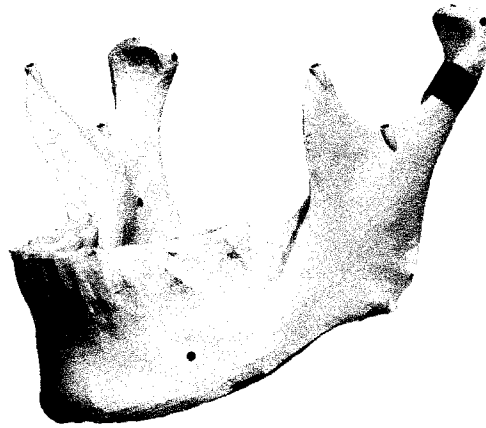


Figure 2-9: Model B with a 9mm vertical condyle asymmetry

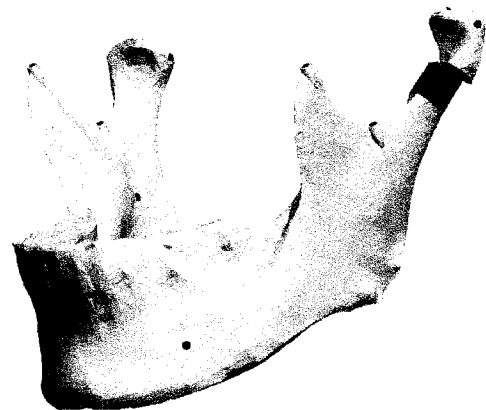


Figure 2-10: Model C with a complex 9mm vertical and 6mm horizontal lateral condyle asymmetry

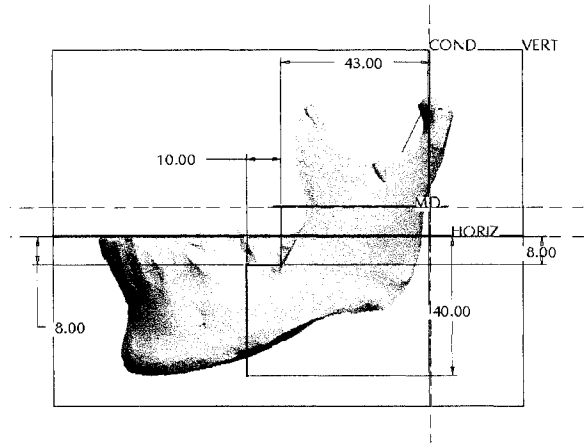


Figure 2-11: Location and design of the body asymmetry

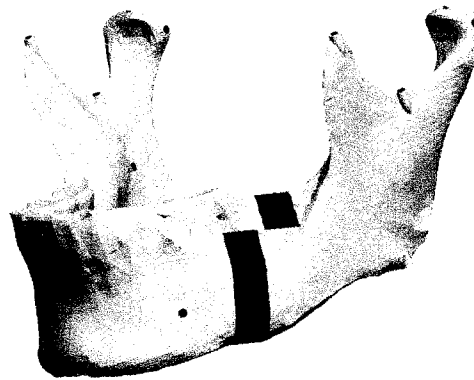


Figure 2-12: Model D with a 9mm anteroposterior body asymmetry

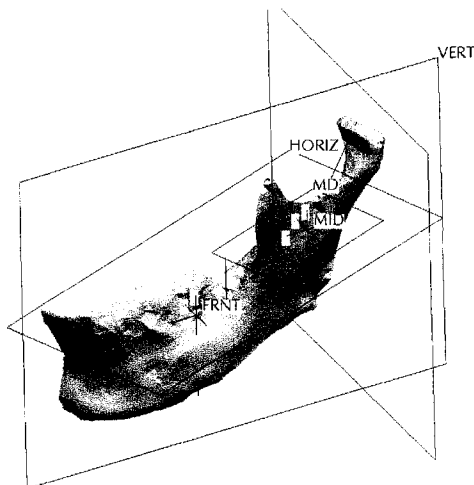


Figure 2-13: Location of the ramus asymmetries

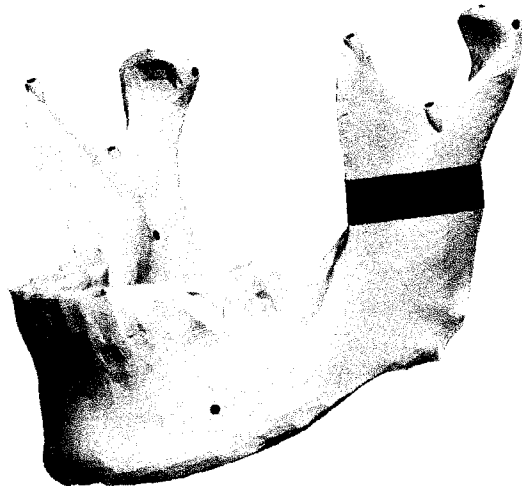


Figure 2-14: Model E with a 9mm vertical ramus asymmetry

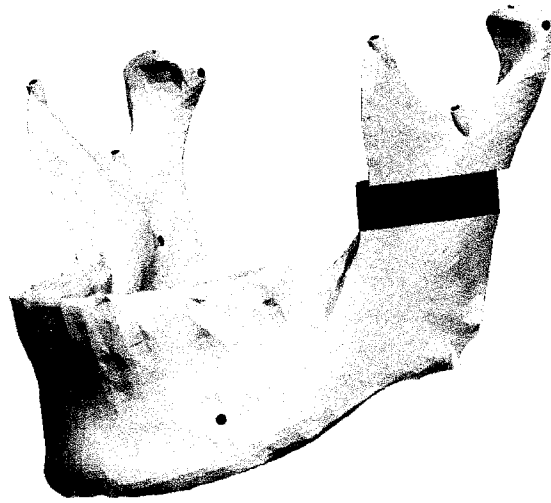


Figure 2-15: Model F with a complex 9mm vertical and 6mm horizontal lateral ramus asymmetry

2.3.2.3 Fabrication of the Mandibles

The STL files of the six pre-selected virtual mandibles were programmed into a rapid prototyping (RP) machine (StratasysTM FDM 8000, Eden Prairie, MA, USA) to generate the STL plastic replica models from the virtual file. This is the process by which the virtual mandible is transformed into a physical mandible and occurs by means

of fabrication of a plastic model through fused deposition modeling (FDM). In other words, the machine is programmed using the pre-established STL program file to feed acrylonitrile-butadiene-styrene (ABS) plastic "wire" through a heated extrusion head where it is melted and deposited in the required pattern. Each pattern delivers the pre-programmed asymmetric mandible desired to an accuracy of 0.62 ± 0.35 mm ($0.56 \pm 0.39\%$)¹³. The RP machine was provided by the Department of Mechanical Engineering, University of Alberta in Edmonton, Alberta, Canada.

2.3.2.4 Coating and Landmarking the Synthetic Mandibles

The constructed, synthetic mandible surface was inspected for gross imperfections and the imperfections were removed using a slow speed turbine handpiece (Kavo, Biberach, Germany) and # 2 round dental bur (Brassler, USA). Each mandible was then coated with an opaque paint to enable detection by the digital panoramic unit. The opaque paint consisted of a mixture of 100 ml of Crayola® (Easton, PA, USA) washable non-toxic white paint with 50 mg of Barium Sulfate (BaSO_4). Due to the fabrication process, the RP models are quite porous. This porosity allowed the custom paint to penetrate beneath the surface. Each mandible was coated with the paint four times to ensure uniform consistency and adequate opacity. The landmarks used in the experiment were 1.588 mm diameter, 316 stainless steel grade 100 balls (Small Parts Inc, Miami Lakes, FL, USA). Each landmark position on the synthetic mandibles was identified and the steel balls were fastened into place using cyanoacrylate (Instant Krazy Glue® New York, USA) as per Table 2-1.

2.3.2.5 Experimental Model

The experimental model was constructed in the following manner using the original skull based with intact maxilla and complete maxillary dentition. The maxillary dentition and fabricated, coated and landmarked mandibular jaws were occluded into a clasp-free morphologically sensitive inter-occlusal thermoset plastic splint. The splint approximated the lower posterior teeth into a protruded position by positioning the anterior teeth in an edge to edge incisor position with an anterior gap of 4mm vertical and 8mm wide for the insertion of the panoramic unit's bite block. The splint acted to hold the maxilla and each one of the series of synthetic mandibles in a secure and reproducible position throughout the experiment. The splint was constructed using IMPAK® (CMP Industries, Albany, NY, USA) elastic acrylic resin. The temporomandibular joints were seated into a uniformly thick 3mm synthetic disc which approximated the joint space. The artificial disc was constructed of Regisil® (Dentsply, York, PA, USA) bite registration material. The disc was maintained in a slightly to allow for translated position within the glenoid fossa as the asymmetry changed and was held in position by mechanical retention. The disc was removed from the original skull following the experiment. The skull and positioned mandibles were mounted onto an OT-S28V camera tripod (Opus® Ontario, Canada) using a custom designed mounting assembly. The custom mounting assembly consisted of a piece of 76.2 mm long by 38.1 mm diameter, 3 mm gauge polyvinyl tubing that was fastened to a Denar® (Waterpik Technologies, Fort Collins, CO, USA) cast mounting ring. The ring was mounted to the tubing using hot glue resin sticks (3M™ Caulk, Ca, USA). To reproduce the relative position of a patient's neck and posture, the assembly was attached to the skull over the

foramen magnum using the same hot glue resin. The hot glue resin was used to facilitate easy removal at project completion. The Denar[®] mounting ring threaded firmly to the mounting screw supplied with the camera tripod.

2.3.2.6 Imaging the Experimental Model

Each of the six experimental models were positioned into A Kodak 8000 Digital Panoramic System (Kodak, USA) and imaged 35 times per model to a total of 210 acquired images. The panoramic unit was set to 60 kV and 2 mA for tube voltage and current respectively. The Kodak 8000 Digital Panoramic Systems captured each panoramic image in real time over 13.9 seconds and the subsequent images were stored as a tagged image file format (TIFF) for further analysis. For each image acquired, the experimental model was positioned into the unit by precisely following the manufacturer's instructions which included centering the midsagittal plane of the skull by utilizing the frontal optical positioning guides. The midsagittal plane was centered horizontally left to right by aligning the frontal optical guide to project onto the center of the anterior nasal spine of the maxilla and further passing through the two midline steel balls of the synthetic mandible. The skull was positioned vertically by placing the skull into the machine in a clinically relevant position whereby the Frankfort horizontal plane was parallel to the floor. Frankfort horizontal was established by using the panoramic unit's lateral optical marker to overly an imaginary line that extended through porion (Po) and orbitale (Or). The optical light markers projecting onto the midline structures frontally and Frankfort horizontal position laterally was useful in maintaining repeatability for obtaining the images. Figure 2-16 depicts an example of the experimental model positioned into the panoramic unit.

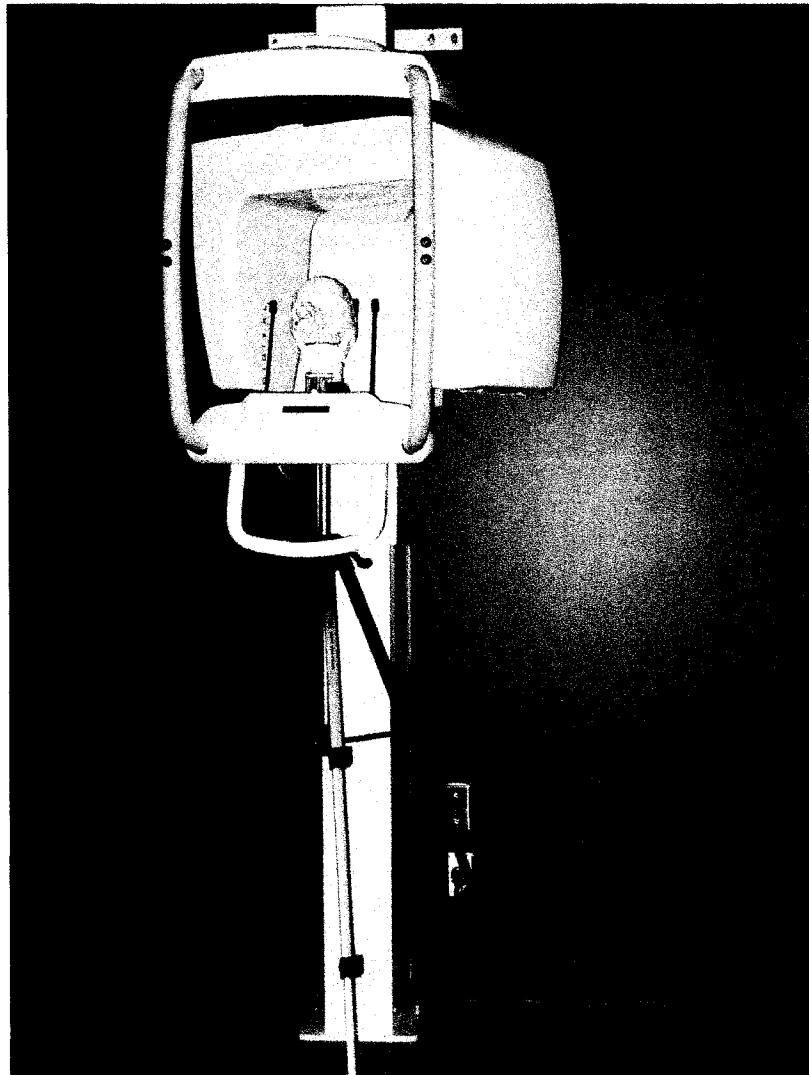


Figure 2-16: Experimental model positioned in panoramic unit

The experimental models (Model A through F) were randomly selected for each image obtained and each experimental model was imaged thirty-five times. The set-up was removed, disassembled, reassembled and repositioned between each image. All images obtained were exported as a TIFF for future analysis. Figure 2-17 is an example of a TIFF image obtained by the Kodak 8000 digital panoramic unit.

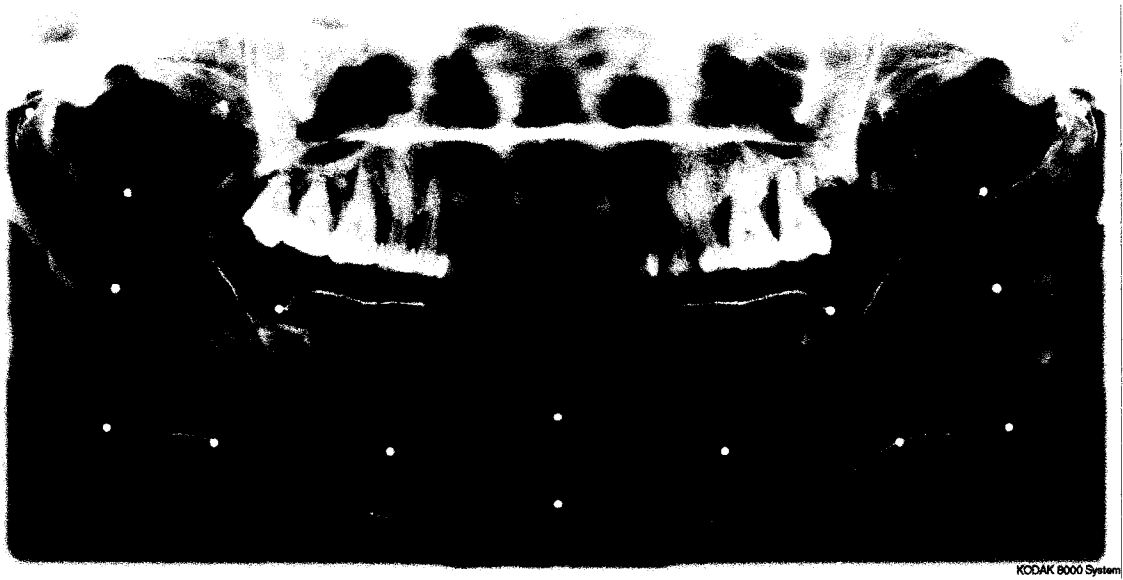


Figure 2-17: An example of a TIFF image

2.4 Discussion

The method developed to fabricate an anatomically realistic human mandible by means of rapid prototyping was described. The resultant model proved to be suitable for imaging using digital panoramic and cone beam computed tomography (CBCT). Methodology for providing surface finish, landmarking and development of a reproducible experimental model were also described. The mandibles were constructed as a plastic model by rapid prototyping using STL files programmed into a FDM printing machine. Interestingly, there are various means to obtain STL files suitable for the production of synthetic objects available as resources. Some authors have used 3-D computed tomography image files and converted them to STL files to fabricate models.^{14,15} The methodology used in this project employed a non-touch laser scanner. Other authors have used similar technology to scan anatomical parts for production of prosthetic replacements.¹⁶ The ability to use laser scanning techniques enabled efficient collection of surface data and easy conversion to STL files. Manipulation of the STL

files that were obtained from the laser scanner were successfully altered using an engineering program to generate the series of asymmetric mandibles. The asymmetric mandibles were produced for future experiments including linear, angular and shape analysis projects.

2.5 Conclusion

Fabrication of a series of thirty asymmetric mandibles including one symmetric mandible suitable for imaging by various radiological techniques was established. It was determined that asymmetries in the condyle, ramus and body of the mandible can be successfully designed and fabricated by rapid prototyping to construct a STL model of a human mandible. Inter rater reliability was established from the subsequent radiographic images of the mandibles. The methodology developed was then used in other projects to determine shape changes, linear differences and angular changes between the left and right sides of digital panoramic radiographs taken on the synthetic mandibles.

References

1. D'Urso PS, Anderson RL, Weidmann MJ, Redmond MJ, Hall BI, Earwaker WJ et al. Biomodelling of skull base tumours. *J Clin Neurosci* 1999;6:31-35.
2. D'Urso PS, Thompson RG, Atkinson RL, Weidmann MJ, Redmond MJ, Hall BI et al. Cerebrovascular biomodelling: a technical note. *Surg Neurol* 1999;52:490-500.
3. D'Urso PS, Thompson RG. Fetal biomodelling. *Aust N Z J Obstet Gynaecol* 1998;38:205-207.
4. Jiao T, Zhang FQ, Ye M, Wang CT. [Using laser scanning to 3-D reconstruct an ear model]. *Zhonghua Kou Qiang Yi Xue Za Zhi* 2003;38:261-263.
5. Bill JS, Reuther JF, Dittmann W, Kubler N, Meier JL, Pistner H et al. Stereolithography in oral and maxillofacial operation planning. *Int J Oral Maxillofac Surg* 1995;24:98-103.
6. Cheung LK, Wong MC, Wong LL. Refinement of facial reconstructive surgery by stereo-model planning. *Ann R Australas Coll Dent Surg* 2002;16:129-132.
7. Muller A, Krishnan KG, Uhl E, Mast G. The application of rapid prototyping techniques in cranial reconstruction and preoperative planning in neurosurgery. *J Craniofac Surg* 2003;14:899-914.
8. Wulf J, Vitt KD, Erben CM, Bill JS, Busch LC. Medical biomodelling in surgical applications: results of a multicentric European validation of 466 cases. *Stud Health Technol Inform* 2003;94:404-406.
9. Poukens J, Haex J, Riediger D. The use of rapid prototyping in the preoperative planning of distraction osteogenesis of the cranio-maxillofacial skeleton. *Comput Aided Surg* 2003;8:146-154.
10. Sarment DP, Sukovic P, Clinthorne N. Accuracy of implant placement with a stereolithographic surgical guide. *Int J Oral Maxillofac Implants* 2003;18:571-577.
11. Barker TM, Earwaker WJ, Lisle DA. Accuracy of stereolithographic models of human anatomy. *Australas Radiol* 1994;38:106-111.
12. Santler G, Karcher H, Gaggl A, Kern R. Stereolithography versus milled three-dimensional models: comparison of production method, indication, and accuracy. *Comput Aided Surg* 1998;3:248-256.
13. Choi JY, Choi JH, Kim NK, Kim Y, Lee JK, Kim MK et al. Analysis of errors in medical rapid prototyping models. *Int J Oral Maxillofac Surg* 2002;31:23-32.

14. Asaumi J, Kawai N, Honda Y, Shigehara H, Wakasa T, Kishi K. Comparison of three-dimensional computed tomography with rapid prototype models in the management of coronoid hyperplasia. *Dentomaxillofac Radiol* 2001;30:330-335.
15. Bouyssie JF, Bouyssie S, Sharrock P, Duran D. Stereolithographic models derived from x-ray computed tomography. Reproduction accuracy. *Surg Radiol Anat* 1997;19:193-199.
16. Zhang R, Li L, Yu LN, Bai RJ, Zhang FQ, Wang CT et al. [3D solid model of mandible with dental arch via LOM method]. *Shanghai Kou Qiang Yi Xue* 2000;9:240-242.

**Chapter 3 - The Accuracy of Digital Panoramic Unit for
Detection of Mandibular Asymmetry Using Coordinate
Derived Size and Shape Analysis (Paper 2)**

3.1 Abstract

Background: Panoramic radiographs are obtained on nearly every orthodontic patient as part of diagnostic records collection prior to orthodontic treatment. Judgment of asymmetry from panoramic images may be a useful screening method for orthodontists prior to obtaining further three dimensional images for diagnosis. The aim of this study is to utilize shape analysis for the purpose of evaluating asymmetry from digital panoramic images. Clarity in this subject area may reduce the need for further diagnostic information for treatment planning. **Methods:** Digital panoramic images (Kodak 8000) were obtained from a series of six synthetic asymmetric mandibles and dry human skull bases (experimental model). Coordinates from mandibular landmarks were selected and shape analysis using a software program (R-analysis) was gathered. **Results:** Shape and size analysis of digital panoramic radiographs did not accurately describe known amounts of asymmetry but size analysis of the radiographs was found to detect left-right asymmetries between the images gathered from the six experimental models. **Conclusion:** Shape analysis did not provide sufficient information for describing known amounts of asymmetry. Increasing the overall number of landmark locations to more adequately define the perimeter of the mandibles by offering more X,Y coordinates may lend to more descriptive results. Size analysis describes known mandibular asymmetries although it is unclear as to how additional coordinates may affect the results. More investigation in this area of research is required to offer definitive results.

3.2 Introduction

Shape analysis as a means to determine soft tissue and skeletal asymmetries is an area that has been relatively well researched over the past couple of decades. Many authors¹⁻⁷ have established analysis, formulas, techniques and methods for assessing shapes of faces and soft tissue asymmetries while other authors have similarly evaluated and focused on assessing underlying skeletal asymmetries.⁸⁻¹¹ A few articles have explored facial shape descriptions and facial analysis using three-dimensional analysis.¹² Some of the three-dimensional studies have employed video imaging¹³ and others have used photogrammetry.¹⁴⁻¹⁶

There has been some research looking specifically at form and shape of the mandible or mandibular components. Ogawa et al set out to investigate, using Fourier series analysis, mandibular form as it relates to overall facial morphology. The authors surmised that mandibular form could indeed be associated with overall facial form.¹⁷ Fourier series, simply stated, is a method of assigning values to shapes using a combination of sine and cosine functions with increasing frequencies and varying amplitudes that are further analyzed by mathematical formulas. Another study looking specifically at condylar shape also used the Fourier series to compare and analyze condylar shape. The authors noticed that there was a significant condylar asymmetry when considering the shape and size between left and right within the same subject being tested.¹⁸ Some authors have utilized elliptical Fourier functions to specifically assess mandibular shape and shape changes over time.^{19,20}

Studies that focus specifically on describing mandibular outline, shape and form have also appeared as a subject of interest in the literature. Edler et al conducted a study

comprising 66 patients divided into three subject groups ranging from no noticeable mandibular asymmetry to visible asymmetry to mandibular asymmetry requiring orthognathic surgery for correction. They tested four methods of measurement for usefulness in discerning mandibular asymmetries from digital photographs of the subject's faces. Three of the methods used to evaluate mandibular asymmetry (area, compactness and perimeter), compared right to left mandibular differences while one method was based on an overall percentage using moment ratio. They found that area, compactness and perimeter methods for comparing left to right were sensitive at distinguishing mandibular asymmetry while the moment ratio variable was not.²¹ In a follow-up study, Edler et al compared posteroanterior cephalometric (PA) radiographic images to photographic images on 29 human subjects. The study assessed whether the PA radiographs could be used in a manner similar to their previous study for assessing mandibular asymmetry. The authors digitized the mandibular outline of both images and applied the same four parameters as their earlier study. The authors were able to prove that PA cephalometric radiographs could also be used in a similar manner as the previously established photographic methods for assessing mandibular asymmetry, however area, compactness and moment were more sensitive but in this case perimeter was not.²² In an additional study, again using the same variables, the authors compared before and after photographs of 16 patients that had undergone corrective orthognathic surgery for mandibular asymmetry. They found that all four parameters were adequate for comparing pre and post surgical mandibular asymmetry correction. The authors also indicated that they felt their technique for measurement could be used as a noninvasive means of quantifying treatment outcome.²³ Most recently, a study including some of the

same researchers looked at 66 orthodontic patients ranging from 8 to 19 years of age to assess skeletal discrepancy as it relates to mandibular outline asymmetry. The authors used the same four variables previously described and found that there was a significant relationship between a reduced ANB as well as increased lower face height to mandibular outline asymmetry.²⁴ None of the studies reviewed specifically looked into panoramic radiography.

The aim of this study is to use shape analysis derived from a series of coordinate points to evaluate known amounts of mandibular asymmetry from a series of digital panoramic radiographs of experimental models possessing synthetically produced asymmetric mandibles.

3.3 Materials and Methods

A set of six asymmetric synthetic mandibles were designed and fabricated using fused deposition modeling (FDM), also known as stereolithic modeling, by means of rapid prototyping (Stratasys™ FDM 8000, Eden Prairie, MA, USA) using a methodology previously described in chapter 2 of this thesis. One mandible was designed to be entirely symmetric and the remaining five mandibles were designed with known amounts of asymmetry in either the condylar, ramal or body regions of the mandible. The mandibles were designed in a manner such that the asymmetry was fabricated in the left half while the right half of the mandible remained unchanged to enable a treatment and control in each test subject. Figure 3-1 and Table 3-1 depict and describe the locations and amounts of asymmetry assigned to the condyle, ramus and body.

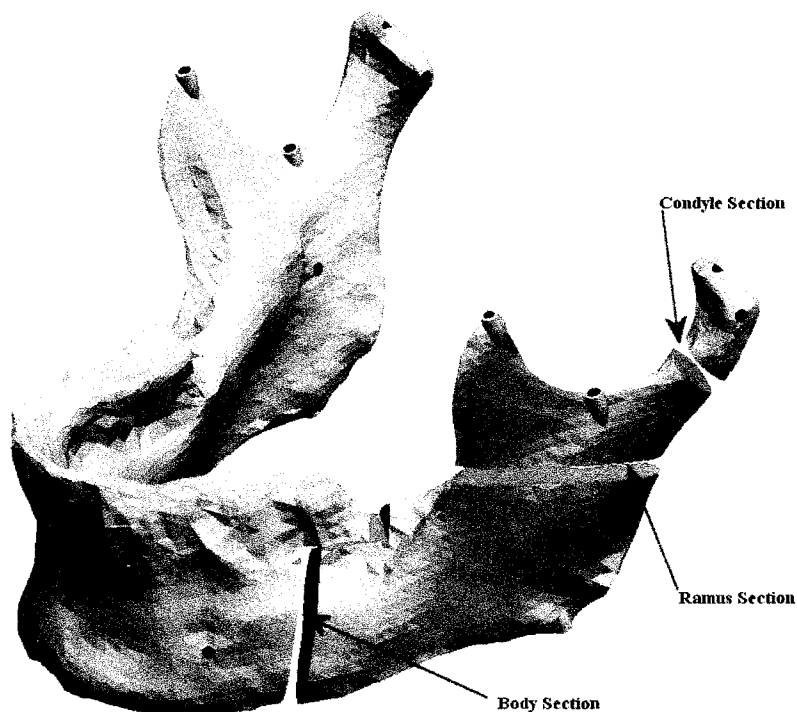


Figure 3-1: Locations of the asymmetries in the synthetic mandibles

Table 3-1: Description of location and amount of asymmetries

Mandible	Location of symmetry	Amount of asymmetry
A	None	Symmetric mandible
B	Condyle	9mm vertical
C	Condyle	9mm vertical and 6mm lateral horizontal
D	Body	9mm horizontal
E	Ramus	9mm vertical
F	Ramus	9mm vertical and 6mm lateral horizontal

Each mandible was coated with a custom radio opaque paint to enable adequate digital radiographic imaging. The coated mandibles were landmarked using 1.588 mm

diameter, 316 stainless steel grade100 balls (Small Parts Inc, Miami Lakes, FL, USA).

Figure 3-2 and Table 3-2 depict the locations and describes the landmark points used in this project.

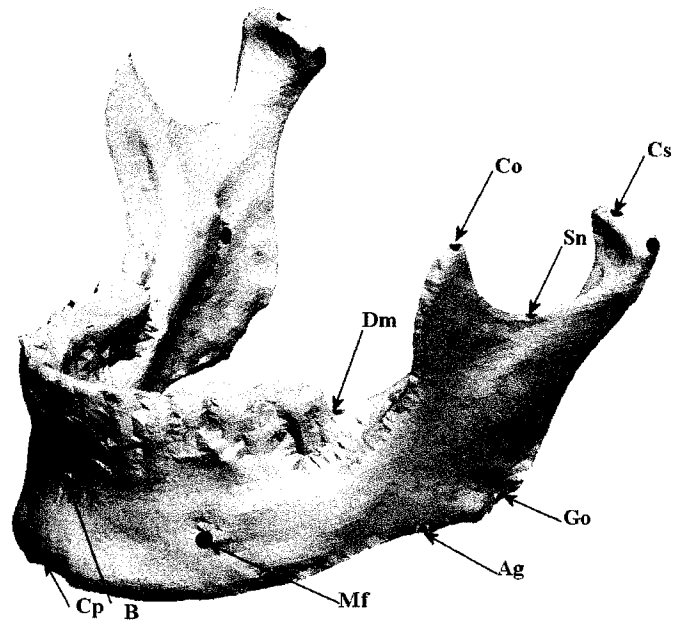


Figure 3-2: Landmark location for synthetic mandibles

Table 3-2: Landmark descriptions

Landmark	Description
B	Depth of curvature above chin point at midline of mandible
Cp	Anterior projection of chin in midline of mandible
Mf	Mental Foramen
Ag	Depth of Antigonial Notch
Go	Anthropometric Gonion
Cs	Superior Point of Condyle
Sn	Depth of Sigmoid Notch
Co	Tip of Coronoid Process
Dm	Distal of Molar at Gingiva

A single human dry skull base and each of the synthetic landmarked and coated mandibles were seated into a custom made inter-occlusal splint. The splint acted to hold the maxilla and series of synthetic mandibles in a secure and reproducible position throughout the experiment. The splint was constructed using IMPAK[®] (CMP Industries, Albany, NY, USA) elastic acrylic resin. The temporomandibular joints were seated into a custom made disc of uniform thickness to approximate the joint space. The disc was made from Regisil[®] (Dentsply, York, PA, USA) bite registration material. To complete the experimental model, the skull and each positioned mandible were mounted onto a camera tripod (Opus[®], On, Canada) using a custom designed mounting assembly. Each of the six experimental models were positioned into a digital panoramic unit (Kodak 8000, Kodak USA) and imaged 35 times per model in random order to a total of 210 acquired images to provide reasonable sample sizing per model. Each experimental model was positioned into the unit by precisely following the manufacturer's instructions which included centering the midsagittal plane of the skull by utilizing the frontal optical positioning guides. The midsagittal plane was centered horizontally by aligning the frontal optical guide to project onto the center of the anterior nasal spine of the maxilla passing through the two midline steel balls of the synthetic mandible. The skull was positioned vertically by placing the skull into the machine in a clinically relevant position whereby the Frankfort horizontal plane was parallel to the floor. Frankfort horizontal was established by using the panoramic unit's lateral optical marker to overly an imaginary line that extended through porion (Po) and orbitale (Or). Images were obtained and stored as a tagged image file format (TIFF) for further digitization

and analysis. Figures 3-3 and 3-4 depict examples of an experimental model in position in the panoramic unit and TIFF image respectively.

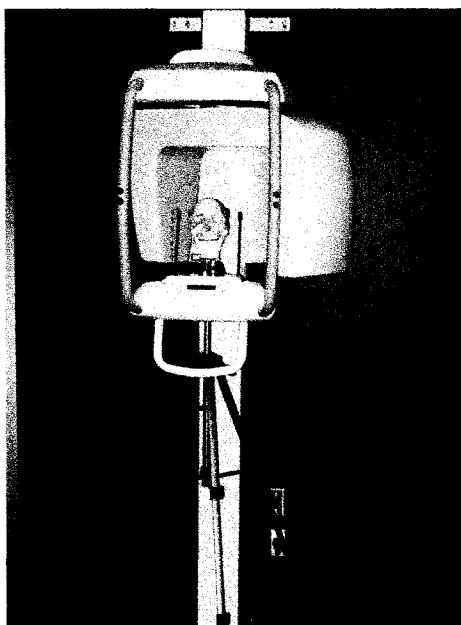


Figure 3-3: Experimental model in the panoramic unit

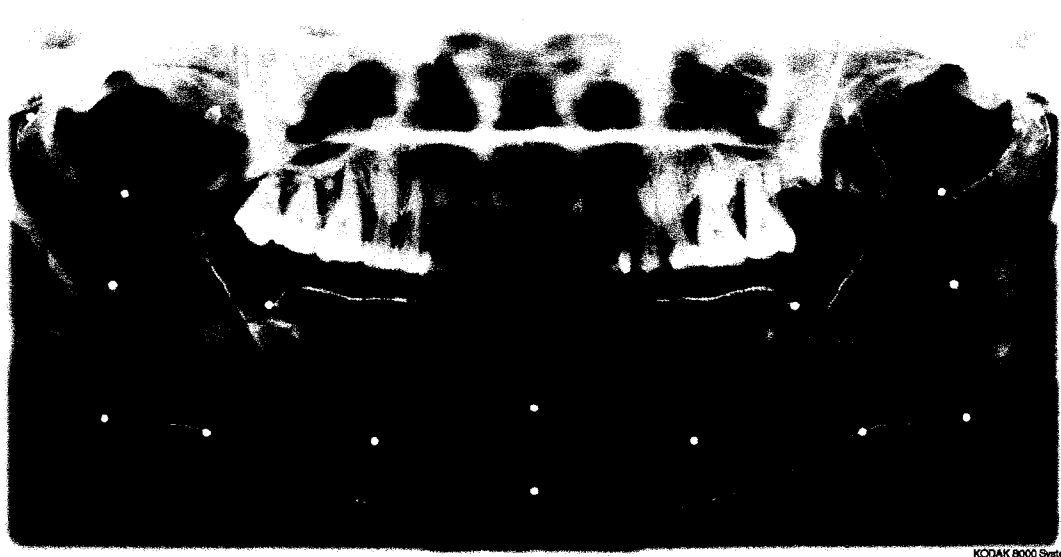


Figure 3-4: Tagged image file format (TIFF) obtained from panoramic unit

Coordinate positions were obtained on the landmarks of the digital radiograph TIFF files using a web based (freeware) measurement software (Image J, NIH Image,

Md, USA, <http://rsb.info.nih.gov/ij/index.html>) and then used to define the asymmetries.

The evaluation process was separated into two sections. The first section was designed to compare **shape** differences between the digital panoramic images for each model.

The second part of the study was designed to compare overall **size** differences between the models. Tables 3-3 and 3-4 provide summaries of average coordinate measurements for each model that were obtained from the digital panoramic images. The raw data values obtained are unit-less as each coordinate was recorded as an X and Y value. The origin of the coordinate system for each image was at B point. Considering X coordinates, a negative value indicated that the point recorded was located physically to the left of point B on the image. The values were deemed unit-less as they are considered pixel positions.

Table 3-3: Average right (unaltered) X and Y coordinate for all models (std. dev.)

Coord	Model A	Model B	Model C	Model D	Model E	Model F
Bx	.00 (.00)	.00 (.00)	.00 (.00)	.00 (.00)	.00 (.00)	.00 (.00)
By	.00 (.00)	.00 (.00)	.00 (.00)	.00 (.00)	.00 (.00)	.00 (.00)
Cpx	-.86 (.43)	.011 (.05)	.30 (.45)	-.64 (.34)	.56 (.35)	.45 (.28)
Cpy	-18.80 (.43)	-19.14 (.14)	-19.06 (.44)	-18.8 (.53)	-18.8 (.53)	-18.94 (.51)
Mfx	36.90 (.43)	36.01 (.71)	36.31 (.73)	37.27 (.39)	35.85 (.38)	36.69 (.45)
Mfy	-7.23 (.42)	-7.55 (.18)	-6.61 (.17)	-7.61 (.61)	-7.05 (.58)	-6.53 (.53)
Agx	75.11 (.56)	75.23 (.66)	75.41 (.69)	76.98 (.54)	74.19 (.39)	74.86 (.68)
Agy	-5.20 (.46)	-6.17 (.38)	-5.33 (.42)	-4.93 (.57)	-7.77 (.50)	-5.06 (.44)
Gox	98.81 (.55)	99.33 (.80)	98.93 (.71)	102.18(.83)	98.49 (.51)	98.69 (.76)
Goy	-1.99 (.52)	-3.25 (.51)	-2.17 (.44)	-1.10 (.49)	-5.48 (.77)	-1.95 (.56)
Csx	111.41(.64)	114.64(.96)	112.91(.74)	114.42(.81)	115.01(.90)	111.26(.73)
Csy	70.21 (.47)	69.14 (.58)	71.57 (.50)	70.92 (.57)	66.31 (.46)	71.54 (.72)
Snx	93.72 (.55)	95.24 (.87)	94.97 (.72)	95.82 (.84)	95.99 (.72)	93.55 (.68)
Sny	48.93 (.53)	48.40 (.50)	50.17 (.43)	49.45 (.50)	46.46 (.45)	50.25 (.57)
Cox	72.76 (.49)	73.75 (.86)	73.65 (.66)	74.18 (.76)	74.92 (.69)	72.61 (.52)
Coy	67.79 (.56)	67.88 (.39)	69.31 (.43)	67.38 (.49)	67.19 (.57)	69.42 (.49)
Dmx	61.06 (.43)	60.35 (.71)	60.10 (.58)	60.11 (.54)	60.54 (.48)	60.57 (.51)
Dmy	23.67 (.48)	23.45 (.30)	24.23 (.35)	24.57 (.52)	21.84 (.36)	24.71 (.47)

For Y coordinates, a negative value indicated that the point recorded was located physically below B point.

Table 3-4: Average left (altered) X and Y coordinates for all models (std. dev.)

Coord	Model A	Model B	Model C	Model D	Model E	Model F
Bx	.00 (.00)	.00 (.00)	.00 (.00)	.00 (.00)	.00 (.00)	.00 (.00)
By	.00 (.00)	.00 (.00)	.00 (.00)	.00 (.00)	.00 (.00)	.00 (.00)
Cpx	-.86 (.43)	.011 (.05)	.30 (.45)	-.64 (.34)	.56 (.35)	.45 (.28)
Cpy	-18.80 (.43)	-19.14 (.14)	-19.06 (.44)	-18.8 (.53)	-18.8 (.53)	-18.94 (.51)
Mfx	-37.51 (.34)	-36.58 (.44)	-37.29 (.60)	-37.32 (.35)	-36.42 (.38)	-37.92 (.47)
Mfy	-7.58 (.34)	-8.63 (.15)	-8.02 (.29)	-6.22 (.49)	-9.25 (.47)	-8.64 (.54)
Agx	-76.35 (.42)	-74.30 (.58)	-78.27 (.49)	-85.88 (.47)	-74.77 (.63)	-79.12 (.58)
Agy	-5.35 (.43)	-8.19 (.20)	-6.52 (.30)	-1.93 (.54)	-10.26 (.36)	-7.87 (.45)
Gox	-100.02 (.63)	-96.92 (.68)	-99.45 (.62)	-106.55 (.64)	-98.41 (.67)	-102.32 (.61)
Goy	-2.10 (.47)	-5.35 (.29)	-4.42 (.43)	1.03 (.55)	-8.06 (.45)	-5.51 (.53)
Csx	-111.39 (.76)	-114.48 (.70)	-113.49 (.63)	-114.48 (.73)	-114.48 (.73)	-113.30 (.75)
Csy	69.76 (.56)	71.99 (.41)	72.57 (.36)	72.37 (.59)	72.41 (.58)	72.53 (.55)
Snx	-94.47 (.58)	-92.78 (.64)	-95.19 (.61)	-99.46 (.64)	-96.13 (.69)	-96.63 (.76)
Sny	48.98 (.47)	45.02 (.26)	47.37 (.34)	51.36 (.61)	53.07 (.50)	52.29 (.43)
Cox	-73.03 (.62)	-72.94 (.59)	-74.47 (.58)	-78.20 (.47)	-76.47 (.72)	-76.72 (.69)
Coy	67.93 (.48)	64.35 (.21)	66.35 (.38)	70.17 (.52)	73.15 (.44)	71.36 (.41)
Dmx	-60.97 (.46)	-60.52 (.63)	-61.63 (.56)	-59.60 (.47)	-61.44 (.62)	-61.67 (.54)
Dmy	23.06 (.38)	22.18 (.32)	22.66 (.48)	25.58 (.67)	20.06 (.41)	22.07 (.38)

Excluding model A, which was designed to be symmetric from left to right, it was expected that variation would exist among designated landmark points and that asymmetry would appear by comparison of bilateral X and Y coordinate points depending on the region of asymmetry. For example, model B with a 9mm condylar asymmetry, would be anticipated to reveal an asymmetry for landmark Cs when comparing coordinate points obtained at point Cs between the left and right sides of the image. Table 3-5 itemizes the landmark points and depicts those that would be expected to project asymmetry or symmetry by model based on the region of asymmetry within that given model. To determine shape and size differences between the models, as a result of the known asymmetries, each model was evaluated for significant left right differences using the web based statistical analysis program R (R 2.2.1, Statistics Department of the University of Auckland, New Zealand).

Table 3-5: Models and landmarks where symmetry and asymmetry were expected

Coord	Model A	Model B	Model C	Model D	Model E	Model F
B	Symmetric	Symmetric	Symmetric	Symmetric	Symmetric	Symmetric
Cp	Symmetric	Symmetric	Symmetric	Symmetric	Symmetric	Symmetric
Mf	Symmetric	Symmetric	Symmetric	Symmetric	Symmetric	Symmetric
Ag	Symmetric	Symmetric	Symmetric	<i>Asymmetric</i>	Symmetric	Symmetric
Go	Symmetric	Symmetric	Symmetric	<i>Asymmetric</i>	Symmetric	Symmetric
Cs	Symmetric	<i>Asymmetric</i>	<i>Asymmetric</i>	<i>Asymmetric</i>	<i>Asymmetric</i>	<i>Asymmetric</i>
Sn	Symmetric	Symmetric	Symmetric	<i>Asymmetric</i>	<i>Asymmetric</i>	<i>Asymmetric</i>
Co	Symmetric	Symmetric	Symmetric	<i>Asymmetric</i>	<i>Asymmetric</i>	<i>Asymmetric</i>
Dm	Symmetric	Symmetric	Symmetric	<i>Asymmetric</i>	Symmetric	Symmetric

Each model possessing one or more asymmetric features (all but model A) were anticipated to indicate a statistically significant difference for both size and shape. Through programming efforts using the statistical program R, each coordinate value was transformed, downloaded, coded and subsequently used to assign an overall outline to each model based on the averages established in tables 3-3 and 3-4. The X,Y coordinates of each landmark point were essentially connected creating a “virtual” perimeter outline of left and right sides of each image. Although, not actually overlain on the image, Figure 3-5 depicts a representation of how the “virtual” outline would appear by selecting the landmark to landmark points using the coordinates to create a shape using R.

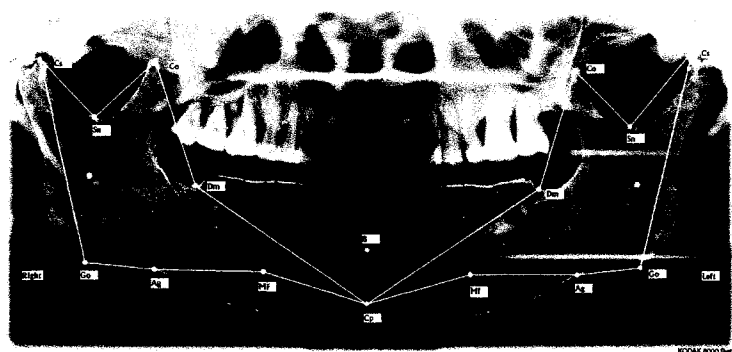


Figure 3-5: Representation of “virtual” perimeter created using R statistics program

As noted, point B was selected for zeroing the original coordinate set but was not used for the analysis. The remaining eight landmarks (Cp, Mf, Ag, Go, Cs, Sn, Co and Dm) were compared left to right using point Cp as the midline axis. All size and shape comparisons of left to right therefore included the common point Cp.

3.4 Results

Repeatability (K) was verified statistically using the following formula:

Equation 3-1:

$$K = \frac{\sum_{i,j=1}^{35} d^2(\sigma_{1i}, \sigma_{1j}) + \sum_{i,j=1}^{35} d^2(\sigma_{2i}, \sigma_{2j}) + \sum_{i,j=1}^{35} d^2(\sigma_{3i}, \sigma_{3j})}{\sum_{i,j=1}^{35} d^2(\sigma_{1i}, \sigma_{1j}) + \sum_{i,j=1}^{35} d^2(\sigma_{2i}, \sigma_{2j}) + \sum_{i,j=1}^{35} d^2(\sigma_{3i}, \sigma_{3j}) + \sum_{i=1}^{35} d^2(\sigma_{1i}, \sigma_{2i}) + \sum_{i=1}^{35} d^2(\sigma_{1i}, \sigma_{3i}) + \sum_{i=1}^{35} d^2(\sigma_{2i}, \sigma_{3i})}$$

Where d^2 was defined as the ordinary Procrustes sum of squares between the configurations with $0 \leq K \leq 1$ where no repeatability was 0 and complete repeatability was 1. It was calculated that repeatability for coordinate selection for this project was ≈ 0.99 .

Table 3-6 summarizes the findings of the shape analysis and the significance of the Hotelling's T^2 -test performed by the statistical program R.

Table 3-6: P-values for shape analysis per model

Shape	Model A	Model B	Model C	Model D	Model E	Model F
ρ^1	0.01	0.05	0.03	0.06	0.06	0.04
RMS ²	0.0075	0.0059	0.0077	0.0073	0.0068	0.0082
p-value	<.001	<.001	<.001	<.001	<.001	<.001

¹ ρ = Procrustes distance

² RMS = Root mean square for the Procrustes distance from each configuration to the mean shape.

To measure overall **shape** variability, the root mean square (RMS) was obtained for the Procrustes distance from each configuration to the mean shape and was further subject to statistical analysis in R. Testing all models for shape similarity using the R program employed a Hotelling's one sample T^2 test. The one sample Hotelling's T^2 test revealed that all models (A through F) had a statistically significant difference ($P<.05$) between left side and right sides suggesting shape differences and thus asymmetry for all models.

Table 3-7 summarizes the findings of the **size** analysis, a unit-less measure of coordinate position, and the significance the paired t-test performed by the statistical program R

Table 3-7: P-values for size analysis per model

Size	Model A	Model B	Model C	Model D	Model E	Model F
Size R	134.89	136.74	136.95	136.95	135.51	135.76
Size L	135.17	135.46	137.33	140.09	142.91	141.37
SD (R-L)	0.88	0.82	0.60	0.97	0.92	0.78
p-value	0.07	<.001	0.012	<.001	<.001	<.001

From **size** analysis using a paired t-test in the statistical program R it was illustrated model A was *not* statistically different ($P>.05$) in size when comparing left and right sides. The remaining models (B through F) revealed a statistically significant difference ($P<.05$) when comparing each model's left and right sides for size. All models were individually compared for shape and size from side to side about point Cp.

3.5 Discussion

It has been suggested that when both size and shape are available for analysis that: either analyze size and shape separately or size and shape jointly. It is further stated that if the real interest is in shape alone that shape and size be studied separately

to ensure less modeling assumptions are made²⁵. Dryden and Mardia define configuration as the set of landmarks on a particular object and the pre-shape as the configuration which is invariant translation and scaling.²⁵ Dryden and Mardia also define shape as the geometrical information that remains when location, scale and rotational effects are filtered out from an object²⁵. This definition was applied for the coordinate driven shape and subsequent shape comparisons using the R program. It was expected that shape differences would have been evident as a result of the inherent asymmetries constructed into the individual models as defined in Table 3-5. In fact, all asymmetric models had a statistically significant difference between left and right sides using Hotelling's one sample T^2 test which is based on the Procrustes tangent space coordinates. Procrustes distance (ρ) is defined as the closest great circle distance between the pre-shapes²⁵ on the pre-shape sphere. Equivalently, ρ can be considered as the smallest angle between the pre-shapes over rotations of the pre-shapes and is explained as $0 \leq \rho \leq \pi/2$ where 0 is exactly the same and $\pi/2$ is furthest distance away.

In terms of shape, it was not surprising that the Hotelling's T^2 test revealed that all asymmetric models had a statistically significant difference between left side and right sides. The small number of available landmarks from which coordinates were obtained to deliver shapes suggested that shape differences due to the small variation in overall asymmetry within each model would be detected. Small variations in coordinate position from image to image within a single model would exaggerate the amount of actual change from this sensitive test. Each model typically possessed a single landmark point across the region of asymmetry making very small coordinate differences detectable as an asymmetry. Statistically speaking, there was a detectable

significant difference between left and right sides for both models. Figure 3-6 is a composite of graphs depicting results of the shape analysis for each model.

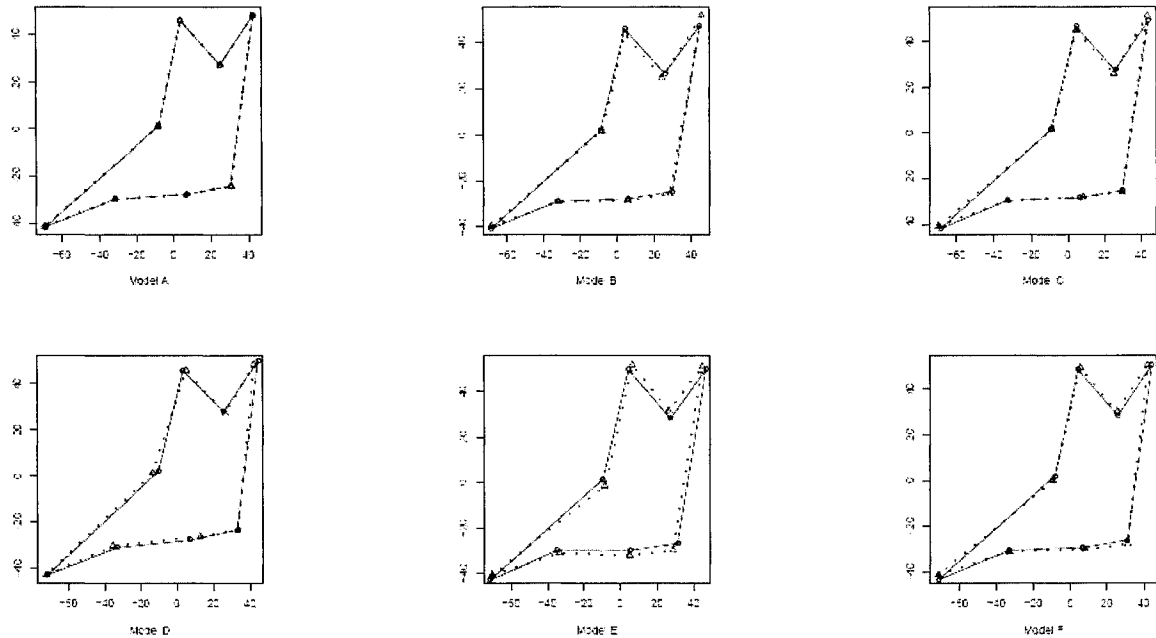


Figure 3-6: Shape superimpositions for mean shapes of left and right all models

In the figure, the perforated line indicates the left (symmetric) outline superimposed over the right (asymmetric) solid line.

From the above argument, it was reasoned that increasing the number of landmark points would provide a higher likelihood of distinguishing areas of actual asymmetry versus areas that reveal little change by relying on more coordinates to define the area of asymmetry. From the information described, using single point coordinates, there is no clinically relevant information that can be gathered from the shape analysis. Figure 3-7 is a representative example of how adding landmarks could change the outcome of shape analysis. Both images depict a condylar asymmetry, but the image on the right would have employed multiple landmark points in the condylar

region where the left image selected a single coordinate as was done in this project. Again, the perforated line would indicate the asymmetric side and the solid line would indicate the symmetric side.

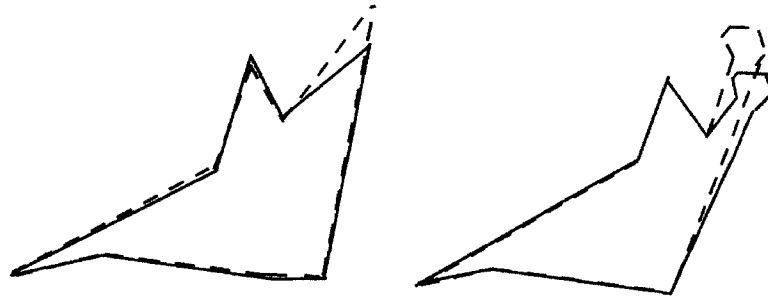


Figure 3-7: Example of how adding landmarks changes the outcome of shape analysis

It was expected that size differences would be observed as a result of the known asymmetries constructed into the individual models as defined in Table 3-5. The average centroid size for each model was compared from left side to right through paired t-test using the statistical program R. The centroid size is the square root of squared Euclidean distances between the center of the mass and each coordinate derived landmark selected. Figure 3-8 is a diagrammatic representation of how the centroid size was used to determine the shape size.

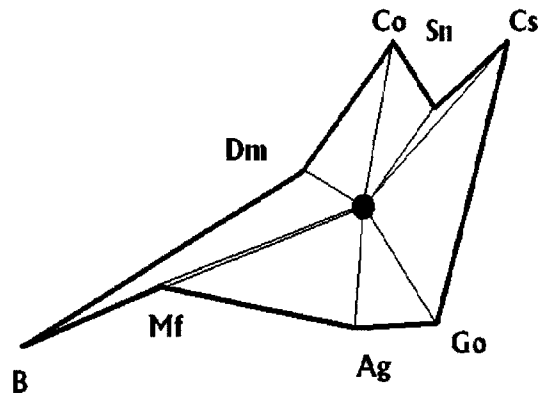


Figure 3-8: Depiction of centroids used by statistics program R

From the results of the paired t-test it was demonstrated that model A was symmetric with no statistically significant difference in size when comparing left and right sides. The remaining models (B through F) all revealed a statistically significant difference for the same comparisons. Determination of overall size was clearly more representative of the actual models for describing the asymmetries.

3.6 Conclusion

Shape analysis did not provide sufficient information for describing known amounts of asymmetry. Increasing the overall number of landmark locations to more adequately define the perimeter of the mandibles by offering more X,Y coordinates may provide more descriptive results. Size analysis describes known mandibular asymmetries although it is unclear as to how additional coordinates may affect the results. More investigation in this area of research is required to offer definitive results.

References

1. Naftel AJ, Trenouth MJ. Stereo-assisted landmark detection for the analysis of changes in 3-D facial shape. *Med Inform Internet Med* 2004;29:137-155.
2. Rose AD, Woods MG, Clement JG, Thomas CD. Lateral facial soft-tissue prediction model: analysis using Fourier shape descriptors and traditional cephalometric methods. *Am J Phys Anthropol* 2003;121:172-180.
3. Ferrario VF, Sforza C, Guazzi M, Montorsi F, Taroni A. Effect of growth and development on human soft tissue facial shape: a Fourier analysis. *Int J Adult Orthodon Orthognath Surg* 1996;11:155-163.
4. Ferrario VF, Sforza C, Schmitz JH, Miani A, Jr., Taroni G. Fourier analysis of human soft tissue facial shape: sex differences in normal adults. *J Anat* 1995;187 (Pt 3):593-602.
5. Coblenz A, Mollard R, Ignazi G. Three-dimensional face shape analysis of French adults, and its application to the design of protective equipment. *Ergonomics* 1991;34:497-517.
6. Farkas LG, Kolar JC, Munro IR. Craniofacial disproportions in Apert's syndrome: an anthropometric study. *Cleft Palate J* 1985;22:253-265.
7. Halazonetis DJ. Morphometrics for cephalometric diagnosis. *Am J Orthod Dentofacial Orthop* 2004;125:571-581.
8. Kim YH, Sato K, Mitani H, Shimizu Y, Kikuchi M. Asymmetry of the sphenoid bone and its suitability as a reference for analyzing craniofacial asymmetry. *Am J Orthod Dentofacial Orthop* 2003;124:656-662.
9. Rossi M, Ribeiro E, Smith R. Craniofacial asymmetry in development: an anatomical study. *Angle Orthod* 2003;73:381-385.
10. Ono I, Ohura T, Narumi E, Kawashima K, Matsuno I, Nakamura S et al. Three-dimensional analysis of craniofacial bones using three-dimensional computer tomography. *J Craniomaxillofac Surg* 1992;20:49-60.
11. McIntyre GT, Mossey PA. Size and shape measurement in contemporary cephalometrics. *Eur J Orthod* 2003;25:231-242.
12. Sforza C, Peretta R, Grandi G, Ferronato G, Ferrario VF. Three-dimensional facial morphometry in skeletal Class III patients A non-invasive study of soft-tissue changes before and after orthognathic surgery. *Br J Oral Maxillofac Surg* 2006.

13. Nanda RS, Ghosh J, Bazakidou E. Three-dimensional facial analysis using a video imaging system. *Angle Orthod* 1996;66:181-188.
14. Ferrario VF, Sforza C, Schmitz JH, Santoro F. Three-dimensional facial morphometric assessment of soft tissue changes after orthognathic surgery. *Oral Surg Oral Med Oral Pathol Oral Radiol Endod* 1999;88:549-556.
15. Ferrario VF, Sforza C, Miani A, Jr., Serrao G. A three-dimensional evaluation of human facial asymmetry. *J Anat* 1995;186 (Pt 1):103-110.
16. Ferrario VF, Sforza C, Poggio CE, Tartaglia G. Distance from symmetry: a three-dimensional evaluation of facial asymmetry. *J Oral Maxillofac Surg* 1994;52:1126-1132.
17. Ogawa T, Kawasaki H, Takahashi O, Aboshi H, Kasai K. Application of a Fourier series to analysis of the relationship between mandibular form and facial morphology. *J Oral Sci* 2000;42:93-100.
18. Ferrario VF, Sforza C, Miani A, Jr., Sigurta D. Asymmetry of normal mandibular condylar shape. *Acta Anat (Basel)* 1997;158:266-273.
19. Ferrario VF, Sforza C, Guazzi M, Serrao G. Elliptic Fourier analysis of mandibular shape. *J Craniofac Genet Dev Biol* 1996;16:208-217.
20. Chen SY, Lestrel PE, Kerr WJ, McColl JH. Describing shape changes in the human mandible using elliptical Fourier functions. *Eur J Orthod* 2000;22:205-216.
21. Edler R, Wertheim D, Greenhill D. Mandibular outline assessment in three groups of orthodontic patients. *Eur J Orthod* 2002;24:605-614.
22. Edler R, Wertheim D, Greenhill D. Comparison of radiographic and photographic measurement of mandibular asymmetry. *Am J Orthod Dentofacial Orthop* 2003;123:167-174.
23. Edler R, Wertheim D, Greenhill D. Outcome measurement in the correction of mandibular asymmetry. *Am J Orthod Dentofacial Orthop* 2004;125:435-443.
24. Good S, Edler R, Wertheim D, Greenhill D. A computerized photographic assessment of the relationship between skeletal discrepancy and mandibular outline asymmetry. *Eur J Orthod* 2006.
25. Dryden I.L. MKV. *Statistical Shape Analysis*. John Wiley & Sons LTD; 1998.(pages 1, 13, 24, 63, 64, 151 and 189)

Chapter 4 - The Accuracy of Digital Panoramic Unit for Linear Measurements (Paper 3)

4.1 Abstract

Background: The use of linear measurements obtained from panoramic images to evaluate asymmetry has been discussed infrequently throughout the orthodontic literature. The aim of this study was to assess accuracy of various linear distances of landmark to landmark locations made on digital panoramic radiographs of known asymmetric synthetic mandibles. A further aim was to assess the validity of linear measurements from digital panoramic for quantifying known mandibular asymmetries.

Methods: A total of 210 Digital panoramic radiographs (Kodak 8000, USA) were acquired on six experimental models (dry skull base with an asymmetric synthetic mandible). Horizontal, oblique and vertical measurements were gathered across ramal, condylar and body asymmetries (Image J, USA) which were subsequently compared to true known mandibular asymmetries measured (Newtom[®]-3G, Italy and Amira[™] software, USA) from the synthetic mandibles.

Results: Model accuracy and validation of measurement technique as well as comparison of panoramic lengths to true values was established. Measurement of six linear distances between left and right sides of digital panoramic radiographs were compared to one another, expressed as a percentage and statistically analyzed. The results of the one sample t-test analysis indicated that asymmetry can be statistically described for some linear measurements in some cases while clinical explanations may provide explanation for others.

Conclusions: More accurate measurements for expected asymmetries are revealed when measurements are made directly across the area of asymmetry along the same axis as the asymmetry. The only length found to be accurate for measuring mandibular asymmetries was vertical ramus measurement from antgonial to sigmoid notches.

4.2 Introduction

Panoramic radiographs are routinely obtained during the initial records collection phase of orthodontics and have proven useful for diagnosis and treatment planning. The desire to use panoramic images for more than a screening/assessment tool has been explored in the orthodontic literature since its inception and subsequent use in mainstream dental and orthodontic treatment. Many authors have attempted to measure specific variables directly from panoramic images despite the fact that magnification and distortion issues often are of concern. The ability to obtain reproducible linear measurements from panoramic images remains a topic of debate.

In 1979, Alpern studied various vertical and horizontal linear measurements obtained from panoramic images. Using dry human skulls, linear skeletal measurements were analyzed for ranges of magnification and the author found that basal skull magnification varied anatomically both vertically and horizontally, but were calculable. As a further observation, the author felt that vertical magnification appeared to be consistent enough in the mandibular ramus area to permit assessment the posterior facial height.¹ Using a study model, constructed to resemble a human mandible, Habets et al determined that as long as the position of the subject being imaged had less than 10 mm variation from original position, vertical differences between the left and right sides less than 6% were likely due to technical errors.² In 1988, Habets et al evaluated vertical condylar and ramal measurements on panoramic images of 152 patients. The symmetry between the right (R) and the left (L) side was calculated with the formula: $[(R-L)/(R + L)]$ and recorded as a percentage. From their earlier study, they designated a 6% cutoff be used to detect clinical asymmetry. Variations of this percentage formula has been

used in the literature by several researchers³⁻⁸ and has become the common method for comparing vertical ramal and condylar asymmetries. The use of this formula has been applied mostly to posterior vertical height assessments in ramal, condylar and overall posterior mandibular vertical height. In a subsequent study, Habets et al compared asymmetry measurements from lateral tomography and panoramic images of thirty-one patients. They concluded that the relationship of condylar asymmetry with the radiological findings of an Orthopantomogram[®] needed to be further evaluated in studies possessing of a larger patient group.⁹

Kjellberg et al reported good validity when looking at the relative size of the condyle in relation to the ramus height on panoramic images.¹⁰ Mattila et al further attempted to develop and refine a method to quantitatively establish ramus and condyle heights. The method incorporated tangential lines of the condylar head, sigmoid notch and lower border of the mandible to establish condyle and ramal heights for posterior vertical measurement. Using this method in addition to the application of Habets et al formula, the authors felt they were able to successfully evaluate asymmetries.⁵ Miller and Bodner also used Habets et al formula to correlate asymmetry with age and reported that condylar asymmetry was successfully determined from panoramic radiographs but had no correlation to patient's age.⁷ Another study using skeletal pattern as a variable attempted to determine the affects of skeletal pattern on measurement of condylar asymmetry of panoramic radiographs.¹¹ The author concluded that individual condylar and ramal measurements were unaffected by varying ANB, but combined condylar plus ramus was affected.

Some authors refute the idea that symmetry measurements can routinely be conducted on panoramic radiographs. Larheim states that horizontal variables are clearly more unreliable.¹² Boratto et al conducted a study using 100 human dry skulls to assess condylar and mandibular asymmetry and concluded that there was a lack of correlation between the anatomical and radiological measurement of asymmetry. The authors did however feel that the lack of correlation was likely due to change in head position between actual and radiographic measurement techniques.³ Turp et al also reported low correlation between left and right condyles and rami heights when comparing measurements of panoramic images to 25 macerated skulls.⁶ In a more contemporary study, there was an attempt to determine error in linear measurements from panoramic radiographs. Laster et al conducted the study using panoramic radiographs of 30 dry human skulls whereby the examiners measured horizontal lengths as well as vertical posterior lengths on the radiographed mandible while the skulls were positioned in “ideal, shifted and rotated positions”. They reported the greatest differences were in horizontal and shifted skull positions and that accuracy for detecting asymmetry from panoramic images was 67%, 70% and 47% for ideal, rotated and shifted skull positions respectively. They also concluded that panoramic radiographs should be used with caution when making absolute measurements or relative comparisons.¹³

In a very recent study, Kambylafkas et al using full profile laminographs as the gold standard found that total ramal height was reliable in diagnosing vertical asymmetry with some under diagnosis, but condylar height was unreliable. The

reported mean difference between the two images was 2.23% for total height and 11.9% for condyle height.⁸

Although various studies on linear measurements from panoramic images, most have focused on either linear or vertical measures, the aim of this study was to assess accuracy of oblique, horizontal and vertical linear distances of landmark to landmark locations made on digital panoramic radiographs of known asymmetric synthetic mandibles. A further aim was to assess the validity of linear measurements from digital panoramic for quantifying known mandibular asymmetries.

4.3 Materials and Methods

4.3.1 Data Acquisition

One symmetric and five asymmetric synthetic mandibles, as seen in Figure 4-1, were designed and fabricated using fused deposition modeling (FDM), also known as stereolithic modeling (SL), by means of rapid prototyping (StratasysTM FDM 8000, Eden Prairie, MA, USA) as per the methodology described in chapter 2 of this thesis. The five asymmetric mandibles were designed with asymmetry in either the condylar, ramal or body regions of the mandible. The mandibles were constructed such that the asymmetry was on the left side while the right half of the mandible remained unchanged to allow for comparison of the sides of each test subject. The mandibles consisted of one of each:

- A. Symmetric mandible
- B. 9mm vertical condylar asymmetry
- C. Complex condylar consisting of a 9mm vertical plus 6mm lateral asymmetry
- D. 9mm anteroposterior body asymmetry

E. 9mm vertical ramus asymmetry

F. Complex ramal with a 9mm vertical plus a 6mm lateral asymmetry.

Each mandible was coated with a custom radio opaque paint and landmarked using 1.588 mm, stainless steel grade100 balls (Small Parts Inc, Miami Lakes, FL, USA).

Figure 4-2 depicts the location and Table 4-1 describes the landmark points measured.

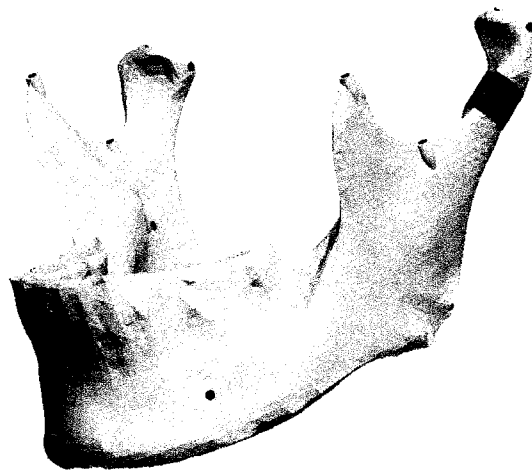


Figure 4-1: Example of Asymmetric Synthetic Mandible from Fused Deposition Modeling (FDM) Process

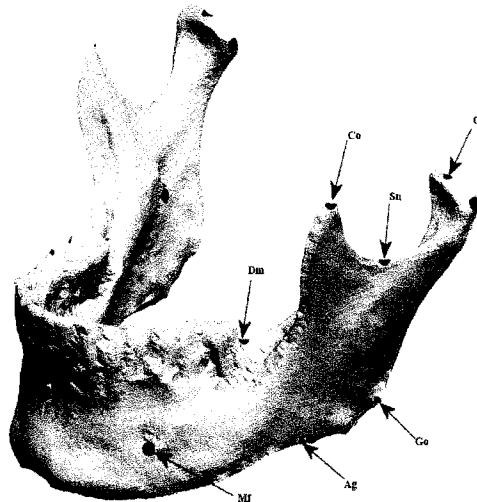


Figure 4-2: Landmark locations and description for Synthetic mandibles

Table 4-1: Landmark anatomical description

Landmark	Description
Mf	Mental Foramen
Ag	Depth of Antigonial Notch
Go	Anthropometric Gonion
Cs	Superior Point of Condyle
Sn	Depth of Sigmoid Notch
Co	Tip of Coronoid Process
Dm	Distal of Molar at Gingiva

To create the experimental model, each synthetic mandible was attached to a human dry skull base with a custom fit inter-occlusal splint. The splint acted to hold the maxilla and series of synthetic mandibles in a secure and reproducible position throughout the experiment. The condyle was seated into the glenoid fossa by creating a uniform 3mm thick disc in the joint space using Regisil® (Dentsply, York, PA, USA) bite registration material. The skull and positioned mandibles were mounted onto an OT-S28V camera tripod (Opus®, On, Canada) using a custom designed mounting assembly. Each of the six experimental models were positioned into a Kodak 8000 Digital Panoramic System (Kodak, USA) and imaged in random order 35 times per model to a total of 210 acquired images. The models were each imaged 35 times to generate an adequate sample size for each range of asymmetry tested. Each model was positioned into the unit by precisely following the manufacturer's instructions which included centering the midsagittal plane of the skull by utilizing the frontal optical positioning guides and vertically by placing the skull into the machine in a clinically relevant position whereby the Frankfort horizontal plane was parallel to the floor.

Figure 4-3 shows an experimental model positioned into the panoramic unit for imaging.

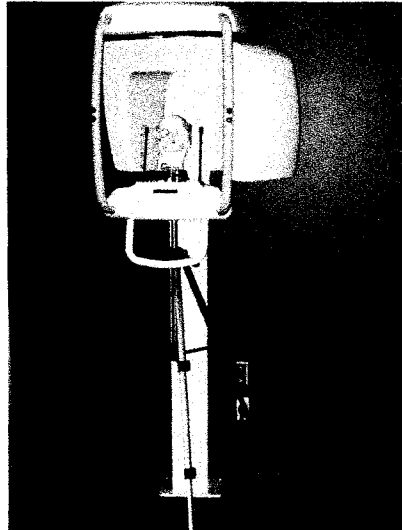


Figure 4-3: Experimental model positioned into the panoramic unit for imaging

Figure 4-4 is an example of an image obtained by the digital panoramic unit from which the linear measurements were gathered and evaluated. The digital panoramic radiographic images were stored as a tagged image file format (TIFF) and the subsequent linear measurements were conducted using the web based measurement software Image J (NIH Image, Maryland, MA, USA, <http://rsb.info.nih.gov/ij/index.html>).

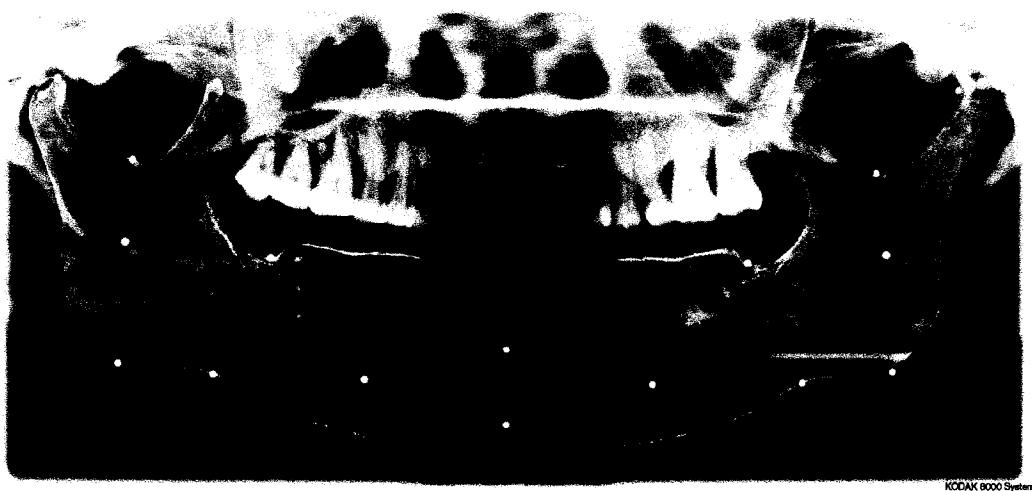


Figure 4-4: Example of tagged image file format (TIFF) obtained from the panoramic unit

Image measurements were performed on the digital radiographs in an effort to define asymmetry. The evaluation process was divided into two sections. The first section of the study was designed to compare the linear measurements of the panoramic images to a gold standard. In this case, a NewTom[®] 3G cone beam volumetric scanner (CBCT) (Aperio Services LLC Sarasota, FL, USA) was used to obtain 3-D images of the synthetic mandibles and measurements with Amira[™] (Advanced 3-D Visualization and Volume Modeling, Berlin Germany) software determined true linear measurements. The measurements from this technique were used as the gold standard. Left and right side measurements of the symmetric mandible (model A) were gathered to assess model accuracy. The remaining models (B through F) were subject to left side measurements only as they were expected to possess the same right side linear measurements as model A due to the right side remaining unchanged throughout the experiment. The gold standard (true) measurements of left and right sides for model A and left sides for models B through F were then compared to the equivalent panoramic linear measurements for magnification. Table 4-2 is a summary of the average true linear measurements for each synthetic mandible in millimeters obtained from the CBCT and Amira[™] evaluation. The average was obtained by imaging once and measuring three times on three separate occasions at least one week apart.

Table 4-2: True linear measurements in millimeters (std. dev.) from CBCT (n=3)

Mandible	Mf-Ag L	Mf-Sn L	Mf-Cs L	Ag-Sn L	Ag-Cs L	Sn-Cs L
A	33.69 (.11)	68.70 (.06)	92.60 (.11)	48.30 (.18)	71.60 (.13)	24.60 (.31)
B	34.61 (.20)	71.41 (.11)	102.80(.06)	49.60 (.07)	80.50 (.08)	33.20 (.15)
C	35.59 (.13)	70.50 (.26)	99.81 (.13)	49.10 (.17)	76.40 (.14)	29.90 (.08)
D	44.12 (.24)	77.50 (.19)	101.20(.09)	48.90 (.12)	70.90 (.21)	24.10 (.24)
E	34.60 (.33)	76.59 (.16)	101.10(.19)	58.00 (.21)	80.60 (.16)	25.60 (.16)
F	36.50 (.17)	75.50 (.12)	98.90 (.14)	55.70 (.32)	76.80 (.18)	24.20 (.23)

The second section compared anatomic right side (symmetric) and left side (asymmetric) measurements for each of the panoramic images. The measurements were established from center point to center point of each of the landmarks and the results were recorded in millimeters on an excel spreadsheet. All measurements were carried out by the principal investigator (SR) and were randomly collected by selecting each image independent of the rest and measuring that image once. Measurement error was determined using Intraclass coefficient analysis in SPSS (SPSS, 14.0 LEAD Technologies Inc., USA). Table 4-3 summarizes the average linear measurement (in millimeters) obtained from the 210 total TIFF digital radiographs with standard deviations for each experimental model of the six synthetic mandibles.

Table 4-3: Average linear measurements in millimeters (std. dev.) for models from panoramic images (n=35)

Length	Model A	Model B	Model C	Model D	Model E	Model F
Mf-AgL	38.56 (.26)	37.79 (.24)	40.45 (.30)	48.52 (.32)	38.26 (.29)	41.62 (.23)
Mf-AgR	38.62 (.24)	38.86 (.26)	38.85 (.19)	39.79 (.27)	38.34 (.24)	38.39 (.29)
Mf-SnL	79.92 (.32)	77.75 (.27)	79.72 (.30)	84.6 (.28)	86.35 (.20)	84.60 (.24)
Mf-SnR	79.95 (.30)	81.46 (.32)	81.53 (.35)	81.59 (.32)	80.56 (.24)	80.21 (.30)
Mf-CsL	106.77(.27)	112.17 (.29)	110.58(.27)	110.47(.26)	113.04 (.24)	110.84 (.25)
Mf-CSR	107.98(.37)	109.70 (.34)	109.31(.31)	109.94(.32)	108.13 (.29)	107.50 (.29)
Ag-SnL	57.24 (.21)	56.33 (.17)	56.42 (.15)	55.25 (.15)	66.82 (.18)	62.58 (.19)
Ag-SnR	57.28 (.21)	58.27 (.12)	58.91 (.15)	57.40 (.15)	57.95 (.16)	58.12 (.15)
Ag-CsL	83.00 (.23)	89.64 (.14)	86.63 (.20)	80.14 (.24)	91.74 (.27)	87.24 (.24)
Ag-CsR	83.53 (.22)	85.10 (.19)	85.44 (.21)	84.48 (.18)	84.22 (.20)	84.14 (.30)
Sn-CsL	26.94 (.19)	34.61 (.13)	31.30 (.18)	26.19 (.19)	26.66 (.19)	26.21 (.17)
Sn-CsR	27.52 (.16)	28.26 (.12)	27.81 (.17)	28.43 (.14)	27.60 (.17)	27.39 (.18)

4.3.2 Panoramic Image to True Length (CBCT) Comparison

The left side horizontal (Mf-Ag), oblique (Mf-Sn, Mf-Cs) and vertical (Ag-Sn, Ag-Cs and Sn-CS) lengths were identified and measured for true distance to a total of three times on separate occasions one week apart by a co-researcher (ML) using the CBCT and the Amira™ software program. Each set of three measurements on the six lengths were averaged and the average distance obtained was recorded as the true linear distance for each length studied on the synthetic models. The same six linear measurements were collected for both the left and right sides on each of the 35 TIFF digital radiographic images obtained per model (Table 4-2).

Comparison of the panoramic to true lengths was carried out in two segments. The first segment compared the amount of magnification between panoramic and true linear measurements on both left and right sides using the symmetric model A with the following magnification calculations.

$$\textit{Equation 4-1: Magnification Left} = \left| \frac{(PanL)}{(NewTomL)} \right|$$

and

$$\textit{Equation 4-2: Magnification Right} = \left| \frac{(PanR)}{(NewTomR)} \right|$$

The left true to left panoramic and right true to right panoramic image magnifications for model A were subsequently exposed to statistical analysis using a one sample t-test using SPSS.

The second segment compared the magnification between panoramic and true linear measurements of the left side only for the remaining asymmetric models (models

B through F). The right side for the remaining models remained unaltered throughout the experiment, thus no further comparisons were made following analysis of model A.

For models B through F, the magnification factor of left side panoramic linear distances to left side true linear distances were calculated using the following formula.

$$\text{Equation 4-3: Magnification Left} = \left| \frac{(PanL)}{(NewTomL)} \right|$$

The left panoramic to left true magnifications were subsequently exposed to statistical analysis using a one sample t-test using SPSS.

To determine overall length disagreement between panoramic and true lengths the mean difference between true lengths and panoramic lengths were established. The percent difference for true left-right measurements was established using right side of model A to left side of the remaining models as right side was unchanged throughout the experiment. The mean differences were expressed as an absolute value of percent disagreement using the following formula:

$$\text{Equation 4-4: Mean Disagreement} = \left| \overline{\Delta\%Pan_{A-F}} - \overline{\Delta\%True_A} \right|$$

Where $\overline{\Delta\%Pan_{A-F}}$ is defined as the average sum of percent differences between left and right sides measurements of the panoramic images for each of the models A through F and where $\overline{\Delta\%True_A}$ is average sum of the percent differences between left and right side measurements of the true model lengths for model A. The disagreement was recorded as an absolute value. The mean disagreement was further exposed to statistical analysis using a one sample t-test using SPSS.

4.3.3 Panoramic Image Left to Right Comparison

The left and right panoramic measurements were converted to percent differences for the 35 trials on each of the experimental models A through F. The left-right percent difference calculation was obtained using a version of the formula discussed previously in the literature where % difference was determined by $[(R-L)/(R + L)]$.² The difference between the above formula and the formula used in this project was that the formula in this project represented percent difference based on the actual average difference versus a scaled average distance as was the case in the other experiments:

$$\text{Equation 4-5: Pan Left to Pan Right \% Difference} = \frac{(R - L)}{R}(100)$$

The left-right percent differences were subsequently exposed to statistical analysis using a one sample t-test using SPSS.

4.4 Results

Intraclass correlation coefficient analysis revealed very high repeatability $\approx .99$ for measurements of the panoramic images following a method statistical analysis outlined by Fleiss et al.¹⁴⁻¹⁶

4.4.1 Panoramic Image to True Length (CBCT) Comparison

True linear measurement as a gold standard was established using a CBCT along with Amira™ software. The CBCT and Amira™ software provided true linear distances in millimeters for measurements conducted on the left and right halves of each synthetic mandible for the horizontal, oblique and vertical length measurements. Each

panoramic image measurement was compared to true measurement and recorded as a magnification factor. The magnification factor was subject to a one sample t-test. For the symmetric mandible (model A), the right and left side measures of the panoramic images were compared to the respective true right and left side measurement (CBCT and Amira™). The magnification and millimeter differences were revealed and noted in Table4-4.

Table 4-4: Magnification (std. dev.) and length differences (mm) for model A between panoramic and true by side (n=35)

Length	Right			Left		
	Mag.	P-value	mm difference	Mag.	P-value	mm difference
Mf-Ag	1.15 (.0070)	<.001	-5.01 (.23)	1.14 (.0075)	<.001	-4.85 (.25)
Mf-Sn	1.16 (.0044)	<.001	-10.85 (.30)	1.16 (.0047)	<.001	-11.22 (.32)
Mf-Cs	1.17 (.0042)	<.001	-15.38 (.38)	1.15 (.0029)	<.001	-14.16 (.27)
Ag-Sn	1.18 (.0042)	<.001	-8.87 (.20)	1.19 (.0045)	<.001	-8.94 (.22)
Ag-Cs	1.16 (.0031)	<.001	-11.82 (.22)	1.16 (.0033)	<.001	-11.40 (.23)
Sn-Cs	1.12 (.0061)	<.001	-3.02 (.15)	1.10 (.0080)	<.001	-2.34 (.20)

For model A, the magnification ranges from 1.10 on vertical condyle length Sn-CS on the left to 1.19 for vertical ramus length Ag-Sn on the left with the overall average being 1.15 ± 0.04 . The remaining mandibles representing models B through F also underwent comparison of left side panoramic to left side true (CBCT) for the horizontal, oblique and vertical measurements. The magnification factors and the linear differences between the panoramic images and true left and right measurements revealed a statistically significant difference between all compared measures ($P < .05$). The models ranged in magnification from 1.04 for vertical condyle length Sn-Cs on models B, C and E to 1.15 for vertical ramus length Ag-Sn on models C and E with an overall average of $1.11 \pm .05$ for all models B through F. Again the magnification factor and linear

differences between panoramic image and true left measurements for the models B through F indicated a statistically significant difference between all compared measures (P<.05).

Table 4-5: Magnification (std. dev.) and length differences (mm) for models B through F between panoramic and true left side (n=35)

Model	Length	Magnification	p-value	mm difference
B	Mf-Ag	1.09 (.0068)	<.001	-3.19 (.24)
	Mf-Sn	1.09 (.0039)	<.001	-6.34 (.28)
	Mf-Cs	1.09 (.0029)	<.001	-9.33 (.29)
	Ag-Sn	1.14 (.0031)	<.001	-6.73 (.16)
	Ag-Cs	1.11 (.0017)	<.001	-9.14 (.14)
	Sn-Cs	1.04 (.0041)	<.001	-1.39 (.14)
C	Mf-Ag	1.14 (.0085)	<.001	-4.87 (.30)
	Mf-Sn	1.13 (.0043)	<.001	-9.22 (.30)
	Mf-Cs	1.11 (.0026)	<.001	-10.79 (.26)
	Ag-Sn	1.15 (.0031)	<.001	-7.31 (.15)
	Ag-Cs	1.13 (.0025)	<.001	-10.22 (.23)
	Sn-Cs	1.04 (.0063)	<.001	-1.4 (.19)
D	Mf-Ag	1.10 (.0073)	<.001	-4.42 (.32)
	Mf-Sn	1.09 (.0036)	<.001	-7.11 (.28)
	Mf-Cs	1.09 (.0025)	<.001	-9.27 (.26)
	Ag-Sn	1.13 (.0030)	<.001	-6.33 (.15)
	Ag-Cs	1.13 (.0033)	<.001	-9.24 (.23)
	Sn-Cs	1.09 (.0179)	<.001	-2.09 (.18)
E	Mf-Ag	1.11 (.0084)	<.001	-3.67 (.29)
	Mf-Sn	1.13 (.0025)	<.001	-9.75 (.19)
	Mf-Cs	1.12 (.0023)	<.001	-11.93 (.23)
	Ag-Sn	1.15 (.0030)	<.001	-8.81 (.17)
	Ag-Cs	1.14 (.0032)	<.001	-11.23 (.25)
	Sn-Cs	1.04 (.0076)	<.001	-1.06 (.19)
F	Mf-Ag	1.14 (.0058)	<.001	-5.12 (.21)
	Mf-Sn	1.12 (.0032)	<.001	-9.1 (.23)
	Mf-Cs	1.12 (.0027)	<.001	-11.93 (.26)
	Ag-Sn	1.12 (.0033)	<.001	-6.87 (.18)
	Ag-Cs	1.14 (.0030)	<.001	-10.44 (.23)
	Sn-Cs	1.08 (.0070)	<.001	-2 (.17)

Magnification factor for all cases combined (model A left and right and models B through F left only) averaged 1.12 ± 0.08 . Table 4-5 summarizes the left to left comparisons of the remaining mandibles B through F for magnification as well as millimeter differences.

The mean percent panoramic (left-right differences) were compared to the mean percent left-right differences of the true measurements to determine overall disagreement between panoramic and true lengths. The mean disagreement for horizontal length Mf-Ag was 2.85%. Oblique measures Mf-Sn and Mf-Cs had mean differences of 2.59% and 4.43% respectively. Posterior vertical lengths were calculated as 1.89% for Ag-Sn, 3.72% for Ag-Cs and 6.04% for length Sn-Cs. The average difference for all lengths combined was 3.59%. The mean disagreement between panoramic and linear left-right percent differences revealed a statistically significant difference between all compared measures ($P < .05$) when subject to the one-sample t-test. Table 4-6 summarizes the mean disagreement between panoramic image and true lengths per model.

Table 4-6: Mean disagreement in percent (std. dev.) between panoramic and true lengths

Model	Mf-Ag	Mf-Sn	Mf-Cs	Ag-Sn	Ag-Cs	Sn-Cs
A	0.15 (.56)	0.55 (.39)	1.12 (.29)	0.16 (.32)	0.48 (.31)	1.67 (.87)
B	1.86 (.46)	4.53 (.45)	7.04 (.43)	3.04 (.40)	6.99 (.38)	10.74(1.12)
C	2.01 (.51)	2.22 (.38)	9.3 (.31)	1.44 (.45)	5.32 (.41)	13.06(1.07)
D	7.02 (.60)	6.09 (.41)	5.7 (.29)	2.4 (.40)	5.03 (.35)	6.9 (.79)
E	1.27 (.48)	1.27 (.39)	2.65 (.38)	2.2 (.29)	2.46 (.33)	1.65 (.71)
F	4.77 (.53)	0.87 (.41)	0.76 (.37)	2.08 (.67)	2.05 (.45)	2.22 (.87)
Ave diff	2.85 (2.55)	2.59 (2.24)	4.43 (3.46)	1.89 (.99)	3.72 (2.44)	6.04 (5.00)
p-value	<.001	<.001	<.001	<.001	<.001	<.001

4.4.2 Panoramic Image Left to Right Comparison

The same six linear measurements from each of the left and right sides of the 35 TIFF images of the digital panoramic radiographs obtained on the six experimental models consisting of synthetic mandibles (models A through F) were measured and sequentially compared to one another and recorded as a difference between left and right in Table 4-7. Apart from model A, it was expected that differences would exist and that asymmetry would appear across the measurements that span regions of asymmetry. For example, model B (9mm condylar asymmetry) was anticipated to display asymmetry for each linear measurement that spans from any origin to point Cs. Table 4-7 indicates lengths that would be projected to reveal symmetry or asymmetry based on the location where the asymmetry was designed. For model A, there was no statistical difference ($P>.05$) between left and right measurements of horizontal length Mf-Ag, oblique length Mf-Sn and vertical length Ag-Sn. The remaining measurements revealed a statistical difference ($P<.05$) from left side to right side lengths. There was a statistically significant difference ($P<.05$) for all left to right measures of the panoramic images of model B, model C and model D. Model E revealed a statistical difference ($P<.05$) between the left and right measurements for all six linear measurements with the exception of horizontal linear measurement Mf-Ag which indicated no statistically significant difference ($P>.05$) between left and right. Model F revealed a statistical difference ($P<.05$) between all left and right measurements.

Table 4-7: Left to right percent and millimeter (std. dev.) differences (n=35)

Model	Length	% difference	p-value	mm difference	Expect	Revealed
A	Mf-Ag	.15 (.82)	.294	0.06 (.32)	Symmetry	Symmetry
	Mf-Sn	.03 (.61)	.744	0.03 (.49)	Symmetry	Symmetry
	Mf-Cs	1.12 (.44)	<.001	1.22 (.48)	Symmetry	<i>Asymmetry</i>
	Ag-Sn	.05 (.68)	.649	0.03 (.39)	Symmetry	Symmetry
	Ag-Cs	.62 (.47)	<.001	0.52 (.39)	Symmetry	<i>Asymmetry</i>
	Sn-Cs	2.08 (1.06)	<.001	0.57 (.30)	Symmetry	<i>Asymmetry</i>
B	Mf-Ag	2.79 (1.12)	<.001	1.09 (.44)	Symmetry	<i>Asymmetry</i>
	Mf-Sn	4.56 (.70)	<.001	3.71 (.58)	Symmetry	<i>Asymmetry</i>
	Mf-Cs	-2.21 (0.54)	<.001	-2.43 (.58)	<i>Asymmetry</i>	<i>Asymmetry</i>
	Ag-Sn	3.34 (.39)	<.001	1.94 (.23)	Symmetry	<i>Asymmetry</i>
	Ag-Cs	-5.35 (.32)	<.001	-4.55 (.26)	<i>Asymmetry</i>	<i>Asymmetry</i>
	Sn-Cs	-22.44 (.81)	<.001	-6.34 (.21)	<i>Asymmetry</i>	<i>Asymmetry</i>
C	Mf-Ag	-4.13 (.84)	<.001	-1.61 (.33)	Symmetry	<i>Asymmetry</i>
	Mf-Sn	2.23 (.62)	<.001	1.82 (.51)	Symmetry	<i>Asymmetry</i>
	Mf-Cs	-1.17 (.41)	<.001	-1.28 (.45)	<i>Asymmetry</i>	<i>Asymmetry</i>
	Ag-Sn	4.23 (.46)	<.001	2.49 (.27)	Symmetry	<i>Asymmetry</i>
	Ag-Cs	-1.37 (.40)	<.001	-1.17 (.34)	<i>Asymmetry</i>	<i>Asymmetry</i>
	Sn-Cs	-12.57 (1.07)	<.001	-3.49 (.28)	<i>Asymmetry</i>	<i>Asymmetry</i>
D	Mf-Ag	-22.00 (1.19)	<.001	-8.74 (.43)	<i>Asymmetry</i>	<i>Asymmetry</i>
	Mf-Sn	-3.71 (.60)	<.001	-3.03 (.48)	<i>Asymmetry</i>	<i>Asymmetry</i>
	Mf-Cs	-.49 (.43)	<.001	-0.54 (.47)	<i>Asymmetry</i>	<i>Asymmetry</i>
	Ag-Sn	3.77 (.42)	<.001	2.16 (.25)	Symmetry	<i>Asymmetry</i>
	Ag-Cs	5.13 (.43)	<.001	4.34 (.37)	Symmetry	<i>Asymmetry</i>
	Sn-Cs	7.85 (.95)	<.001	2.23 (.28)	Symmetry	<i>Asymmetry</i>
E	Mf-Ag	.20 (1.17)	.327	0.08 (.45)	Symmetry	Symmetry
	Mf-Sn	-7.18 (.49)	<.001	-5.79 (.38)	<i>Asymmetry</i>	<i>Asymmetry</i>
	Mf-Cs	-4.53 (.46)	<.001	-4.90 (.48)	<i>Asymmetry</i>	<i>Asymmetry</i>
	Ag-Sn	-15.28 (.52)	<.001	-8.86 (.28)	<i>Asymmetry</i>	<i>Asymmetry</i>
	Ag-Cs	-8.94 (.48)	<.001	-7.53 (.39)	<i>Asymmetry</i>	<i>Asymmetry</i>
	Sn-Cs	3.40 (1.04)	<.001	0.94 (.29)	Symmetry	<i>Asymmetry</i>
F	Mf-Ag	-8.40 (1.13)	<.001	-3.22 (.41)	Symmetry	<i>Asymmetry</i>
	Mf-Sn	-5.48 (.55)	<.001	-4.39 (.43)	<i>Asymmetry</i>	<i>Asymmetry</i>
	Mf-Cs	-3.10 (.43)	<.001	-3.34 (.45)	<i>Asymmetry</i>	<i>Asymmetry</i>
	Ag-Sn	-7.67 (.51)	<.001	-4.46 (.29)	<i>Asymmetry</i>	<i>Asymmetry</i>
	Ag-Cs	-3.69 (.56)	<.001	-3.10 (.46)	<i>Asymmetry</i>	<i>Asymmetry</i>
	Sn-Cs	4.34 (1.12)	<.001	1.19 (.31)	Symmetry	<i>Asymmetry</i>

The total range of percent difference across all of the models and all of the lengths studied went from -0.03% in oblique length Mf-Sn of model A to -22.44% for vertical length Sn-Cs on model B (Table 4-6). A negative percentage score indicated that the left hand side measurement was of greater length than the equivalent right side measurement while the opposite was true for positive percentages. Considering the horizontal measurement Mf-Ag, the overall percent difference ranged from 0.15% in model A to -22.00% in model D. The oblique linear measurements Mf-Sn and Mf-CS were as follows. Length Mf-Sn fell between -0.03% in model A to -7.18% in Model E and length Mf-Cs went from -0.49% in model D to -4.53% for model E. Measurements Ag-Sn, Ag-Cs and Sn-Cs were of vertical mandible height and focused on the posterior mandible. Percent difference for length Ag-Sn ranged from 0.05% in model A to -15.28% in model E. Vertical measurement Ag-Cs went from 0.62% in model A to -8.94% in model E. Finally, measurement Sn-CS ranged from 2.08% in model A to -22.44% in model B.

4.5 Discussion

The purpose of this study was to assess mandibular asymmetry using various linear measurements of point to point landmark lengths on digital panoramic images. As a method to assess for model accuracy and validate the measurement technique, comparison of panoramic lengths to true values were established. Measurement of six linear distances (horizontal, oblique and vertical) between left and right sides of digital panoramic radiographs were compared to one another, expressed as a percentage and statistically analyzed.

4.5.1 Panoramic Length to True Length Measurements

Model accuracy and image magnification factors were established accepting the NewTom[®] 3G (CBCT) and Amira[™] software as the gold standard of measurement for this project. The CBCT and Amira[™] software were previously reported to measure distances in millimeters with an accuracy of 0.6mm with a measurement error between 0.2 and 0.3mm.¹⁷ This value was suitable for measurements made on stereolithic (STL) models and compared very well with values reported by Choi et al who noted error 0.62 +/- 0.35 mm for comparing linear distances between human and STL replicated skulls.¹⁸ Synthetic mandible A revealed symmetry with an average left to right difference of 0.13mm (± 0.40 mm) as measured by Amira[™]. The difference converts to an accuracy of 99.29 -99.77% in symmetry between left and right sides. This range of accuracy in replication also compared well with the 97.7-99.12% dimensional accuracy of STL models reported by Barker et al when they analyzed certain linear measurements.¹⁹ Both left and right measurements were conducted for mandible A (symmetric mandible) whereas left only (asymmetric side) measurements were made on remaining mandibles B through F. From the accuracy determined on measurements of model A, it was determined that all remaining true measurements possessed accuracy in excess of 99%.

For comparison of the true to panoramic measurements, the differences were expressed as both magnification and millimeter differences (tables 4-4 and 4-5) and were further compared for mean disagreement (Table 4-6). The CBCT (true) measurements were consistently smaller than the panoramic measurements as noted by negative millimeter values. The difference between the panoramic image and true measurements was considered a magnification factor which was recorded as a unit free

absolute value. The measurement differences revealed object distortion with larger magnification in some lengths than others with a pooled magnification of $1.12 \pm .04$ (combined for all models). From this range in magnification, it is evident that there was distortion that brings into question the clinical significance of image for judging asymmetry. Despite the various ranges of measurements and subsequent magnifications, the results compared well with other studies²⁰⁻²² and were lower than the reported 1.27 magnification noted in the manufacturer's specifications (www.kodak.com). In 1998, Catic et al demonstrated a consistent amount of magnification for vertical, horizontal and oblique measurements providing that the measurements were all conducted on one side of the mandible and that it was possible to precisely measure any vertical, horizontal and oblique distances on that side.²¹ Scarfe et al also reported a range of magnification where vertical spanned from 1.27 to 1.37 and horizontal was from 1.01 to 1.63.²⁰ In a study looking into implant dentistry, Frei et al calculated a vertical magnification factor of $1.27 \pm .01$. No mention of horizontal magnification was made.²² This reduction in magnification factor from manufacturer's recommendation and overall decrease from other reports may have been a result of proper and consistent head positioning within the unit. It was evident from the low standard deviations among repeated measured (Table 4-2) that there were no large variations due to head positioning errors on the panoramic radiographs.

From a clinical perspective using an average magnification value may give the observer an overall feel for different landmark to landmark lengths but a true determination or actual measurement should not be relied on due to the variations in magnification and distortion noted from each length to length assessment on the models.

Over or underestimation of true length would be the direct result of measuring lengths from panoramic radiographs and applying a magnification factor, but the amount is variable based on the amount of magnification for the region being measured. As an example, when looking at unilateral measurements of symmetric model A from Table 4-4, condyle length Sn-Cs has considerably less magnification (1.12-right and 1.10-left) than does the posterior vertical length Ag-Cs (1.18-right and 1.19-left). This difference in magnification would indicate that there is something different in the condyle region that exasperates the level of distortion. The greatest amount of magnification occurred in the posterior vertical height, in particular ramus height on length Ag-Sn at 1.15 ± 0.02 indicating a high level of distortion. The least amount of magnification and therefore lower distortion amounts for this unit were in the condylar height measurement Sn-Cs with 1.07 ± 0.03 magnifications. Fluctuation of magnification within various regions of the panoramic unit makes determining true linear measurements very difficult and is therefore not advisable.

Habets et al previously reported that differences between left and right side measurements of less than 6% were due to inherent machine error.² Kambylafkas et al also used the 6% cutoff as the threshold of clinical significance in their experiment despite finding a maximum disagreement for total ramus height to be 5.38%.⁸ Based on previous studies and the average mean disagreement between the true left-right and the panoramic left-right being 3.59% with the highest being 6.04% (Table 4-6), the 6% cutoff was used for all oblique, horizontal and vertical linear measurements for determining measurable mandibular asymmetry. It is worth noting that variation in formulas used between Habets et al $[(R-L)/(R+L)]$, Kambylafkas et al $[(R-L)/(R+L)/2]$

and in this project [(R-L)/R] reveal slight variations in reported “errors” of 6%, 5.38% and 6.04% respectively.

4.5.2 Panoramic Image Left to Right Comparison

Panoramic left to right side differences were compared on all models in an attempt to determine which lengths were best suited to describe the known asymmetries. It was calculated that the overall left to right percent difference among expected symmetric lengths (Table 4-7) was 3.07% with some variability among the models. This value compares well with the average mean disagreement of 3.59%. The difference is likely accounted for by a combination of fabrication error, positioning error, inherent machine error and measurement error. From this it can be stated that there was an overall range of error in data acquisition of 3.07-3.59%. This number is higher but still comparable to the 2.1% inherent machine error reported by Kambylafkas et al⁸ and much less than the 6% reported by Habets et al.² The higher value for this project compared to Kambylafkas et al was due to combining all sources of error as well as pooling all length measurements. When looking specifically at mean disagreement of ramus height for this project, the 1.89% (Table 4-6) difference compares nicely to the 2.23% total height asymmetry Kambylafkas et al reported for mean disagreement from their gold standard (laminograph).⁸

When looking at the models individually, using the 6% cutoff to determine measurement asymmetry, the following observations were made from the values reported in Table 4-7. Only linear measurements directly crossing areas of asymmetries were expected to reveal asymmetry between left and right. Negative percentages indicate that the left side of the model was larger than the right side for each observed

length. Model A was designed to be a symmetric model with no inherent asymmetry fabricated into the mandible. Despite the fact that there was a statistically significant difference for left to right lengths Mf-Cs and Sn-Cs, comparison of linear measurements from the digital panoramic radiographs all fell well below the 6% cutoff range indicating symmetry for this model.

Model B was designed and fabricated with a 9mm vertical condylar asymmetry. It was expected that oblique measurement Mf-Cs and vertical measurements Ag-CS and Sn-Cs would reveal measurement asymmetries. Although they revealed a statistical asymmetry, they failed to demonstrate an asymmetry in excess of the 6% cutoff. Vertical measurement Sn-Cs, the shortest point to point across the asymmetric area, expressed an asymmetry of -22.44% representing a measurement asymmetry in the condylar region. All other lengths (Mf-Ag, Mf-Sn and Ag-Sn), as expected, revealed symmetry as they did not span the region of asymmetry.

For Model C, a complex condylar asymmetry with 9mm vertical and 6mm lateral (horizontal) movement of the condylar head was designed and fabricated into the model. Again, oblique length Mf-Cs and vertical lengths Ag-Cs and Sn-CS were expected to provide asymmetries in excess of the 6% cutoff. In this case, Mf-Cs and Ag-Cs again reported statistically significant asymmetry but both fell under the 6% cutoff. As in the last case, all other lengths (Mf-Ag, Mf-Sn and Ag-Sn), revealed symmetry as they did not span the region of asymmetry. Again vertical length Sn-Cs, the shortest point to point across the asymmetric area, indicated a measured asymmetry at -12.57%. It should be noted that the amount of asymmetry decreased as the condylar head was repositioned in a more lateral direction with the 6mm lateral offset.

Model D was developed and produced with a 9mm anteroposterior body asymmetry in a horizontal direction. Horizontal measurement Mf-Ag and oblique lengths Mf-Sn and Mf-Cs spanned the asymmetric area and were expected to display more than 6% asymmetry. Horizontal measurement Mf-Ag, the length measuring the shortest point to point distance across the body asymmetry and in the direction of the asymmetry, indicated a -22.00% asymmetry while the remaining two measures failed to provide measurement confirmation. Interestingly, vertical length Sn-Cs indicated an asymmetry of 7.85% indicating a longer right side measurement despite the assumption that it would remain symmetric as it did not cross the region of asymmetry. This anomaly may be a result of displacing the opposing condyle near to or out of the panoramic machine's focal trough.

Model E was designed and fabricated with a 9mm ramus asymmetry in a straight vertical direction. Oblique (Mf-Sn and Mf-Cs) and Vertical (Ag-Sn and Ag-Cs) measurements were of interest for providing asymmetries greater than 6%. Oblique length Mf-Sn reported asymmetry at -7.18% while Mf-Cs did not despite revealing a statistical asymmetry. Both vertical lengths indicated asymmetry with Ag-Sn being the shortest point to point distance across the asymmetry, at -15.28% followed by Ag-Cs at -8.94%.

Finally, model F was designed as a complex ramal asymmetry with 9mm vertical and 6mm lateral (horizontal) asymmetry. The same oblique (Mf-Sn and Mf-Cs) as well as the same vertical (Ag-Sn and Ag-Cs) were lengths of expected asymmetry. All measurements with one exception failed to produce measurement asymmetries over 6% despite their statistically significant differences. The only measurement to indicate

asymmetry was Ag-Sn, also measuring from the points closest to and directly across the region of asymmetry, displayed an asymmetry of -7.67%. Horizontal length Mf-Ag indicated asymmetry of -8.40% indicating a longer left side measurement despite the assumption that it would remain symmetric as it did not cross the region of asymmetry. This anomaly may also be a result of displacing one of the landmarks near to or out of the panoramic machine's focal trough. As was the case for model C, as the condyle becomes repositioned more laterally, the amount of clinical asymmetry also decreases.

When looking only at the shortest point to point measurement by model, and factoring the average magnification factor for that measurement, there was a general pattern toward under-sizing the clinical length of the measurement with a few exceptions. Length Sn-Cs for model B revealed 22.44% possessing a 6.34mm length difference between left and right sides with the left being longer. Considering the magnification factor for this model and length of 1.04 from table 4-8, the corrected value for this length was calculated to be -6.59mm. This value is roughly 27% shorter than the true 9mm constructed into the model. Employing the same rationale and calculations, length Sn-Cs for model C was 60% shorter than the true value. In this model the condyle underwent a vertical as well as lateral shift. Model F, also containing a lateral shift of the condyle due to a 9mm vertical and 6mm lateral asymmetry in the ramal region indicated that length Ag-Sn was roughly 50% of the true asymmetry value. The exceptions were for Model E, possessing a 9mm vertical ramus difference, displaying a 2% over-sizing for length Ag-Sn and the single horizontal measurement length Mf-Ag on model D revealing an over-sizing of length Mf-Ag of roughly 7% greater than the true value for the length. The differences in amounts of magnification

and varying measurements as the condyles were moved laterally as in models C and F indicate that distortion plays a major role in complex asymmetries.

4.6 Conclusion

From a magnification and distortion perspective, linear measurements can be made, with caution, by applying a 1.12X magnification factor at least for this panoramic unit. The actual length will be roughly 83% of the measured length in nearly all regions of the panoramic image with less magnification in the condyle region.

Horizontal measurements can be used to describe asymmetries for anteroposterior mandibular body asymmetries but were found to over-describe the asymmetry by roughly 7%. Caution must be used with this measurement as asymmetry was noted in this region when none was expected when a complex ramus asymmetry was present.

Vertical measurements can be used to describe vertical asymmetries. Straight vertical and complex condylar asymmetries were best described using sigmoid notch to superior condyle landmarks but underestimated the asymmetry by 27% for straight and 60% for complex asymmetries. Vertical ramus asymmetries were best described when measured from antgonial notch to sigmoid notch with an underestimation of 50% for complex ramus and overestimation of 2% for straight vertical asymmetry. Distortion causing further underestimation of asymmetry occurred in complex asymmetry cases, which were those that translated the condyle laterally.

The most accurate measurement for assessing mandibular asymmetry was measuring a straight vertical ramus asymmetry from antgonial notch to sigmoid notch.

Much caution is advised using all other measurements and measuring all other forms of asymmetry due to the highly variable degree of distortion and magnifications.

References

1. Alpern MC. Analysis of panoramic cephalometrics using skeletal cephalostat. *Angle Orthod* 1979;49:110-20.
2. Habets LL, Bezuur JN, van Ooij CP, Hansson TL. The orthopantomogram, an aid in diagnosis of temporomandibular joint problems. I. The factor of vertical magnification. *J Oral Rehabil* 1987;14:475-480.
3. Boratto R, Gambardella U, Micheletti P, Pagliani L, Preda L, Hansson TL. Condylar-mandibular asymmetry, a reality. *Bull Group Int Rech Sci Stomatol Odontol* 2002;44:52-56.
4. Habets LL, Bezuur JN, Naeiji M, Hansson TL. The Orthopantomogram, an aid in diagnosis of temporomandibular joint problems. II. The vertical symmetry. *J Oral Rehabil* 1988;15:465-471.
5. Mattila M, Kononen M, Mattila K. Vertical asymmetry of the mandibular ramus and condylar heights measured with a new method from dental panoramic radiographs in patients with psoriatic arthritis. *J Oral Rehabil* 1995;22:741-745.
6. Turp JC, Vach W, Harbich K, Alt KW, Strub JR. Determining mandibular condyle and ramus height with the help of an Orthopantomogram--a valid method? *J Oral Rehabil* 1996;23:395-400.
7. Miller VJ, Bodner L. Condylar asymmetry measurements in patients with an Angle's Class III malocclusion. *J Oral Rehabil* 1997;24:247-249.
8. Kambylafkas P, Murdoch K, Gilda E, Tallents R, Kyrkanides S. Validity of Panoramic Radiographs for Measuring Mandibular Asymmetry. *Angle Orthod* 2006;76:388-393.
9. Habets LL, Bezuur JN, Jimenez Lopez V, Hansson TL. The OPG: an aid in TMJ diagnostics. III. A comparison between lateral tomography and dental rotational panoramic radiography (Orthopantomography). *J Oral Rehabil* 1989;16:401-406.
10. Kjellberg H, Ekestubbe A, Kiliaridis S, Thilander B. Condylar height on panoramic radiographs. A methodologic study with a clinical application. *Acta Odontol Scand* 1994;52:43-50.
11. Saglam AM. The condylar asymmetry measurements in different skeletal patterns. *J Oral Rehabil* 2003;30:738-742.
12. Larheim TA, Svanaes DB. Reproducibility of rotational panoramic radiography: mandibular linear dimensions and angles. *Am J Orthod Dentofacial Orthop* 1986;90:45-51.

13. Laster WS, Ludlow JB, Bailey LJ, Hershey HG. Accuracy of measurements of mandibular anatomy and prediction of asymmetry in panoramic radiographic images. *Dentomaxillofac Radiol* 2005;34:343-349.
14. Fleiss JL, Mann J, Paik M, Goultchin J, Chilton NW. A study of inter- and intra-examiner reliability of pocket depth and attachment level. *J Periodontal Res* 1991;26:122-128.
15. Fleiss JL, Slakter MJ, Fischman SL, Park MH, Chilton NW. Inter-examiner reliability in caries trials. *J Dent Res* 1979;58:604-609.
16. Fleiss JL, Fischman SL, Chilton NW, Park MH. Reliability of discrete measurements in caries trials. *Caries Res* 1979;13:23-31.
17. Lagravère. Accuracy of Three Dimensional images obtained from a Cone-Beam Computerized Tomographer. Edmonton, Alberta; 2006: p. 15.
18. Choi JY, Choi JH, Kim NK, Kim Y, Lee JK, Kim MK et al. Analysis of errors in medical rapid prototyping models. *Int J Oral Maxillofac Surg* 2002;31:23-32.
19. Barker TM, Earwaker WJ, Lisle DA. Accuracy of stereolithographic models of human anatomy. *Australas Radiol* 1994;38:106-111.
20. Scarfe WC, Eraso FE, Farman AG. Characteristics of the Orthopantomograph OP 100. *Dentomaxillofac Radiol* 1998;27:51-57.
21. Catic A, Celebic A, Valentic-Peruzovic M, Catovic A, Jerolimov V, Muretic I. Evaluation of the precision of dimensional measurements of the mandible on panoramic radiographs. *Oral Surg Oral Med Oral Pathol Oral Radiol Endod* 1998;86:242-248.
22. Frei C, Buser D, Dula K. Study on the necessity for cross-section imaging of the posterior mandible for treatment planning of standard cases in implant dentistry. *Clin Oral Implants Res* 2004;15:490-497.

Chapter 5 - The Accuracy of Digital Panoramic Unit for Mandibular Angular Measurements (Paper 4)

5.1 Abstract

Background: The use of angular measurements from panoramic images to evaluate asymmetry has been discussed very infrequently throughout the orthodontic literature. The aim of this study was to examine various angular measurements taken from digital panoramic images and describe their ability for describing known asymmetries. **Methods:** A total of 210 Digital panoramic radiographs (Kodak 8000, Kodak USA) were acquired on six experimental models (dry skull base with an asymmetric synthetic mandible). Each experimental model was designed using a previously fabricated synthetic mandible of known asymmetry ranging from 0 to 9mm in the condylar, ramal and body regions of the mandible. Angular measurements (Image J, USA) were gathered across the ramal, condylar and body asymmetries which were subsequently compared to the actual known mandibular asymmetries measured (Newtom-3G, Italy and AmiraTM software, Germany) from the synthetic mandibles. **Results:** Some mandibular asymmetries were revealed when measuring angles on digital panoramic images. **Conclusions:** With caution, Vertical posterior asymmetries can be determined by bilaterally comparing angles between the sigmoid notch, the superior point of the condyle and the antgonial notch with the vertex being superior condyle. Anteroposterior body asymmetries may be analyzed looking at bilateral angles between mental foramen sigmoid notch (or superior condyle) and antgonial notch with the vertex being either superior condyle or sigmoid notch.

5.2 Introduction

Since the inception of dental radiography clinicians have been studying, testing and challenging the qualities and techniques of the various instruments employed for imaging along with testing the interpretive value of the images in an attempt to maximize their diagnostic value. The usefulness of panoramic radiography for measurements of asymmetry among bilateral structures has been of primary interest to many authors.¹⁻⁶ Most of the research conducted by these investigators has contemplated linear measurements. There has been considerably less research involving angular measurements of panoramic images for the same purpose. Some of the work dealing with angular measurements has focused on tooth position as is the case with impacted cuspids⁷ and third molars.⁸ Early studies indicated that angular measurements from panoramic images could be obtained with some mathematical correction.⁹ More recent research deals with dental alignment by assessing tooth position and tooth angulation.¹⁰⁻¹² For the most part, these comparisons were made to adjacent structures and reference lines versus bilateral comparisons. Akcam et al looked at possible links between cephalometric and panoramic angles.¹³

Despite the abundant use of panoramic radiology in clinical orthodontic practice few studies involved the use of angular measurement in an attempt to describe asymmetry. One author reported that panoramic film angles were almost identical to those measured on the dry mandible when assessing the gonial angle.¹⁴ Another author noted that there was no difference in accuracy of angular measurements of teeth when observed on panoramic images when comparing to lateral oblique projections.¹⁵ Kubota et al further support the use of panoramic images for determining asymmetries.¹⁶

Akcam et al. investigated the possibility of using panoramic radiography as a prediction tool for cephalometric measurements by looking at various linear and angular measurements on panoramic radiographs.¹³ A unique study described the use of panoramic images for comparison of left and right side changes using two angular measurements following distraction osteogenesis.¹⁷

In view of the relative lack of available literature, the aim of this study was to assess accuracy of various angular measurements of landmark to landmark to landmark locations made on digital panoramic radiographs of known asymmetric synthetic mandibles. A further aim was to assess the validity of angular measurements from digital panoramic for quantifying known mandibular asymmetries.

5.3 Materials and Methods

5.3.1 Data Acquisition

Fused deposition Modeling (FDM) by means of rapid prototyping (Stratasys™ FDM 8000, Eden Prairie, MA, USA) was employed to construct a series of six synthetic mandibles (mandibles A, B, C, D, E and F) using a procedure described in chapter 2 of this thesis. Of the six synthetic mandibles, one (mandible A) was designed to be symmetric between the left and right sides when considering the halves of the mandible and was split through the chin point extending between the position of lower central incisors. All remaining mandibles (B through F) were fabricated with an asymmetry fabricated into the left half of the mandible. Mandible B possessed a vertical asymmetry of 9mm in the left condylar neck while mandible C was constructed with a 9mm vertical and 6mm horizontal asymmetry in the condylar neck forming a complex asymmetry. Mandible D consisted of a 9mm anteroposterior asymmetry in the

body of the mandible. Mandible E was designed with asymmetry in the ramus of the model of 9mm vertical. Finally, mandible F possessed a 9mm vertical with 6mm lateral horizontal asymmetry. To summarize the models used:

- A. Symmetric mandible
- B. 9mm vertical condylar asymmetry
- C. Complex condylar consisting of a 9mm vertical plus 6mm lateral asymmetry
- D. 9mm anteroposterior body asymmetry
- E. 9mm vertical ramus asymmetry
- F. Complex ramal with a 9mm vertical plus a 6mm lateral asymmetry.

Figure 5-1 shows an example of a synthetic mandible, in this case, mandible D consisting of a 9mm anteroposterior body asymmetry.

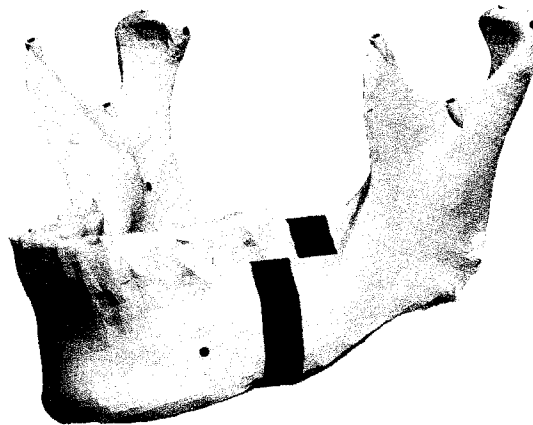


Figure 5-1: Mandible F with a 9mm horizontal body asymmetry

Each synthetic mandible was prepared for imaging by coating with a custom radio opaque paint and landmarked using 1.588 mm, stainless steel grade100 balls (Small Parts Inc, Miami Lakes, FL, USA). Figure 5-2 and Table 5-1 depict the location and describe the landmark points for the angular measurements.

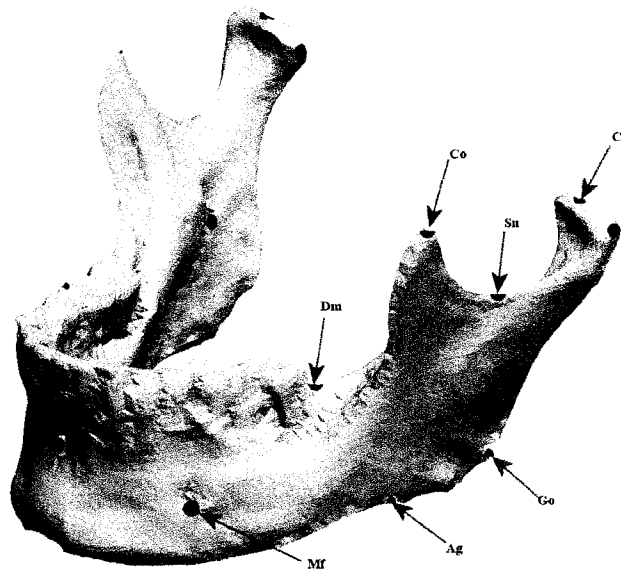


Figure 5-2: Landmark locations and description for Synthetic mandibles

Table 5-1: Landmark description for the points used for angular measurements

Landmark	Description
Mf	Mental Foramen
Ag	Depth of Antigonial Notch
Go	Anthropometric Gonion
Cs	Superior point of Condyle
Sn	Depth of Sigmoid Notch
Co	Tip of Coronoid Process
Dm	Distal of molar at Gingiva

An experimental model formed by coupling each asymmetric synthetic mandible to a single dry human skull base using a series of custom fabricated inter-occlusal splints. The condyles were seated into the glenoid fossa and artificial discs (Regisil[®] York, PA, USA) of uniform thickness were employed for reproducibility. The skull and synthetic mandible pairs were mounted onto a camera tripod (Opus[®], On, Canada) using a custom designed mounting assembly. Each of the six experimental models were

positioned into the digital panoramic unit (Kodak 8000, Kodak, USA) and imaged 35 times per model to a total of 210 images. Each model was imaged 35 times for statistical reasons to generate an adequate sample size for each range of asymmetry tested. The models were aligned in the unit by precisely following the manufacturer's instructions whereby the Frankfort horizontal plane was parallel to the floor and frontal alignment was gained through use of the optical light positioning feature of the panoramic machine. Figure 5-3 shows an experimental model positioned into the panoramic unit for imaging.

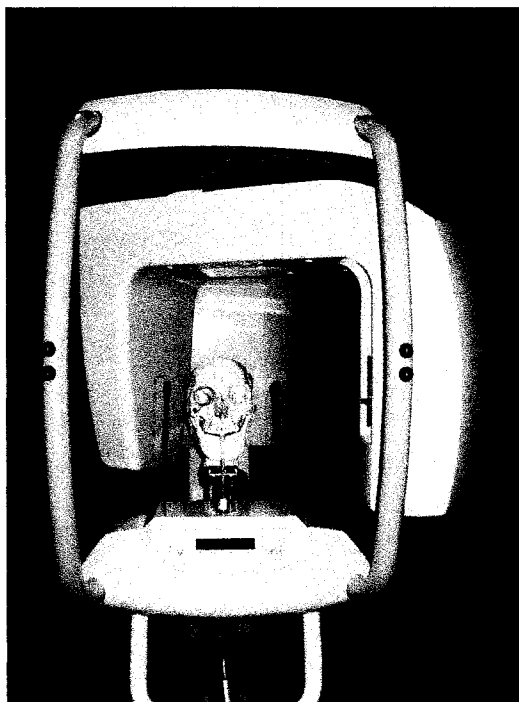


Figure 5-3: Experimental model positioned into the panoramic unit for imaging

The subsequent images were stored as a tagged image file format (TIFF) for future analysis as seen in Figure 5-4. Angular measurements were obtained from the

TIFF tiles using a web based (freeware) measurement software (Image J, NIH Image, Md, USA, <http://rsb.info.nih.gov/ij/index.html>).

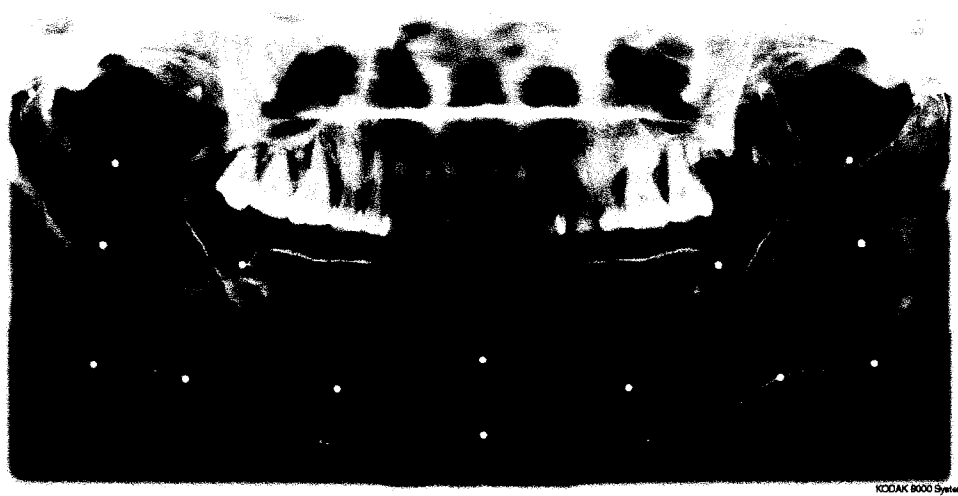


Figure 5-4: Example of tagged image file format (TIFF) obtained for angular measurements from digital panoramic

The angular measurements were performed on digital radiographs of models possessing known amounts of asymmetry in an effort to define the asymmetry. The evaluation process was separated into two sections. The first section was planned to compare the angular measurements of the digital panoramic images to true angles from a gold standard. To obtain the gold standard angular measurements, a NewTom[®] 3G cone beam volumetric scanner (CBCT) (Aperio Services LLC Sarasota, FL, USA) was used to obtain 3-D images of the synthetic mandibles and measurements were made using Amira[™] (Advanced 3-D Visualization and Volume Modeling, Berlin Germany) software to determine true angular measurements in degrees. Left and right side measurements of model A were gathered to assess model symmetry and image accuracy. Since the right side remained unchanged throughout the experiment, the remaining models (B through F) were subject to left side angular measurements only.

The true angular measurements of left and right sides for model A and left sides for models B through F were then compared to the equivalent panoramic angular measurements. Table 5-2 is a summary of the average true angular measurements for each synthetic mandible in degrees that were obtained from the CBCT and measured with Amira™.

Table 5-2: True angular measurements in degrees (std. dev.) from CBCT (n=3)

Mandible	Mf- Ag-Sn	Ag- Sn-Mf	Sn-Mf- Ag	Mf- Ag-Cs	Ag-Cs- Mf	Cs-Mf- Ag	Ag-Sn- Cs	Sn-Cs- Ag	Cs-Ag- Sn
A	111.0 (.01)	27.9 (.00)	41.0 (.01)	118.2 (.05)	18.9 (.01)	42.7 (.04)	155.9 (.01)	15.8 (.02)	8.5 (.04)
B	114.0 (.00)	26.7 (.02)	39.7 (.00)	122.9 (.02)	16.3 (.02)	41.1 (.00)	156.0 (.02)	14.1 (.02)	8.9 (.03)
C	111.1 (.01)	29.1 (.01)	40.0 (.01)	119.0 (.03)	18.9 (.02)	41.8 (.01)	158.0 (.04)	14.2 (.03)	8.4 (.02)
D	114.2 (.02)	30.8 (.00)	34.4 (.00)	121.1 (.01)	21.5 (.02)	37.1 (.03)	154.1 (.00)	16.8 (.01)	8.6 (.02)
E	109.0 (.00)	25.1 (.02)	46.3 (.02)	115.9 (.2)	17.7 (.04)	47.0 (.01)	152.8 (.01)	18.5 (.00)	8.6 (.01)
F	110.1 (.01)	27.3 (.01)	42.6 (.00)	117.0 (.03)	19.2 (.01)	43.6 (.00)	152.2 (.01)	19.2 (.01)	8.8 (.02)

The second section compared right side and left side angular measurements for each of the panoramic images. The measurements were established from center point to center point of each of the landmarks and the results were recorded in degrees on an excel spreadsheet. All measurements were carried out by the principal investigator (SR) and were randomly collected by selecting each image independent of the rest and measuring that image once. Measurement error was determined using interclass coefficient analysis in SPSS (SPSS 14.0, LEAD Technologies, Inc. USA).

Table 5-3 summarizes the average angular measurement (in degrees) obtained from the 210 total TIFF digital radiographs with standard deviations for each experimental model of the six synthetic mandibles. Aside from model A, it was

expected that differences would exist and that asymmetry would appear across the angles that spanned regions of asymmetry. For example, model B (9mm condylar asymmetry) would be anticipated to display asymmetry for each angular measurement that was inclusive of Cs within its set.

Table 5-3: Average angular measurements (°) for synthetic mandible models. (n=35)

Side	Angle	Model A	Model B	Model C	Model D	Model E	Model F
Left	Mf-Ag-Sn	111.45 (.19)	109.90(.25)	109.52 (.17)	109.12 (.13)	107.29 (.13)	107.04 (.14)
	Ag-Sn-Mf	26.75 (.23)	27.17 (.17)	28.64 (.21)	32.80 (.26)	25.05 (.17)	28.02 (.18)
	Sn-Mf-Ag	41.84 (.20)	42.98 (.17)	41.89 (.13)	38.12 (.14)	47.69 (.19)	44.98 (.21)
	Mf-Ag-Cs	118.05 (.21)	117.30 (.22)	116.29 (.18)	116.10 (.19)	114.28 (.15)	113.83 (.19)
	Ag-Cs-Mf	18.64 (.16)	17.41 (.12)	19.19 (.17)	23.29 (.21)	18.00 (.13)	20.13 (.13)
	Cs-Mf-Ag	43.36 (.18)	45.30 (.17)	44.55 (.16)	40.63 (.14)	47.73 (.15)	46.08 (.19)
	Ag-Sn-CS	159.33 (.19)	160.37 (.18)	161.22 (.18)	157.91 (.16)	155.31 (.20)	156.32 (.20)
	Sn-Cs-Ag	14.15 (.14)	12.22 (.15)	12.11 (.15)	15.05 (.16)	17.72 (.19)	16.77 (.16)
	Cs-Ag-Sn	6.61 (.10)	7.44 (.10)	6.70 (.08)	7.07 (.09)	7.01 (.06)	6.93 (.09)
Right	Mf-Ag-Sn	111.71 (.18)	112.52 (.19)	111.39 (.16)	113.14 (.18)	112.08 (.17)	110.31 (.16)
	Ag-Sn-Mf	26.56 (.20)	26.13 (.19)	26.31 (.19)	26.53 (.22)	26.17 (.12)	26.70 (.18)
	Sn-Mf-Ag	41.75 (.20)	41.40 (.20)	42.32 (.21)	40.36 (.22)	41.78 (.16)	43.03 (.17)
	Mf-Ag-Cs	118.52 (.23)	119.80 (.19)	118.09 (.18)	120.18 (.18)	119.08 (.17)	117.33 (.22)
	Ag-Cs-Mf	18.37 (.17)	17.92 (.12)	18.30 (.15)	18.22 (.12)	18.07 (.09)	18.53 (.13)
	Cs-Mf-Ag	43.15 (.19)	42.31 (.19)	43.64 (.20)	41.63 (.17)	42.88 (.19)	44.17 (.23)
	Ag-Sn-CS	158.91 (.24)	157.69 (.23)	158.87 (.24)	159.59 (.26)	158.20 (.22)	157.85 (.18)
	Sn-Cs-Ag	14.30 (.16)	15.08 (.17)	14.39 (.17)	14.35 (.19)	14.83 (.17)	15.11 (.15)
	Cs-Ag-Sn	6.83 (.12)	7.27 (.09)	6.77 (.11)	7.10 (.10)	7.00 (.08)	7.05 (.11)

5.3.2 Panoramic to True Angular Comparison (CBCT)

Each of the nine angular measurements (Mf-Ag-Sn, Ag-Sn-Mf, Sn-Mf-Ag, Mf-Ag-Cs, Ag-Cs-Mf, Cs-Mf-Ag, Ag-Sn-Cs, Sn-Cs-Ag and Cs-Ag-Sn) were identified and measured for true angles to a total of three times on separate occasions one week apart by a co-researcher (ML) using the CBCT and Amira™ software program. Each set of three measurements was averaged and the average angle obtained was used as the true degrees of measure for each angle studied on the synthetic models (Table 5-2). The same nine left side angular measurements were gathered for the 35 digital panoramic radiographic images obtained for each model.

Comparison of the panoramic to true angles was conducted as two segments. The first compared the amount of magnification between the panoramic and true angles for both the left and right hand sides of model A by means of the following equation.

$$\textit{Equation 5-1: Magnification Left} = \left| \frac{(PanL)}{(NewTomL)} \right|$$

and

$$\textit{Equation 5-2: Magnification Right} = \left| \frac{(PanR)}{(NewTomR)} \right|$$

The left and right angular panoramic to true measurements (magnification factors) of experimental model A was subsequently exposed to a one sample t-test using SPSS.

The second portion for assessing the gold standard related the left side measurements of the digital panoramic to the left side true angular measurements for the remaining models B through F. The right side angle measurements for the remaining models remained unaltered throughout the experiment, thus were not compared.

For models B through F, the magnification factor was calculated using the formula:

$$\text{Equation 5-3: Magnification Left} = \left| \frac{(PanL)}{(NewTomL)} \right|$$

The left side magnification factors for models B through F were subject to statistical analysis using a one sample t-test in SPSS.

To determine overall angle disagreement between panoramic and true angles the mean difference between true angles and panoramic angles was established. The percent difference for true left-right measurements was established using right side of model A to left side of the remaining models as right side was unchanged throughout the experiment. The mean differences were expressed as an absolute value of percent disagreement using the following formula:

$$\text{Equation 5-4: Mean Disagreement} = \left| \left[\overline{\Delta\%Pan_{A-F}} - \overline{\Delta\%True_A} \right] \right|$$

Where $\overline{\Delta\%Pan_{A-F}}$ is defined as the average sum of percent differences between left and right sides measurements of the panoramic images for each of the models A through F and where $\overline{\Delta\%True_A}$ is the average sum of the percent differences between left and right side measurements of the true model angles for model A. The disagreement was recorded as an absolute value. The mean angular disagreement was further exposed to statistical analysis using a one sample t-test using SPSS.

5.3.3 Panoramic Image Left to Right Side Comparison

Panoramic digital image left to right side measurements (degrees) were converted to a percentage using a version of the formula $[(R-L)/(R+L)]$ reported in previous literature¹ and adapted from chapter 4 of this thesis.

$$\textit{Equation 5-5: Pan Left to Pan Right Percent Difference} = \frac{(R-L)}{R}(100)$$

The left-right percent differences were subject to statistical analysis using a one sample t-test in SPSS.

5.4 Results

Intraclass correlation coefficient analysis revealed very high repeatability $\approx .99$ in measurement of angles from the digital panoramic images following a method of statistical analysis outlined by Fleiss et al.¹⁸⁻²⁰

5.4.1 Panoramic Image to True Angular (Newtom[®] and Amira[™]) Comparison

True angular measurement determination was established using a CBCT with Amira[™] software for the six synthetic mandibles. The CBCT and Amira[™] software provided true angles in degrees for measurements conducted on the left and right halves of each synthetic mandible and was considered the gold standard. Each of the digital panoramic image measurements of angles were compared to their respective true angular measurements collected from the CBCT and Amira[™] software and recorded as a magnification factor. The magnification factor and degree difference were subject to a one sample t-test using SPSS for left and right sides of model A. Table 5-4 reflects the magnification factor as well as measured degree difference for model A. The degree and magnification differences between the panoramic images and the true measurements revealed a statistically significant difference ($P < .05$) for all left hand and right side measurements on model A as determined by the one sample t-test except for angle Mf-

Ag-Cs on the left which revealed that there was not a statistically significant difference (P>.05) between panoramic and true.

Table 5-4: Magnification and degree difference (std. dev.) for model A (n=35)

Angle	Right			Left		
	Magnification	p-value	° difference	Magnification	p-value	° difference
Mf-Ag-Sn	0.99 (.0016)	<.001	-.29 (.18)	0.99 (.0017)	<.001	.45 (.19)
Ag-Sn-Mf	.97 (.0074)	<.001	-.74 (.20)	.97 (.0083)	<.001	-.85 (.23)
Sn-Mf-Ag	1.04 (.0049)	<.001	1.55 (.20)	1.04 (.0051)	<.001	1.64 (.20)
Mf-Ag-Cs	0.99 (.0019)	<.001	-.49 (.17)	1.00 (.0017)	.206	.05 (.21)
Ag-Cs-Mf	.99 (.0091)	<.001	-.14 (.17)	.99 (.0083)	<.001	-.16 (.16)
Cs-Mf-Ag	1.04 (.0046)	<.001	1.85 (.19)	1.04 (.0043)	<.001	1.65 (.18)
Ag-Sn-CS	1.02 (.0015)	<.001	2.41 (.24)	1.02 (.0012)	<.001	3.33 (.19)
Sn-Cs-Ag	.93 (.0104)	<.001	-1.00 (.16)	.89 (.0091)	<.001	-1.65 (.14)
Cs-Ag-Sn	.82 (.0141)	<.001	-1.53 (.12)	.78 (.0116)	<.001	-1.85 (.10)

For model A, the magnification ranged from 0.78 for angle Cs-Ag-Sn on the left side to 1.04 for two bilateral angles (Sn-Mf-Ag, Cs-Mf-Ag) and the difference of degrees went from -1.85° for angle Cs-Ag-Sn on the left to 1.85° Cs-Mf-Ag on the right. The remaining mandibles, models B through F underwent the same comparison of left side only for panoramic image to true (CBCT) measurement of degrees. One sample t-test was performed between the left and right magnification and angular difference for models B through F. There was a statistically significant difference (P<.05) for all compared measures except for angle Ag-Sn-Mf on model E which revealed that there was not a statistically significant difference (P>.05) between panoramic and true for the angle. The range of magnification for the remaining models went from 0.77 on angle Cs-Ag-Sn of model C to 1.11 for angle Sn-Mf-Ag on model D. The difference of degrees went from 0.04° for angle Mf-Ag-Cs on model B to -5.70° for angle Mf-Ag-Cs on model C. The average magnification factor for **all** cases pooled (model A left and right and models B through F left only) revealed 0.98 ± 0.08.

Table 5-5: Panoramic to true magnification and ° differences (std. dev.) (n=35)

Model	Angle	Magnification	p-value	° difference
B	Mf-Ag-Sn	.96 (.0022)	<.001	-4.10 (.25)
	Ag-Sn-Mf	1.02 (.0065)	<.001	.47 (.17)
	Sn-Mf-Ag	1.08 (.0044)	<.001	1.64 (.20)
	Mf-Ag-Cs	.95 (.0018)	<.001	.04 (.21)
	Ag-Cs-Mf	1.07 (.0071)	<.001	-.16 (.16)
	Cs-Mf-Ag	1.10 (.0040)	<.001	1.65 (.18)
	Ag-Sn-CS	1.02 (.0012)	<.001	3.33 (.19)
	Sn-Cs-Ag	.89 (.0107)	<.001	-1.65 (.14)
C	Cs-Ag-Sn	.84 (.0111)	<.001	-1.85 (.10)
	Mf-Ag-Sn	.99 (.0015)	<.001	-1.48 (.17)
	Ag-Sn-Mf	.98 (.0071)	<.001	-.46 (.21)
	Sn-Mf-Ag	1.05 (.0034)	<.001	3.28 (.17)
	Mf-Ag-Cs	.98 (.0015)	<.001	-5.70 (.22)
	Ag-Cs-Mf	1.02 (.0090)	<.001	1.11 (.12)
	Cs-Mf-Ag	1.07 (.0037)	<.001	4.20 (.17)
	Ag-Sn-CS	1.01 (.0011)	<.001	4.37 (.18)
D	Sn-Cs-Ag	.85 (.0103)	<.001	-1.48 (.15)
	Cs-Ag-Sn	.77 (.0091)	<.001	-1.46 (.10)
	Mf-Ag-Sn	.96 (.0012)	<.001	-4.88 (.13)
	Ag-Sn-Mf	1.06 (.0084)	<.001	2.00 (.26)
	Sn-Mf-Ag	1.11 (.0039)	<.001	1.89 (.13)
	Mf-Ag-Cs	.96 (.0016)	<.001	-2.71 (.18)
	Ag-Cs-Mf	1.08 (.0096)	<.001	.29 (.16)
	Cs-Mf-Ag	1.10 (.0038)	<.001	2.74 (.16)
E	Ag-Sn-CS	1.03 (.0011)	<.001	2.22 (.18)
	Sn-Cs-Ag	.93 (.0097)	<.001	-2.19 (.15)
	Cs-Ag-Sn	.83 (.0105)	<.001	-1.98 (.08)
	Mf-Ag-Sn	.98 (.0012)	<.001	-1.71 (.13)
	Ag-Sn-Mf	1.00 (.0084)	.126	-.05 (.17)
	Sn-Mf-Ag	1.03 (.0041)	<.001	3.72 (.14)
	Mf-Ag-Cs	.99 (.0013)	<.001	-4.90 (.19)
	Ag-Cs-Mf	1.02 (.0072)	<.001	1.79 (.21)
F	Cs-Mf-Ag	1.02 (.0031)	<.001	3.53 (.14)
	Ag-Sn-CS	1.03 (.0013)	<.001	3.91 (.16)
	Sn-Cs-Ag	.96 (.0103)	<.001	-1.15 (.16)
	Cs-Ag-Sn	.84 (.0075)	<.001	-1.48 (.06)
	Mf-Ag-Sn	.97 (.0013)	<.001	-2.97 (.14)
	Ag-Sn-Mf	1.03 (.0058)	<.001	.72 (.16)
	Sn-Mf-Ag	1.06 (.0049)	<.001	1.39 (.19)
	Mf-Ag-Cs	.97 (.0016)	<.001	-1.72 (.15)
F	Ag-Cs-Mf	1.05 (.0068)	<.001	.30 (.13)
	Cs-Mf-Ag	1.06 (.0042)	<.001	.73 (.15)
	Ag-Sn-CS	1.03 (.0013)	<.001	3.31 (.20)
	Sn-Cs-Ag	.83 (.0080)	<.001	-.78 (.19)
F	Cs-Ag-Sn	.79 (.0098)	<.001	-1.34 (.06)

Looking at the degree (°) difference on Tables 5-4 and 5-5, there was a range of difference between panoramic and true values for all angles measured where a negative value indicated that panoramic angular measurement were smaller than true angle and a positive value indicated the panoramic angular measurement was larger than the true angle. The range of difference in angles (all models) from panoramic to true was from 0.04° for angle Mf-Ag-CS on model B to -5.70° for angle Mf-Ag-Cs on model C. Table 5-5 summarizes the left side to left side comparison of mandibles B through F for magnification and degree differences of panoramic to true. The average absolute difference for the pooled angular measurements was 1.85° ± 0.71 for all cases.

The mean percent (right minus left) from panoramic were compared to the mean percent difference of the true angles to determine the overall disagreement between panoramic and true measures. Table 5-6 is a summary of each percent difference (average) by angle for the six experimental models.

Table 5-6: Mean disagreement in percent (std. dev.) between panoramic and true angles

Model	Mf-Ag-Sn	Ag-Sn-Mf	Sn-Mf-Ag	Mf-Ag-Cs	Ag-Cs-Mf	Cs-Mf-Ag	Ag-Sn-Cs	Sn-Cs-Ag	Cs-Ag-Sn
A	0.66 (.24)	0.38 (.27)	0.22 (.22)	0.44 (.17)	0.13 (.13)	0.50 (.45)	0.06 (.18)	2.19 (.91)	2.21 (.77)
B	0.57 (.29)	1.78 (.98)	2.50 (1.15)	1.25 (.49)	9.02 (1.21)	6.34 (1.21)	1.37 (.55)	8.49 (1.33)	4.03 (1.11)
C	0.80 (.31)	1.90 (.68)	0.53 (.27)	1.54 (.76)	2.63 (.98)	0.85 (.75)	0.13 (.12)	10.71 (1.45)	2.84 (.98)
D	1.83 (.79)	8.31 (1.33)	8.73 (1.22)	1.78 (.88)	8.21 (1.25)	7.74 (1.21)	1.17 (.56)	1.08 (.78)	1.84 (.79)
E	1.69 (.88)	3.72 (.75)	1.96 (.87)	1.59 (.74)	3.98 (1.11)	3.08 (1.19)	1.03 (.32)	3.19 (1.01)	0.05 (.12)
F	1.22 (.62)	4.83 (1.01)	1.54 (.77)	1.35 (.67)	4.51 (1.15)	1.33 (.69)	1.91 (.87)	13.94 (1.55)	3.78 (.99)
Ave diff	1.13 (.54)	3.49 (2.84)	2.58 (3.13)	1.33 (.47)	4.75 (3.37)	3.31 (3.06)	0.95 (.72)	6.60 (5.21)	2.46 (1.46)
p-value	<.001	<.001	<.001	<.001	<.001	<.001	<.001	<.001	<.001

The mean disagreement for angle Mf-Sn-Ag was 1.13% between the models while angles Ag-Sn-Mf and Sn-Mf-Ag were 3.49% and 2.58% respectively. Angle Mf-Ag-Cs had a mean percent disagreement of 1.33% between true and panoramic angles while angle Ag-Cs-Mf was 4.75% and Cs-Mf-Ag was 3.31%. Finally angles Ag-Sn-Cs, Sn-Cs-Ag and Cs-Ag-Sn respectively demonstrated 0.95%, 6.60% and 2.46% panoramic to true mean percent differences. The average mean disagreement among the angles for all models was 3.10%.

5.4.2 Panoramic Image Left to Right Comparison

Nine angular measurements from each of the left and right sides of 35 TIFF images gathered from panoramic radiographs obtained on six synthetic mandibles (Models A through F) were measured and sequentially compared to one another and recorded as a percent difference between left and right. Table 5-7 is a summary of the left to right percent differences and degree differences for all models. Table 5-7 also displays angles to which statistically significant asymmetries were expected as well as those which revealed asymmetries based on the statistical analysis. One sample t-test was performed between the left and right percentages to test for significant differences. The overall percent differences varied depending on the angle and asymmetric model studied. For model A, there was no statistically significant difference ($P > .05$) between left and right degree measurement for angle Sn-Mf-Ag. In addition, models D and E indicated no statistically significant difference ($P > .05$) for angle Cs-Ag-Sn. All remaining angular measurements on the rest of the models revealed statistically significant differences ($P < .05$). The overall range of percent difference between left and

right angles measured from the digital panoramic images ranged from -0.17% for angle Cs-Ag-Sn of model E to -24.42% for angle Ag-Cs-Mf of model D.

Looking at the various asymmetries for each model individually, certain asymmetries were evident using 6% cutoff as being the threshold of observed measurement significance.^{1,6} As noted from the observed values in Table 5-7, only the angular measurements crossing areas of asymmetry were expected to reveal a statistical or measurement difference (asymmetry) between left and right sides. To understand signage, angles displaying a negative left-right percent difference were more obtuse on left compared to right while the positive left-right differences became more acute.

Table 5-7: Left to right percent and degree (std. dev) differences (n=35)

Model	Angle	% difference	p-value	° difference	Expected	Revealed
A	Mf-Ag-Sn	.23 (.26)	<.001	-.26 (.29)	Symmetric	<i>Asymmetric</i>
	Ag-Sn-Mf	-.72 (1.05)	<.001	.19 (.28)	Symmetric	<i>Asymmetric</i>
	Sn-Mf-Ag	-.22 (.61)	.039	.09 (.25)	Symmetric	Symmetric
	Mf-Ag-Cs	.40 (.32)	<.001	-.47 (.39)	Symmetric	<i>Asymmetric</i>
	Ag-Cs-Mf	-1.49 (1.19)	<.001	.28 (.22)	Symmetric	<i>Asymmetric</i>
	Cs-Mf-Ag	-.47 (.69)	<.001	.20 (.30)	Symmetric	<i>Asymmetric</i>
	Ag-Sn-CS	-.26 (.17)	<.001	.41 (.27)	Symmetric	<i>Asymmetric</i>
	Sn-Cs-Ag	1.07 (1.36)	<.001	-.15 (.19)	Symmetric	<i>Asymmetric</i>
	Cs-Ag-Sn	3.29 (2.47)	<.001	-.22 (.17)	Symmetric	<i>Asymmetric</i>
B	Mf-Ag-Sn	2.36 (.31)	<.001	-2.62 (.35)	Symmetric	<i>Asymmetric</i>
	Ag-Sn-Mf	-3.97 (.83)	<.001	1.06 (.22)	Symmetric	<i>Asymmetric</i>
	Sn-Mf-Ag	-3.74 (.79)	<.001	1.58 (.33)	Symmetric	<i>Asymmetric</i>
	Mf-Ag-Cs	2.11 (.30)	<.001	-2.50 (.36)	<i>Asymmetric</i>	<i>Asymmetric</i>
	Ag-Cs-Mf	2.87 (.96)	<.001	-.51 (.17)	<i>Asymmetric</i>	<i>Asymmetric</i>
	Cs-Mf-Ag	-6.83 (.72)	<.001	2.99 (.31)	<i>Asymmetric</i>	<i>Asymmetric</i>
	Ag-Sn-CS	-1.69 (.19)	<.001	2.69 (.31)	<i>Asymmetric</i>	<i>Asymmetric</i>
	Sn-Cs-Ag	20.94(1.49)	<.001	-2.86 (.21)	<i>Asymmetric</i>	<i>Asymmetric</i>
	Cs-Ag-Sn	-2.43 (2.11)	<.001	.18 (.16)	<i>Asymmetric</i>	<i>Asymmetric</i>

Continued on next page....

Table 5-7: Continued

Model	Angle	% difference	p-value	° difference	Expected	Revealed
C	Mf-Ag-Sn	1.69 (.20)	<.001	-1.87 (.22)	Symmetric	<i>Asymmetric</i>
	Ag-Sn-Mf	-8.49 (.70)	<.001	2.33 (.19)	Symmetric	<i>Asymmetric</i>
	Sn-Mf-Ag	1.03 (.56)	<.001	-.43 (.24)	Symmetric	<i>Asymmetric</i>
	Mf-Ag-Cs	1.54 (.26)	<.001	-1.80 (.31)	<i>Asymmetric</i>	<i>Asymmetric</i>
	Ag-Cs-Mf	-4.79 (1.06)	<.001	.90 (.20)	<i>Asymmetric</i>	<i>Asymmetric</i>
	Cs-Mf-Ag	-2.06 (.60)	<.001	.91 (.26)	<i>Asymmetric</i>	<i>Asymmetric</i>
	Ag-Sn-CS	-1.47 (.20)	<.001	2.35 (.32)	<i>Asymmetric</i>	<i>Asymmetric</i>
	Sn-Cs-Ag	17.24(1.88)	<.001	-2.28 (.25)	<i>Asymmetric</i>	<i>Asymmetric</i>
	Cs-Ag-Sn	.99 (2.10)	.009	-.07 (.14)	<i>Asymmetric</i>	<i>Asymmetric</i>
D	Mf-Ag-Sn	3.62 (.19)	<.001	-4.02 (.21)	<i>Asymmetric</i>	<i>Asymmetric</i>
	Ag-Sn-Mf	-21.13 (.92)	<.001	6.27 (.28)	<i>Asymmetric</i>	<i>Asymmetric</i>
	Sn-Mf-Ag	5.7 (.61)	<.001	-2.24 (.24)	<i>Asymmetric</i>	<i>Asymmetric</i>
	Mf-Ag-Cs	3.46 (.23)	<.001	-4.09 (.27)	<i>Asymmetric</i>	<i>Asymmetric</i>
	Ag-Cs-Mf	-24.42 (.76)	<.001	5.07 (.17)	<i>Asymmetric</i>	<i>Asymmetric</i>
	Cs-Mf-Ag	2.43 (.56)	<.001	-1.00 (.23)	<i>Asymmetric</i>	<i>Asymmetric</i>
	Ag-Sn-CS	.43 (.18)	<.001	-.68 (.28)	Symmetric	<i>Asymmetric</i>
	Sn-Cs-Ag	-4.80 (1.55)	<.001	.70 (.23)	Symmetric	<i>Asymmetric</i>
	Cs-Ag-Sn	.43 (1.94)	.195	-.03 (.14)	Symmetric	Symmetric
E	Mf-Ag-Sn	4.37 (.20)	<.001	-4.79 (.23)	<i>Asymmetric</i>	<i>Asymmetric</i>
	Ag-Sn-Mf	4.34 (.91)	<.001	-1.11 (.23)	<i>Asymmetric</i>	<i>Asymmetric</i>
	Sn-Mf-Ag	-13.21 (.62)	<.001	5.91 (.28)	<i>Asymmetric</i>	<i>Asymmetric</i>
	Mf-Ag-Cs	4.11 (.22)	<.001	-4.80 (.25)	<i>Asymmetric</i>	<i>Asymmetric</i>
	Ag-Cs-Mf	.36 (.77)	<.001	-.07 (.14)	<i>Asymmetric</i>	<i>Asymmetric</i>
	Cs-Mf-Ag	-10.72 (.57)	<.001	4.86 (.25)	<i>Asymmetric</i>	<i>Asymmetric</i>
	Ag-Sn-CS	1.85 (.20)	<.001	-2.90 (.31)	<i>Asymmetric</i>	<i>Asymmetric</i>
	Sn-Cs-Ag	-17.72(1.8)	<.001	2.88 (.30)	<i>Asymmetric</i>	<i>Asymmetric</i>
	Cs-Ag-Sn	-.17 (1.52)	.506	.01 (.11)	<i>Asymmetric</i>	Symmetric
F	Mf-Ag-Sn	3.01 (.23)	<.001	-3.27 (.25)	<i>Asymmetric</i>	<i>Asymmetric</i>
	Ag-Sn-Mf	-4.83 (.96)	<.001	1.32 (.26)	<i>Asymmetric</i>	<i>Asymmetric</i>
	Sn-Mf-Ag	-4.43 (.77)	<.001	1.95 (.34)	<i>Asymmetric</i>	<i>Asymmetric</i>
	Mf-Ag-Cs	3.03 (.30)	<.001	-3.50 (.35)	<i>Asymmetric</i>	<i>Asymmetric</i>
	Ag-Cs-Mf	-8.29 (.93)	<.001	1.60 (.28)	<i>Asymmetric</i>	<i>Asymmetric</i>
	Cs-Mf-Ag	-4.23 (.78)	<.001	1.91 (.35)	<i>Asymmetric</i>	<i>Asymmetric</i>
	Ag-Sn-CS	.97 (.17)	<.001	-1.52(.26)	<i>Asymmetric</i>	<i>Asymmetric</i>
	Sn-Cs-Ag	-10.38(1.3)	<.001	1.66 (.21)	<i>Asymmetric</i>	<i>Asymmetric</i>
	Cs-Ag-Sn	1.72 (2.02)	<.001	-.12 (.14)	<i>Asymmetric</i>	<i>Asymmetric</i>

Model A was designed as a symmetric model with no inherent asymmetry

fabricated into the mandible. Despite the fact that there was a statistically significant

difference for left to right angles for all that were measured on model A, with the exception of Sn-Mf-Ag indicating no statistical difference ($P>.05$), comparison of angular measurements from the digital panoramic radiographs all fell well below the 6% cutoff revealing symmetry for this model.

Model B was constructed with a 9mm vertical condylar asymmetry. It was expected that any angle measured using point Cs (superior point of condyle) would reveal a difference between left and right sides due to the asymmetry. Although this was statistically the case, angular measurement confirmation was not evident. Of the nine angles, six were expected to reveal asymmetry of which only two did so. Angle Cs-Mf-Ag became more obtuse displaying a -6.83% difference as point Cs was displaced more vertically on the left side, indicating a left-right difference of 2.99° . For angle Sn-Cs-Ag the change was 20.94% with a -2.86° difference. Figure 5-5 represents an image of model B with angle Sn-Cs-Ag traced on left and right sides for visual comparison of the angle change as point Cs was elevated due to the 9mm condylar asymmetry. It can be noted from the figure that a very large change in position resulted in only a minor change in the angle measured.

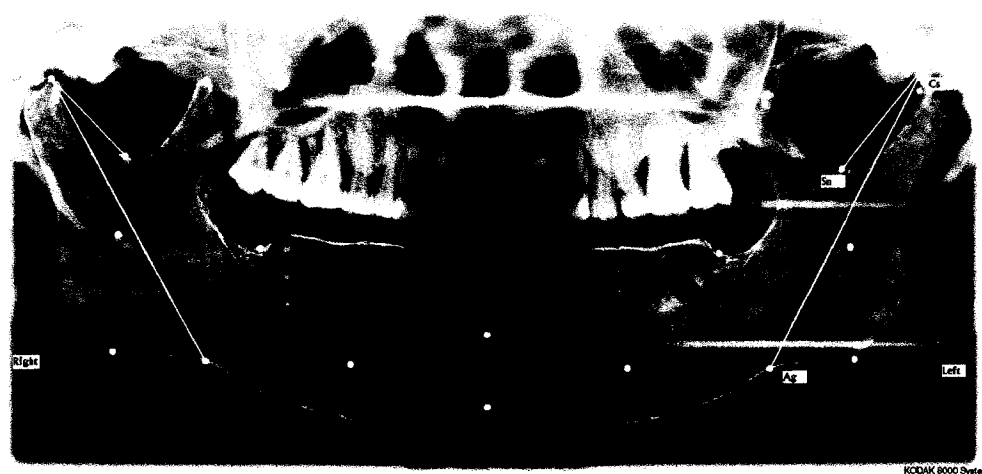


Figure 5-5: Model B with angle Sn-Cs-Ag traced left and right

Model C was designed with a complex asymmetry whereby point Cs was fabricated 9mm vertical and 6mm lateral horizontal in the left condyle. All measured angles, when comparing left to right, indicated a statistically significant difference ($P < .05$). The same six angles as in model B were expected to indicate a measurement asymmetry in addition to the statistical difference. From an angular measurement perspective one angle, Sn-Cs-Ag became more acute by 17.24% from right to left sides due to the asymmetry, a -2.88° angle change. Interestingly, angle Ag-Sn-Mf also changed by becoming more obtuse and indicating an excess of the 6% cutoff and a subsequent asymmetry, however, the angle did not involve the area of asymmetry and was not expected to reveal a measured nor statistical asymmetry. Figure 5-6 represents an image of model C with angle Sn-Cs-Ag traced on left and right sides for visual comparison of the angle change as point Cs was altered due to the 9mm vertical and 6mm horizontal condylar asymmetry.

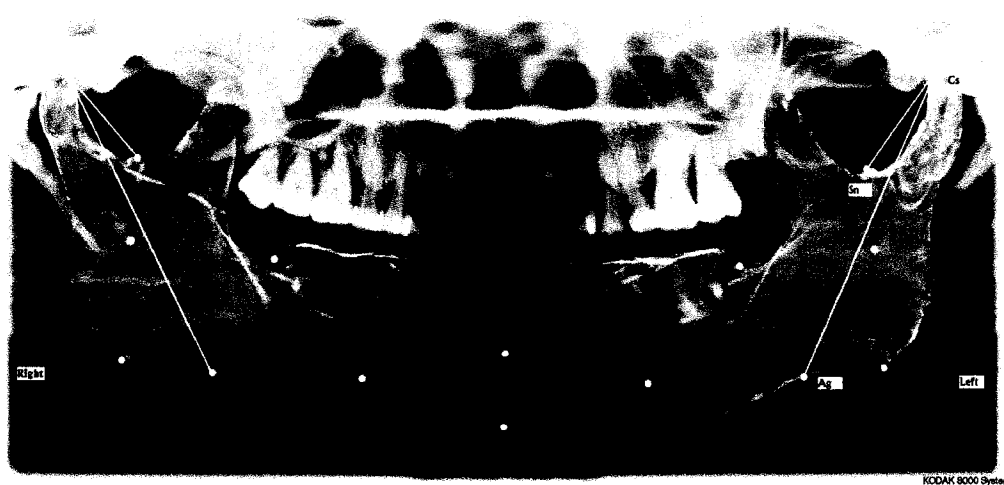


Figure 5-6: Model C with angle Sn-Cs-Ag traced left and right

Model D underwent fabrication consisting of a 9mm anteroposterior horizontal asymmetry in the body of the mandible. The same nine angular measurements were

collected on both left and right sides. All measured angles, when comparing left to right, indicated a statistically significant difference ($P < .05$) with the exception of Cs-Ag-Sn which revealed no statistically significant difference ($P > .05$) between left and right sides. From Table 5-7, this angle was one of three that were expected to be symmetric, the other two being Ag-Sn-Cs and Sn-Cs-Ag which were measured as symmetric. Of the remaining six angles, two revealed an asymmetry by exceeding the 6% cutoff. Ag-Sn-Mf became more obtuse on the left with a -21.13% difference from the right side revealing a 6.27° change due to the asymmetry. Angle Ag-Cs-Mf also became more obtuse with a difference of -24.42% suggesting a 5.07° change. Figure 5-7 represents an image of model D with angles Ag-Sn-Mf and Ag-Cs-Mf overlain on both left and right sides for visual comparison of the angle change as distance Mf-Ag was increased due to the 9mm anteroposterior body asymmetry.

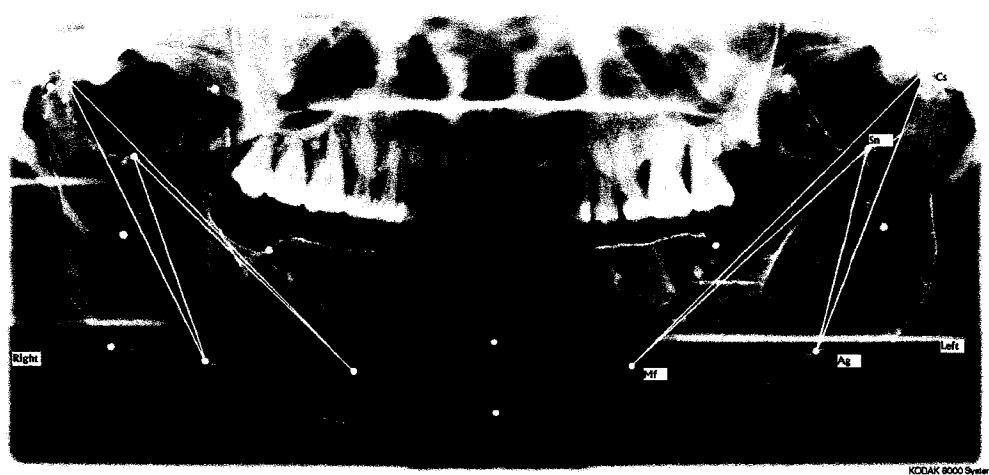


Figure 5-7: Model D with angles Ag-Sn-Mf and Ag-Cs-Mf traced left and right

Model E was constructed with a 9mm vertical ramus asymmetry. It was expected that any angle measured using points Sn and/or Cs (sigmoid notch and/or superior point of condyle) would reveal a difference between left and right sides due to

the asymmetry. All measured angles, when comparing left to right, indicated a statistically significant difference ($P < .05$) with the exception of Cs-Ag-Sn which revealed no statistically significant difference ($P > .05$) between left and right sides. From Table 5-7, this angle, along with the remaining eight were expected to *not* be symmetric both by measurement of the angles and statistically speaking. Of the remaining angles, using the 6% cutoff, three angles specified an asymmetry. Angle Sn-Mf-Ag became more obtuse on the left with a -13.21% difference from the right side revealing a 5.91° change due to the asymmetry. Angle Cs-Mf-Ag also became more obtuse with a -10.71% difference displaying a 4.86° change. Finally, angle Sn-Cs-Ag was also more obtuse on the left with a -17.72% difference from the right side generating a 2.88° change as a result of the asymmetry. Figure 5-8 shows an image of model E with angle Sn-Cs-Ag drawn on both left and right sides as an example of one three angle changes resulting from the 9mm vertical ramus asymmetry.

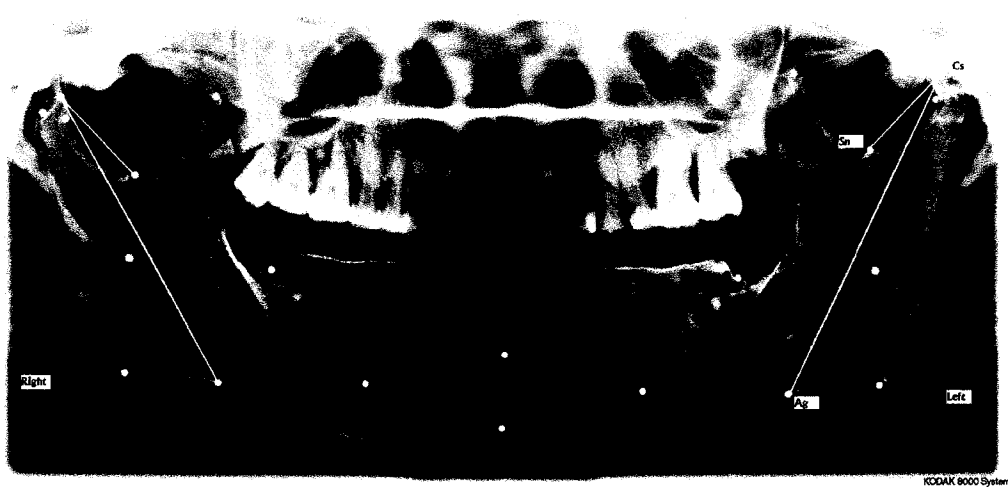


Figure 5-8: Model E with angle Cs-Mf-Ag traced on left and right sides

Finally, model F was designed with a complex asymmetry whereby points Cs and Sn were repositioned as a result of a 9mm vertical and 6mm lateral horizontal

change to the left ramus. All nine angular measurements were collected on both left and right sides. As in model E, it was expected that any angle measured using points Sn and/or Cs would reveal a statistical and observed measurement difference between left and right sides due to the asymmetry. All measured angles, when comparing left to right, indicated a statistically significant difference ($P < .05$). From a clinical perspective, only two of the nine angles indicated asymmetry using the 6% cutoff. Angle Ag-Cs-Mf was more obtuse on the left with a -8.29% difference from the right side presenting a 1.60° change. The second angle, angle Sn-Cs-Ag also became obtuse on the left with a -10.38% difference revealing a 1.66° change due to the asymmetry. Figure 5-9 depicts an image of model F with angle Sn-Cs-Ag overlain on both left and right sides as an example of one of the two angle changes resulting from the 9mm vertical and 6mm lateral complex ramus asymmetry.

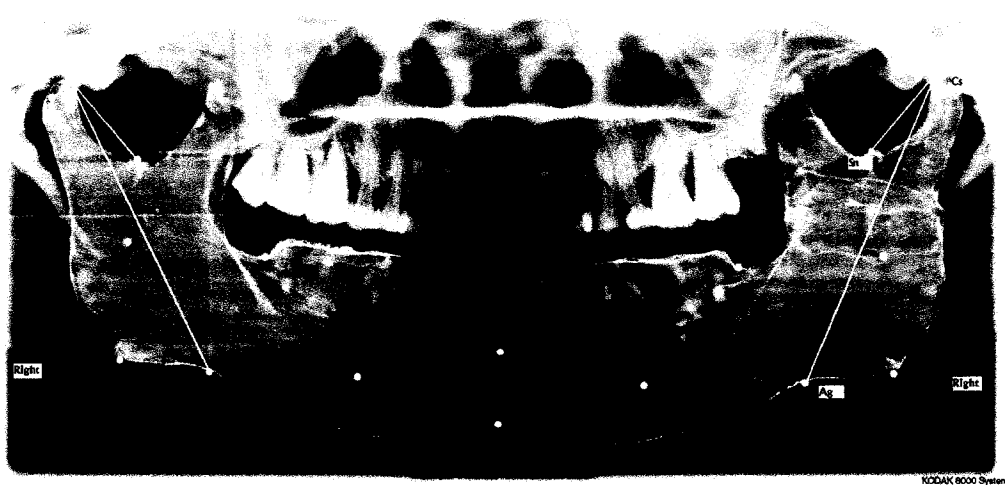


Figure 5-9: Model F with angle Sn-Cs-Ag traced on left and right sides

5.5 Discussion

The purpose of this study was to use angular measurements of landmarks on panoramic images to evaluate known amounts of mandibular asymmetry from a series of synthetically produced asymmetric mandibles.

5.5.1 Panoramic to True Length Measurements

Model accuracy and image magnification factors were established accepting the NewTom[®] 3G (CBCT) and Amira[™] software as the gold standard of measurement for this project. The CBCT and Amira[™] software were previously reported to measure degrees with an accuracy of 0.5° with measurement error of between 0.2° and 0.3°. ²¹ Both left and right measurements were conducted for mandible A (symmetric mandible) whereas left only (asymmetric side) measurements were made on remaining mandibles B through F. Synthetic mandible A revealed angle symmetry with an average left to right difference of 1.80° as measured from Amira[™]. The difference converts to an accuracy of 98.55 - 99.54% in symmetry between left and right sides. This range of accuracy compared well with the 97.7- 99.12% dimensional accuracy of STL models reported by Barker et al. ²² From this information, it was decided that all remaining true measurements possessed an accuracy of over 98%. The differences between digital panoramic measurements of angles obtained from the radiographs and the true angular measurements established from the CBCT and Amira[™] software program (Tables 5-4 and 5-5) indicate nearly a 1:1 relationship. Considering the magnification factor, the measurement differences revealed object distortion with larger magnification in some lengths than others. The magnification factor was a division of one measurement into another and recorded as a unit free absolute value. The pooled magnification for model A left and right and models B through F left side, at 0.98 ± 0.08 was considerably less than the manufacturer's reported magnification of 1.27 (www.kodak.com). The magnification factor corresponds reasonably well with values reported by other authors. Catic et al found a magnification to be 1.05 when looking at bilateral gonial angle

measurements. The authors also found that the measured magnification was considerably less than the manufacturer's reported magnification.²³

From a clinical and measurement perspective using an average magnification value may give the clinician an overall feel for different landmark to landmark to landmark angle differences but a true determination of actual degrees should be made with some caution due to the variations in magnification noted from angle to angle within a given model. Theoretically, rough calculations of angles between structures within an image could be obtained directly from a radiographic image and further considered as an actual angular measurement from the nearly 1.00X magnification factor. In other words the angle measured is equivalent to or very near the angle of the actual structure being measured. Although this information is subject to some variability within the image, it appears to be much better than using the manufacturer's recorded magnification of 1.27X. This reduction in magnification factor from the manufacturer may have been a result of proper and consistent head positioning in the unit. It was realized that there were no large variations due to the head positioning errors on the panoramic radiographs from consistently low standard deviation among the repeated measures.

Habets et al previously reported that differences between left and right side linear measurements of less than 6% were due to inherent machine error.¹ Kambylafkas et al also used the 6% cutoff in their experiment despite the finding a maximum disagreement for total ramus height to be 5.38%.⁶ Although no linear measurements were obtained in this part of the experiment, based on previous studies in addition to the average mean disagreement between the true left-right and the panoramic left-right

being 3.10% with the highest mean disagreement being 6.60% for angle Sn-Cs-Ag (Table 4-6), the 6% cutoff was used for all angular measurements for determining measurement of mandibular asymmetry. There were no Sn-Cs-Ag angles that fell within the 6%-6.6% region therefore the 6% cutoff remained the value above which asymmetry was considered.

5.5.2 Panoramic Image Left to Right Comparison

Panoramic bilateral left-right angular differences (percent) were compared on all models in an attempt to determine which angles could describe asymmetries. The combined percent difference between left and right side panoramic angular measurements from those that were **expected to be symmetric** averaged 1.93% (table 5-7). This average variation in expected symmetries was less, than the average mean disagreement of 3.10% (Table 5-6) for all models. The difference was accounted for by a combination of fabrication error, positioning error, inherent machine error and measurement error. From this it can be stated that there was an overall range of error in data acquisition of 1.93%-3.10%. This number is higher but still comparable to the 2.1% inherent machine error reported by Kambylalkas et al⁶ and much less than the 6% reported by Habets et al for their linear values.¹ The values reported by the aforesaid authors were established for posterior vertical height measurements of linear measurements thus can only be used loosely as a guideline when applied to angles. No other research was available for consideration of angular measurements from panoramic images regarding mandibular asymmetry.

Model A was designed to be symmetric and remaining models (B through F) were designed with various ranges of asymmetries. It was expected that at least one

left-right angle comparison would reveal a measurement asymmetry by exceeding the 6% cutoff for each asymmetric model. It was further anticipated that every angle with at least one landmark point in the region of asymmetry would indicate a clinical asymmetry by revealing a left-right percent difference greater than 6%. Although this was not the case for every asymmetry, each model possessed at least one angle with a measured asymmetry. It was evident that the asymmetry for each model was best described by an angle that had the highest left-right percent difference coupled with the largest difference in angular measurement ($^{\circ}$). For each model, this angle was consistently one which had the arms of the angle spanning across the region of asymmetry and the vertex at the point most perpendicular to the landmark point within the asymmetry (Figures 5-5 to 5-9). From an observation of the measurement values above the 6% cutoff, the difficulty with determining which angular measurement to use lies not only with landmark identification but also increases in complexity with a relative lack of knowledge to precisely where and how the asymmetry is approximated. It was clear from the reduction in percent difference in models C and F that complex asymmetries are more difficult to explain. From this information, it can be surmised that selecting landmark points distant from the asymmetry and choosing a vertex landmark point perpendicular to the axial direction of the asymmetry for bilateral comparison within a panoramic image are key factors. More investigation is required to determine precisely which landmark points should be used.

All of the asymmetric models (B through F) revealed a level of measured angular asymmetry using at least one angle. Models B and C with vertical and complex condylar asymmetries had the asymmetry identified by a change in angle Sn-Cs-Ag.

Model D, with an anteroposterior body asymmetry was identified with two angles (Mf-Sn-Ag and Mf-Cs-Ag). Models E and F, with a vertical ramus and complex ramus asymmetries were best described using angle Sn-Cs-Ag. As a general rule of thumb, vertical posterior asymmetries (condyle and ramus) were all observed using angle Sn-Cs-Ag and the anteroposterior asymmetry (body) was clinically detectable using angles Mf-Sn-Ag and Mf-Cs-Ag.

5.6 Conclusion

Intuitively, it would be expected that an asymmetry could be described by a change in comparative angles however clinically this has proven difficult as landmark positioning changes of several millimeters translate into only a few degrees of angular change. With caution, vertical posterior asymmetries can be determined by comparing bilateral angles between the sigmoid notch and the antigonial notch with a vertex located at the superior condyle. Anteroposterior body asymmetries can be determined by measuring bilateral angles between mental foramen and antigonial notch with the vertex being either superior condyle or sigmoid notch. In addition to the above arguments, large landmark positional changes seem to be required to change an angle by more than a few degrees therefore, intuitively, it would seem that small or moderate asymmetries would be difficult if not impossible to measure.

References

1. Habets LL, Bezuur JN, van Ooij CP, Hansson TL. The orthopantomogram, an aid in diagnosis of temporomandibular joint problems. I. The factor of vertical magnification. *J Oral Rehabil* 1987;14:475-480.
2. Kjellberg H, Ekestubbe A, Kiliaridis S, Thilander B. Condylar height on panoramic radiographs. A methodologic study with a clinical application. *Acta Odontol Scand* 1994;52:43-50.
3. Mattila M, Kononen M, Mattila K. Vertical asymmetry of the mandibular ramus and condylar heights measured with a new method from dental panoramic radiographs in patients with psoriatic arthritis. *J Oral Rehabil* 1995;22:741-745.
4. Miller VJ, Bodner L. Condylar asymmetry measurements in patients with an Angle's Class III malocclusion. *J Oral Rehabil* 1997;24:247-249.
5. Saglam AM. The condylar asymmetry measurements in different skeletal patterns. *J Oral Rehabil* 2003;30:738-742.
6. Kambylafka P, Murdoch K, Gilda E, Tallents R, Kyrkanides S. Validity of Panoramic Radiographs for Measuring Mandibular Asymmetry. *Angle Orthod*. 2006;76:388-393.
7. Warford JH, Jr., Grandhi RK, Tira DE. Prediction of maxillary canine impaction using sectors and angular measurement. *Am J Orthod Dentofacial Orthop* 2003;124:651-655.
8. Castella P, Albright RH, Jr., Straja S, Tuncay OC. Prediction of mandibular third molar impaction in the orthodontic patient from a panoramic radiograph. *Clin Orthod Res* 1998;1:37-43.
9. Frykholm A, Malmgren O, Samfors KA, Welander U. Angular measurements in orthopantomography. *Dentomaxillofac Radiol* 1977;6:77-81.
10. Stramotas S, Geenty JP, Darendeliler MA, Byloff F, Berger J, Petocz P. The reliability of crown-root ratio, linear and angular measurements on panoramic radiographs. *Clin Orthod Res* 2000;3:182-191.
11. Stramotas S, Geenty JP, Petocz P, Darendeliler MA. Accuracy of linear and angular measurements on panoramic radiographs taken at various positions in vitro. *Eur J Orthod* 2002;24:43-52.
12. McKee IW, Williamson PC, Lam EW, Heo G, Glover KE, Major PW. The accuracy of 4 panoramic units in the projection of mesiodistal tooth angulations. *Am J Orthod Dentofacial Orthop* 2002;121:166-175; quiz 192.

13. Akcam MO, Altiok T, Ozdiler E. Panoramic radiographs: a tool for investigating skeletal pattern. *Am J Orthod Dentofacial Orthop* 2003;123:175-181.
14. Larheim TA, Svanaes DB. Reproducibility of rotational panoramic radiography: mandibular linear dimensions and angles. *Am J Orthod Dentofacial Orthop* 1986;90:45-51.
15. Wyatt DL, Farman AG, Orbell GM, Silveira AM, Scarfe WC. Accuracy of dimensional and angular measurements from panoramic and lateral oblique radiographs. *Dentomaxillofac Radiol* 1995;24:225-231.
16. Kubota Y, Takenoshita Y, Takamori K, Kanamoto M, Shirasuna K. Levandoski panoramic analysis in the diagnosis of hyperplasia of the coronoid process. *Br J Oral Maxillofac Surg* 1999;37:409-411.
17. Padwa BL, Zaragoza SM, Sonis AL. Proximal segment displacement in mandibular distraction osteogenesis. *J Craniofac Surg* 2002;13:293-296; discussion 297.
18. Fleiss JL, Mann J, Paik M, Goultchin J, Chilton NW. A study of inter- and intra-examiner reliability of pocket depth and attachment level. *J Periodontal Res* 1991;26:122-128.
19. Fleiss JL, Slakter MJ, Fischman SL, Park MH, Chilton NW. Inter-examiner reliability in caries trials. *J Dent Res* 1979;58:604-609.
20. Fleiss JL, Fischman SL, Chilton NW, Park MH. Reliability of discrete measurements in caries trials. *Caries Res* 1979;13:23-31.
21. Lagravère. Accuracy of Three Dimensional images obtained from a Cone-Beam Computerized Tomographer. Edmonton, Alberta; 2006: p. 15.
22. Barker TM, Earwaker WJ, Lisle DA. Accuracy of stereolithographic models of human anatomy. *Australas Radiol* 1994;38:106-111.
23. Catic A, Celebic A, Valentic-Peruzovic M, Catovic A, Jerolimov V, Muretic I. Evaluation of the precision of dimensional measurements of the mandible on panoramic radiographs. *Oral Surg Oral Med Oral Pathol Oral Radiol Endod* 1998;86:242-248.

Chapter 6 – General Discussion

6.1 Introduction

Objectives of this thesis chapter are several and include the following: Firstly, to discuss the clinical applications, advantages and disadvantages of using panoramic radiography for assessing and measuring mandibular asymmetry. The second objective is to discuss techniques used in this thesis research project for measuring mandibular asymmetry from panoramic radiographs as well as to determine which of the techniques bear relevance and potential functionality for the clinical orthodontist. Further to clinical relevance, what is the feasibility and overall utility for the average practitioner using these techniques? From a clinical and feasibility perspective the following questions have been posed:

- What is the best overall method for measuring asymmetry?
- What measurements within each method are most applicable for determining asymmetry?
- Which techniques are most easily employed in everyday practice?

Exploration of interesting techniques such as shape and size analysis to measure and describe asymmetries was conducted. As with any new technique, questions arise as to the application of their use. Are these techniques helpful with clinical diagnosis and treatment planning or are they most suitable for determining clinical outcomes?

A third objective is to identify and evaluate the limitations found within the current study. The fourth and final objective of this thesis is to recommend future research projects that would continue to enhance the development of newer and more practical methods or aid in the development of ideas for assessing mandibular and other

facial asymmetries. A further goal would be to then develop diagnostic tools that would potentially aid in the detection, diagnosis and treatment of mandibular asymmetries.

6.2 Using Panoramic Radiography to Assess and Measuring Mandibular Asymmetry

Panoramic radiography is used by virtually every orthodontist as a mainstay of diagnosis and treatment planning by providing a general scan of all teeth and supporting structures. Some of the overall advantages to its use have been reported as:

1. Production of relatively undistorted anatomical images.
2. Significant reduction in radiation dose to the patient.
3. Simplicity and rapidity of the procedure.
4. Reduced superimposition of anatomical structures.
5. Minimal infection control procedures.¹
6. Use of panoramic radiography for detecting and evaluating

mandibular asymmetries has received considerable attention in the dental, radiological and orthodontic literature over the decades.

Some authors have attempted to simply classify asymmetries²⁻⁴ based on various clinical characteristics. Other authors⁵⁻¹³ have dedicated their research efforts toward developing measuring techniques of asymmetries from panoramic radiographs. More specifically, attention to horizontal and oblique measurements have focused on the ability to obtain accurate quantitative measurements of lengths for determining bilateral magnification and distortion levels.¹⁴ For a variety of reasons, more attention has been directed toward posterior

vertical height measurements to evaluate and compare asymmetries.^{5,12} The authors focusing on this area have found that total ramus height and to a lesser degree, condylar height asymmetries can be measured.¹² Angular measurements for comparison and evaluation of mandibular asymmetry have been discussed very infrequently. The most interesting literature regarding angular measurements from panoramic radiographs compared before and after surgical treatment of mandibular asymmetries by measuring and comparing pre and post surgical gonial angles.¹⁵ Other authors have also studied and focused on reproducibility of angular measurements.¹⁶ None of the studies to date have concentrated specifically on shape analysis for measurement of mandibular asymmetries using panoramic radiographs. Shape analysis offers an interesting perspective by potentially producing not only information on exact location of asymmetry through comparison of bilateral structures, but also by quantifying the amount of asymmetry using overall size comparisons.

Conceptually, it would be desirable to describe and quantify various asymmetries from panoramic images using one or a combination of these techniques. If proven to be simple, the advantages of measuring asymmetries from panoramic radiographs are many. To name a few, the availability to obtain asymmetry information from images routinely obtained during initial records collection is the most attractive asset. The ability to make predictive and concise determinations of asymmetry to

establish the proper modality of treatment is of great benefit to both patient and practitioner. The avoidance of further imaging to define and quantify the asymmetry decreases radiation exposure and out of pocket expense to the patient.

6.3 Techniques used for Measuring Mandibular Asymmetries and clinical relevance

This study was designed to assess various methods for measuring mandibular asymmetries from the digital panoramic radiographs using a series of synthetic mandibles. One symmetric and five asymmetric synthetic mandibles were designed and fabricated using fused deposition modeling to create a series of stereolithic models. The five asymmetric mandibles were designed with asymmetry in either the condylar, ramal or body regions of the mandible. The mandibles were constructed such that the asymmetry was on the left side while the right half of the mandible remained unchanged to allow for comparison of the sides of each test subject and consisted of one of each:

- A. Symmetric mandible
- B. 9mm vertical condylar asymmetry
- C. Complex condylar consisting of a 9mm vertical plus 6mm lateral asymmetry
- D. 9mm anteroposterior body asymmetry
- E. 9mm vertical ramus asymmetry
- F. Complex ramal with a 9mm vertical plus a 6mm lateral asymmetry.

Using the stereolithic models, three specific measurement techniques were researched.

The first technique employed shape analysis as a method to compare the various asymmetries. The aim of the study was to use shape analysis derived from a series of coordinate points to evaluate known amounts of mandibular asymmetry from the series

of digital panoramic radiographs. Although shape analysis did not specifically define the various asymmetries, size difference was proven to be capable thus promise using this technique remains. As a portion of shape analysis, size differences (or lack thereof for the symmetric model) between the various models were statistically detected among all models and correctly identified as asymmetric (symmetric for the symmetry model). The drawback with the information gathered was that size differences were simply that, differences, and did not provide information on the location of shape to which the asymmetry was located. From a statistical perspective, the information was useful but from a clinical perspective the evidence failed to make a definitive diagnosis of location of asymmetry. Selection of additional coordinate points bilaterally would surely help to define the regions of asymmetry more adequately and deliver more evident information regarding shape and location of asymmetry especially when coupled with the differences in size. The question of clinical application remains paramount. The current methodology for shape analysis has demanded extensive software programming skills which are likely to be out of the scope of the average clinician's skill set. Design, testing and development of a commercially available software program would be a minimum requirement to measure asymmetry using this technique for analysis. In addition, training for landmark identification and selection of appropriate landmarks, not to mention choosing an adequate quantity of coordinates, would need to be standardized to make such a program effective. Studies on the effect of distortion and magnification as they effect coordinate position among the various landmarks would need to be established. Despite the need for further testing, this type of information may be of significant value for evaluating the outcome of treatment. Shape information may be of

particular interest to the clinician when determining if treatment objectives have been met. Comparison of pre and post treatment radiographs using shape analysis would certainly be an attractive method to quantify treatment outcome and contribute to defining success without exposing the patient to additional radiation and financial burden.

The second technique for measuring mandibular asymmetry was aimed to assess accuracy of vertical, oblique and anteroposterior linear distances of landmark to landmark locations made on digital panoramic radiographs of synthetic mandibles. Clinically significant asymmetry was determined using a 6% cutoff for clinical significance.^{5,12} Using the cutoff, it was determined that nearly all oblique measurements were of no diagnostic value for determining the types of asymmetry defined in this project. It was very likely a combination of image distortion and magnification that negatively affected this measurement rendering it statistically and diagnostically useless. It is therefore not recommended that oblique measurements be conducted to quantify mandibular asymmetries. Anteroposterior measurements indicated promise for describing asymmetry in the mandibular body using the suggested cutoff. The results from chapter 4 of this study agree with those found by other authors^{13,14} that horizontal measurements may be used with a slight over-estimation of radiographic size versus the actual measurement. Laster et al recommend that extreme caution be used when conducting horizontal measurements from panoramic radiographs while other authors have discredited the use of such measures entirely.¹⁶ It was determined from this project that horizontal measurements for the detection of anteroposterior body asymmetry could be employed with caution. Vertical measurements have been used to describe vertical

asymmetries by numerous authors^{5,12,14} while a few have opposed the notion.^{8,17} It was found from this project that straight vertical and complex condylar asymmetries were best described using sigmoid notch to superior condyle landmarks but underestimated the asymmetry. This finding is in agreement with other authors.¹² The most unreliable posterior mandibular vertical measurement was derived from the vertical ramus and condylar measurements where there was a complex asymmetry. From this information, it is again recommended that caution be used in measurement of vertical asymmetries, particularly where complex asymmetries are suspected. From a clinical perspective, it is useful to conduct simple linear measurements on panoramic images to determine or confirm quantity of asymmetry. Landmark selection and reliability for measurements need to be established in advance if the practitioner were to use linear measurements for asymmetry analysis. It is recommended that horizontal linear measurements be limited to anteroposterior body asymmetries keeping in mind that there is a slight and expected overestimation of the actual measurement. Vertical measurements for ramus asymmetries should be conducted from antgonial to sigmoid notches and condylar asymmetries from sigmoid notch to the superior point of the condyle expecting some under-estimation. Extreme caution is advised when measuring suspected complex condyle and complex ramus asymmetries due to their high variability in magnification coupled with distortion.

The final technique for measurement of asymmetries investigated in this thesis examined the accuracy and validity of various angular measurements from the radiographs of the known synthetic mandibles. Some authors have used angular measurements to assess outcomes of surgical procedures to correct mandibular

asymmetries.¹⁵ The magnification factor was determined to be nearly 1:1 in this study which was in agreement with other studies.¹⁰ The near 1:1 magnification would clinically suggest that an angle measured from the panoramic image would reflect the anatomical measurement. Despite the 1:1 ratio, variation was found to exist between the models studied and their actual measurements. Other authors have found that small variability exists between measured and true angular measurements as well.¹⁶ Upon measurement analysis, it was evident that a landmark movement of several millimeters due to an asymmetry translated into only a few degrees (or less) of angular change and obvious landmark positional changes were needed to detect the asymmetry in excess of 6% therefore, intuitively, it would seem that small or moderate asymmetries are difficult if not impossible to measure. With caution, vertical posterior asymmetries can be determined by comparing bilateral angles between the sigmoid notch and the antigonial notch with a vertex located at the superior condyle. Anteroposterior body asymmetries were analyzed looking at bilateral angles between mental foramen and antigonial notch with the vertex being either superior condyle or sigmoid notch. Angular measurements indicate promise however more investigation into refining the technique and establishing appropriate measurement and clinical significance levels need to be established as this information was technically difficult to decipher. It was suggested that a better way to decipher a relevant cutoff point for clinical asymmetry using angular measurements would be to use values of angles that were expected to be symmetric. In other words, find the average value and maximum ranges of all angles that should indicate asymmetry to determine a more precise cutoff point between inherent experimental error and actual asymmetry.

Discussion of shape, linear and angular analysis have been argued and described in the chapters three, four and five of this thesis. From a clinical perspective, it would appear that several hurdles need to be overcome to bring shape analysis into mainstream orthodontic practice. It would also seem that more investigation for angular analysis to refine measurement techniques and establish clinically relevant and useable cutoff points to bring these measures into employment. The best overall technique for measuring and quantifying mandibular asymmetries is through linear measurement. Although not entirely accurate the average clinician is easily able to detect and determine within reason bilateral differences using vertical and horizontal linear measurements providing that complex asymmetries are not present.

6.4 Limitations of the current study

As with any research project, certain goals were attained while others required (and continue to require) further investigation and thought. The ability to bring goals into fruition lies within the limitations of study design and methodology. The primary limitation of this research project was the inability to link a “real life” clinical result with the results determined here. Without clinical association, a practitioner would be expected to make a leap of faith that outcome and results are valid and may be applied to their own patient base. One of the most difficult associations to make is the use of steel balls as artificial landmarks. Selecting steel balls as landmark reference points is considerably different than seeking landmarks from a panoramic radiograph of a human patient and selection difference makes a direct comparison to patients difficult. A second limitation is with panoramic unit selection. Consideration for other manufacturing companies of panoramic units, both digital and conventional style, would

undoubtedly reveal slight differences in results. Again, if the clinician were unable to apply the study outcomes to his or her own practice environment then application has limited value. In addition to machine selection, inherent machine error studies and calculations should have been performed to enable more accurate distinction between measurement values and values resulting from inherent machine error.

Although a series of 30 mandibles were fabricated for use, selection of only six models created a study limitation as all but the symmetric possessed maximum ranges of asymmetries. Value would have been added by identifying and utilizing models specifically reflective of clinical asymmetries that would be potentially destined for corrective treatment rather than focusing on maximum ranges only. A pilot study to identify patient asymmetry types and to further compare these types to similar images of synthetic mandibles for selection and study inclusion would have been more useful. The effect of altering the amount of asymmetry within the condyle, ramus and body were not identified. It would have been valuable to note the changes in measurements from a range of asymmetries within each area to establish if the rate of change was linear. One final limitation to this study was limiting the complex asymmetries of vertical and horizontal changes within the areas of interest. Complex asymmetries involving axis rotations and occlusal compensations would have added an interesting component.

6.5 Recommendation for future studies

While this study examined mandibular asymmetry using shape/size analysis, linear and angular measurements, only a single panoramic (Kodak 8000) unit was used. The focus of future studies could be expanded to include other digital and conventional

panoramic units. At the conception of this thesis, there were a total of 30 asymmetric mandibles designed and fabricated with various ranges of vertical, anteroposterior and complex asymmetries. Analyzing the additional ranges and models of mandibular asymmetries would also provide a more concise picture of which areas are most readily measured from the various panoramic units to provide clinically relevant information.

In addition, comparison to panoramic-like images obtained from cone beam volumetric scanning units (CBCT) such as the NewTom® or other three-dimensional imaging systems such as the i-CAT would be of interest. The focus of future studies could be to compare the same shape/size, linear and angular measurements of images from each unit to one another in an effort to determine which machine would provide the most accurate and descriptive information.

Shape and size analysis may provide more interesting and detailed results by utilizing an increased number of landmark points. Increasing the number of landmark points increases the overall number of coordinate points and adding coordinate points theoretically would provide a better outline of perimeter of the mandible, thus describing the overall shape of the asymmetry which would provide a more detailed description of the overall shape. Again, using three dimensional analyses of the coordinate points, adding the Z coordinate would deliver a more detailed overall shape and size comparison of the mandibular asymmetries.

Removing the steel landmarks from the mandibles and imaging the various ranges of asymmetries would be of value for defining landmark reliability from panoramic and three dimensional images. A good transition from model to human studies would be accomplished by identifying anatomic landmarks. A further goal from

this method would be to develop and test a protocol for classification of asymmetry. A classification system could then be tested for application in human studies to provide clinical utility. Techniques for measuring and classifying would then need to be standardized to provide a useful tool for future clinicians when assessing asymmetries.

Reference:

1. Langland OE, Langlais R.P., Preece P.W. Principles of Dental Imaging. Lippincott Williams & Wilkins; 2002.
2. Bruce RA, Hayward JR. Condylar hyperplasia and mandibular asymmetry: a review. *J Oral Surg* 1968;26:281-290.
3. Hinds EC, Reid LC, Burch RJ. Classification and management of mandibular asymmetry. *Am J Surg* 1960;100:825-834.
4. Obwegeser HL, Makek MS. Hemimandibular hyperplasia--hemimandibular elongation. *J Maxillofac Surg* 1986;14:183-208.
5. Habets LL, Bezuur JN, van Ooij CP, Hansson TL. The orthopantomogram, an aid in diagnosis of temporomandibular joint problems. I. The factor of vertical magnification. *J Oral Rehabil* 1987;14:475-480.
6. Kjellberg H, Ekestubbe A, Kiliaridis S, Thilander B. Condylar height on panoramic radiographs. A methodologic study with a clinical application. *Acta Odontol Scand* 1994;52:43-50.
7. Mattila M, Kononen M, Mattila K. Vertical asymmetry of the mandibular ramus and condylar heights measured with a new method from dental panoramic radiographs in patients with psoriatic arthritis. *J Oral Rehabil* 1995;22:741-745.
8. Turp JC, Vach W, Harbich K, Alt KW, Strub JR. Determining mandibular condyle and ramus height with the help of an Orthopantomogram--a valid method? *J Oral Rehabil* 1996;23:395-400.
9. Miller VJ, Bodner L. Condylar asymmetry measurements in patients with an Angle's Class III malocclusion. *J Oral Rehabil* 1997;24:247-249.
10. Catic A, Celebic A, Valentic-Peruzovic M, Catovic A, Jerolimov V, Muretic I. Evaluation of the precision of dimensional measurements of the mandible on panoramic radiographs. *Oral Surg Oral Med Oral Pathol Oral Radiol Endod* 1998;86:242-248.
11. Saglam AM. The condylar asymmetry measurements in different skeletal patterns. *J Oral Rehabil* 2003;30:738-742.
12. Kambylafkas P, Murdoch K, Gilda E, Tallents R, Kyrkanides S. Validity of Panoramic Radiographs for Measuring Mandibular Asymmetry. *Angle Orthod.* 2006;76:388-393.

13. Laster WS, Ludlow JB, Bailey LJ, Hershey HG. Accuracy of measurements of mandibular anatomy and prediction of asymmetry in panoramic radiographic images. *Dentomaxillofac Radiol* 2005;34:343-349.
14. Alpern MC. Analysis of panoramic cephalometrics using s skeletal cephalostat. *Angle Orthod* 1979;49:110-20.
15. Padwa BL, Zaragoza SM, Sonis AL. Proximal segment displacement in mandibular distraction osteogenesis. *J Craniofac Surg* 2002;13:293-296; discussion 297.
16. Larheim TA, Svanaes DB. Reproducibility of rotational panoramic radiography: mandibular linear dimensions and angles. *Am J Orthod Dentofacial Orthop* 1986;90:45-51.
17. Boratto R, Gambardella U, Micheletti P, Pagliani L, Preda L, Hansson TL. Condylar-mandibular asymmetry, a reality. *Bull Group Int Rech Sci Stomatol Odontol* 2002;44:52-56.

Appendices

Appendices for Chapter Four

Reliability

Scale: ALL VARIABLES

Case Processing Summary

		N	%
Cases	Valid	12	100.0
	Excluded ^a	0	.0
	Total	12	100.0

a. Listwise deletion based on all variables in the procedure.

Reliability Statistics

Cronbach's Alpha	Cronbach's Alpha Based on Standardized Items	N of Items
1.000	1.000	3

Inter-Item Correlation Matrix

	Mf-Ag1	Mf-Ag2	Mf-Ag3
Mf-Ag1	1.000	1.000	1.000
Mf-Ag2	1.000	1.000	1.000
Mf-Ag3	1.000	1.000	1.000

Inter-Item Covariance Matrix

	Mf-Ag1	Mf-Ag2	Mf-Ag3
Mf-Ag1	9.248	9.249	9.251
Mf-Ag2	9.249	9.250	9.252
Mf-Ag3	9.251	9.252	9.255

Summary Item Statistics

	Mean	Minimum	Maximum	Range	Maximum / Minimum	Variance	N of Items
Inter-Item Covariances	9.251	9.249	9.252	.003	1.000	.000	3
Inter-Item Correlations	1.000	1.000	1.000	.000	1.000	.000	3

Intraclass Correlation Coefficient

	Intraclass Correlation	95% Confidence Interval		F Test with True Value 0			
		Lower Bound	Upper Bound	Value	df1	df2	Sig
Single Measures	1.000	1.000	1.000	3330323	11	24	.000
Average Measures	1.000	1.000	1.000	3330323	11	24	.000

One-way random effects model where people effects are random.

Case Processing Summary

		N	%
Cases	Valid	12	100.0
	Excluded ^a	0	.0
	Total	12	100.0

a. Listwise deletion based on all variables in the procedure.

Reliability Statistics

Cronbach's Alpha	Cronbach's Alpha Based on Standardized Items	N of Items
1.000	1.000	3

Inter-Item Correlation Matrix

	Mf-Sn1	Mf-Sn2	Mf-Sn3
Mf-Sn1	1.000	1.000	1.000
Mf-Sn2	1.000	1.000	1.000
Mf-Sn3	1.000	1.000	1.000

Inter-Item Covariance Matrix

	Mf-Sn1	Mf-Sn2	Mf-Sn3
Mf-Sn1	6.094	6.095	6.095
Mf-Sn2	6.095	6.097	6.096
Mf-Sn3	6.095	6.096	6.096

Summary Item Statistics

	Mean	Minimum	Maximum	Range	Maximum / Minimum	Variance	N of Items
Inter-Item Covariances	6.095	6.095	6.096	.002	1.000	.000	3
Inter-Item Correlations	1.000	1.000	1.000	.000	1.000	.000	3

Intraclass Correlation Coefficient

	Intraclass Correlation	95% Confidence Interval		F Test with True Value 0			
		Lower Bound	Upper Bound	Value	df1	df2	Sig
Single Measures	1.000	1.000	1.000	1316597	11	24	.000
Average Measures	1.000	1.000	1.000	1316597	11	24	.000

One-way random effects model where people effects are random.

Case Processing Summary

		N	%
Cases	Valid	12	100.0
	Excluded ^a	0	.0
	Total	12	100.0

a. Listwise deletion based on all variables in the procedure.

Reliability Statistics

Cronbach's Alpha	Cronbach's Alpha Based on Standardized Items	N of Items
1.000	1.000	3

Inter-Item Correlation Matrix

	Mf-Cs1	Mf-Cs2	Mf-Cs3
Mf-Cs1	1.000	1.000	1.000
Mf-Cs2	1.000	1.000	1.000
Mf-Cs3	1.000	1.000	1.000

Inter-Item Covariance Matrix

	Mf-Cs1	Mf-Cs2	Mf-Cs3
Mf-Cs1	4.732	4.736	4.745
Mf-Cs2	4.736	4.739	4.748
Mf-Cs3	4.745	4.748	4.757

Summary Item Statistics

	Mean	Minimum	Maximum	Range	Maximum / Minimum	Variance	N of Items
Inter-Item Covariances	4.743	4.736	4.748	.012	1.003	.000	3
Inter-Item Correlations	1.000	1.000	1.000	.000	1.000	.000	3

Intraclass Correlation Coefficient

	Intraclass Correlation	95% Confidence Interval		F Test with True Value 0			
		Lower Bound	Upper Bound	Value	df1	df2	Sig
Single Measures	1.000	1.000	1.000	569124.6	11	24	.000
Average Measures	1.000	1.000	1.000	569124.6	11	24	.000

One-way random effects model where people effects are random.

Case Processing Summary

		N	%
Cases	Valid	12	100.0
	Excluded ^a	0	.0
	Total	12	100.0

a. Listwise deletion based on all variables in the procedure.

Reliability Statistics

Cronbach's Alpha	Cronbach's Alpha Based on Standardized Items	N of Items
1.000	1.000	3

Inter-Item Correlation Matrix

	Ag-Sn1	Ag-Sn2	Ag-Sn3
Ag-Sn1	1.000	1.000	1.000
Ag-Sn2	1.000	1.000	1.000
Ag-Sn3	1.000	1.000	1.000

Inter-Item Covariance Matrix

	Ag-Sn1	Ag-Sn2	Ag-Sn3
Ag-Sn1	10.051	10.054	10.052
Ag-Sn2	10.054	10.057	10.054
Ag-Sn3	10.052	10.054	10.052

Summary Item Statistics

	Mean	Minimum	Maximum	Range	Maximum / Minimum	Variance	N of Items
Inter-Item Covariances	10.053	10.052	10.054	.003	1.000	.000	3
Inter-Item Correlations	1.000	1.000	1.000	.000	1.000	.000	3

Intraclass Correlation Coefficient

	Intraclass Correlation	95% Confidence Interval		F Test with True Value 0			
		Lower Bound	Upper Bound	Value	df1	df2	Sig
Single Measures	1.000	1.000	1.000	1357199	11	24	.000
Average Measures	1.000	1.000	1.000	1357199	11	24	.000

One-way random effects model where people effects are random.

Case Processing Summary

		N	%
Cases	Valid	12	100.0
	Excluded ^a	0	.0
	Total	12	100.0

a. Listwise deletion based on all variables in the procedure.

Reliability Statistics

Cronbach's Alpha	Cronbach's Alpha Based on Standardized Items	N of Items
1.000	1.000	3

Inter-Item Correlation Matrix

	Ag-Cs1	Ag-Cs2	Ag-Cs3
Ag-Cs1	1.000	1.000	1.000
Ag-Cs2	1.000	1.000	1.000
Ag-Cs3	1.000	1.000	1.000

Inter-Item Covariance Matrix

	Ag-Cs1	Ag-Cs2	Ag-Cs3
Ag-Cs1	10.855	10.860	10.858
Ag-Cs2	10.860	10.864	10.862
Ag-Cs3	10.858	10.862	10.861

Summary Item Statistics

	Mean	Minimum	Maximum	Range	Maximum / Minimum	Variance	N of Items
Inter-Item Covariances	10.860	10.858	10.862	.005	1.000	.000	3
Inter-Item Correlations	1.000	1.000	1.000	.000	1.000	.000	3

Intraclass Correlation Coefficient

	Intraclass Correlation	95% Confidence Interval		F Test with True Value 0			
		Lower Bound	Upper Bound	Value	df1	df2	Sig
Single Measures	1.000	1.000	1.000	1954798	11	24	.000
Average Measures	1.000	1.000	1.000	1954798	11	24	.000

One-way random effects model where people effects are random.

Case Processing Summary

		N	%
Cases	Valid	12	100.0
	Excluded ^a	0	.0
	Total	12	100.0

a. Listwise deletion based on all variables in the procedure.

Reliability Statistics

Cronbach's Alpha	Cronbach's Alpha Based on Standardized Items	N of Items
1.000	1.000	3

Inter-Item Correlation Matrix

	Sn-Cs1	Sn-Cs2	Sn-Cs3
Sn-Cs1	1.000	1.000	1.000
Sn-Cs2	1.000	1.000	1.000
Sn-Cs3	1.000	1.000	1.000

Inter-Item Covariance Matrix

	Sn-Cs1	Sn-Cs2	Sn-Cs3
Sn-Cs1	6.489	6.495	6.494
Sn-Cs2	6.495	6.500	6.500
Sn-Cs3	6.494	6.500	6.499

Summary Item Statistics

	Mean	Minimum	Maximum	Range	Maximum / Minimum	Variance	N of Items
Inter-Item Covariances	6.496	6.494	6.500	.006	1.001	.000	3
Inter-Item Correlations	1.000	1.000	1.000	.000	1.000	.000	3

Intraclass Correlation Coefficient

	Intraclass Correlation	95% Confidence Interval		F Test with True Value 0			
		Lower Bound	Upper Bound	Value	df1	df2	Sig
Single Measures	1.000	1.000	1.000	467713.1	11	24	.000
Average Measures	1.000	1.000	1.000	467713.1	11	24	.000

One-way random effects model where people effects are random.

Appendices for Chapter Five

Reliability

Case Processing Summary

		N	%
Cases	Valid	12	100.0
	Excluded ^a	0	.0
	Total	12	100.0

a. Listwise deletion based on all variables in the procedure.

Reliability Statistics

Cronbach's Alpha	Cronbach's Alpha Based on Standardized Items	N of Items
1.000	1.000	3

Inter-Item Correlation Matrix

	Mf-Ag-Sn1	Mf-Ag-Sn2	Mf-Ag-Sn3
Mf-Ag-Sn1	1.000	1.000	1.000
Mf-Ag-Sn2	1.000	1.000	1.000
Mf-Ag-Sn3	1.000	1.000	1.000

Inter-Item Covariance Matrix

	Mf-Ag-Sn1	Mf-Ag-Sn2	Mf-Ag-Sn3
Mf-Ag-Sn1	3.467	3.463	3.466
Mf-Ag-Sn2	3.463	3.459	3.462
Mf-Ag-Sn3	3.466	3.462	3.464

Summary Item Statistics

	Mean	Minimum	Maximum	Range	Maximum / Minimum	Variance	N of Items
Inter-Item Covariances	3.463	3.462	3.466	.004	1.001	.000	3
Inter-Item Correlations	1.000	1.000	1.000	.000	1.000	.000	3

Intraclass Correlation Coefficient

	Intraclass Correlation ^a	95% Confidence Interval		F Test with True Value 0			
		Lower Bound	Upper Bound	Value	df1	df2	Sig
Single Measures	1.000 ^b	1.000	1.000	935120.9	11.0	22	.000
Average Measures	1.000 ^c	1.000	1.000	935120.9	11.0	22	.000

Two-way mixed effects model where people effects are random and measures effects are fixed.

- Type A intraclass correlation coefficients using an absolute agreement definition.
- The estimator is the same, whether the interaction effect is present or not.
- This estimate is computed assuming the interaction effect is absent, because it is not estimable otherwise.

Case Processing Summary

		N	%
Cases	Valid	12	100.0
	Excluded ^a	0	.0
	Total	12	100.0

a. Listwise deletion based on all variables in the procedure.

Reliability Statistics

Cronbach's Alpha	Cronbach's Alpha Based on Standardized Items	N of Items
1.000	1.000	3

Inter-Item Correlation Matrix

	Ag-Sn-Mf1	Ag-Sn-Mf2	Ag-Sn-Mf3
Ag-Sn-Mf1	1.000	1.000	1.000
Ag-Sn-Mf2	1.000	1.000	1.000
Ag-Sn-Mf3	1.000	1.000	1.000

Inter-Item Covariance Matrix

	Ag-Sn-Mf1	Ag-Sn-Mf2	Ag-Sn-Mf3
Ag-Sn-Mf1	4.146	4.145	4.148
Ag-Sn-Mf2	4.145	4.144	4.147
Ag-Sn-Mf3	4.148	4.147	4.150

Summary Item Statistics

	Mean	Minimum	Maximum	Range	Maximum / Minimum	Variance	N of Items
Inter-Item Covariances	4.147	4.145	4.148	.003	1.001	.000	3
Inter-Item Correlations	1.000	1.000	1.000	.000	1.000	.000	3

Intraclass Correlation Coefficient

	Intraclass Correlation ^a	95% Confidence Interval		F Test with True Value 0			
		Lower Bound	Upper Bound	Value	df1	df2	Sig.
Single Measures	1.000 ^b	1.000	1.000	460400.6	11.0	22	.000
Average Measures	1.000 ^c	1.000	1.000	460400.6	11.0	22	.000

Two-way mixed effects model where people effects are random and measures effects are fixed.

- Type A intraclass correlation coefficients using an absolute agreement definition.
- The estimator is the same, whether the interaction effect is present or not.
- This estimate is computed assuming the interaction effect is absent, because it is not estimable otherwise.

Case Processing Summary

		N	%
Cases	Valid	12	100.0
	Excluded ^a	0	.0
	Total	12	100.0

a. Listwise deletion based on all variables in the procedure.

Reliability Statistics

Cronbach's Alpha	Cronbach's Alpha Based on Standardized Items	N of Items
1.000	1.000	3

Inter-Item Correlation Matrix

	Sn-Mf-Ag1	Sn-Mf-Ag2	Sn-Mf-Ag3
Sn-Mf-Ag1	1.000	1.000	1.000
Sn-Mf-Ag2	1.000	1.000	1.000
Sn-Mf-Ag3	1.000	1.000	1.000

Inter-Item Covariance Matrix

	Sn-Mf-Ag1	Sn-Mf-Ag2	Sn-Mf-Ag3
Sn-Mf-Ag1	5.229	5.231	5.227
Sn-Mf-Ag2	5.231	5.233	5.229
Sn-Mf-Ag3	5.227	5.229	5.225

Summary Item Statistics

	Mean	Minimum	Maximum	Range	Maximum / Minimum	Variance	N of Items
Inter-Item Covariances	5.229	5.227	5.231	.004	1.001	.000	3
Inter-Item Correlations	1.000	1.000	1.000	.000	1.000	.000	3

Intraclass Correlation Coefficient

	Intraclass Correlation ^a	95% Confidence Interval		F Test with True Value 0			
		Lower Bound	Upper Bound	Value	df1	df2	Sig
Single Measures	1.000 ^b	1.000	1.000	913527.3	11.0	22	.000
Average Measures	1.000 ^c	1.000	1.000	913527.3	11.0	22	.000

Two-way mixed effects model where people effects are random and measures effects are fixed.

- a. Type A intraclass correlation coefficients using an absolute agreement definition.
- b. The estimator is the same, whether the interaction effect is present or not.
- c. This estimate is computed assuming the interaction effect is absent, because it is not estimable otherwise.

Case Processing Summary

		N	%
Cases	Valid	12	100.0
	Excluded ^a	0	.0
	Total	12	100.0

a. Listwise deletion based on all variables in the procedure.

Reliability Statistics

Cronbach's Alpha	Cronbach's Alpha Based on Standardized Items	N of Items
1.000	1.000	3

Inter-Item Correlation Matrix

	Mf-Ag-Cs1	Mf-Ag-Cs2	Mf-Ag-Cs3
Mf-Ag-Cs1	1.000	1.000	1.000
Mf-Ag-Cs2	1.000	1.000	1.000
Mf-Ag-Cs3	1.000	1.000	1.000

Inter-Item Covariance Matrix

	Mf-Ag-Cs1	Mf-Ag-Cs2	Mf-Ag-Cs3
Mf-Ag-Cs1	3.740	3.744	3.743
Mf-Ag-Cs2	3.744	3.749	3.747
Mf-Ag-Cs3	3.743	3.747	3.746

Summary Item Statistics

	Mean	Minimum	Maximum	Range	Maximum / Minimum	Variance	N of Items
Inter-Item Covariances	3.745	3.743	3.747	.004	1.001	.000	3
Inter-Item Correlations	1.000	1.000	1.000	.000	1.000	.000	3

Intraclass Correlation Coefficient

	Intraclass Correlation ^a	95% Confidence Interval		F Test with True Value 0			
		Lower Bound	Upper Bound	Value	df1	df2	Sig
Single Measures	1.000 ^b	1.000	1.000	780499.9	11.0	22	.000
Average Measures	1.000 ^c	1.000	1.000	780499.9	11.0	22	.000

Two-way mixed effects model where people effects are random and measures effects are fixed.

- a. Type A intraclass correlation coefficients using an absolute agreement definition.
- b. The estimator is the same, whether the interaction effect is present or not.
- c. This estimate is computed assuming the interaction effect is absent, because it is not estimable otherwise.

Case Processing Summary

		N	%
Cases	Valid	12	100.0
	Excluded ^a	0	.0
	Total	12	100.0

a. Listwise deletion based on all variables in the procedure.

Reliability Statistics

Cronbach's Alpha	Cronbach's Alpha Based on Standardized Items	N of Items
1.000	1.000	3

Inter-Item Correlation Matrix

	Ag-Cs-Mf1	Ag-Cs-Mf2	Ag-Cs-Mf3
Ag-Cs-Mf1	1.000	1.000	1.000
Ag-Cs-Mf2	1.000	1.000	1.000
Ag-Cs-Mf3	1.000	1.000	1.000

Inter-Item Covariance Matrix

	Ag-Cs-Mf1	Ag-Cs-Mf2	Ag-Cs-Mf3
Ag-Cs-Mf1	2.606	2.611	2.611
Ag-Cs-Mf2	2.611	2.616	2.616
Ag-Cs-Mf3	2.611	2.616	2.616

Summary Item Statistics

	Mean	Minimum	Maximum	Range	Maximum / Minimum	Variance	N of Items
Inter-Item Covariances	2.613	2.611	2.616	.005	1.002	.000	3
Inter-Item Correlations	1.000	1.000	1.000	.000	1.000	.000	3

Intraclass Correlation Coefficient

	Intraclass Correlation ^a	95% Confidence Interval		F Test with True Value 0			
		Lower Bound	Upper Bound	Value	df1	df2	Sig
Single Measures	1.000 ^b	1.000	1.000	290102.7	11.0	22	.000
Average Measures	1.000 ^c	1.000	1.000	290102.7	11.0	22	.000

Two-way mixed effects model where people effects are random and measures effects are fixed.

- Type A intraclass correlation coefficients using an absolute agreement definition.
- The estimator is the same, whether the interaction effect is present or not.
- This estimate is computed assuming the interaction effect is absent, because it is not estimable otherwise.

Case Processing Summary

		N	%
Cases	Valid	12	100.0
	Excluded ^a	0	.0
	Total	12	100.0

a. Listwise deletion based on all variables in the procedure.

Reliability Statistics

Cronbach's Alpha	Cronbach's Alpha Based on Standardized Items	N of Items
1.000	1.000	3

Inter-Item Correlation Matrix

	Cs-Mf-Ag1	Cs-Mf-Ag2	Cs-Mf-Ag3
Cs-Mf-Ag1	1.000	1.000	1.000
Cs-Mf-Ag2	1.000	1.000	1.000
Cs-Mf-Ag3	1.000	1.000	1.000

Inter-Item Covariance Matrix

	Cs-Mf-Ag1	Cs-Mf-Ag2	Cs-Mf-Ag3
Cs-Mf-Ag1	3.499	3.500	3.502
Cs-Mf-Ag2	3.500	3.501	3.503
Cs-Mf-Ag3	3.502	3.503	3.505

Summary Item Statistics

	Mean	Minimum	Maximum	Range	Maximum / Minimum	Variance	N of Items
Inter-Item Covariances	3.501	3.500	3.503	.003	1.001	.000	3
Inter-Item Correlations	1.000	1.000	1.000	.000	1.000	.000	3

Intraclass Correlation Coefficient

	Intraclass Correlation ^a	95% Confidence Interval		F Test with True Value 0			
		Lower Bound	Upper Bound	Value	df1	df2	Sig
Single Measures	1.000 ^b	1.000	1.000	349559.7	11.0	22	.000
Average Measures	1.000 ^c	1.000	1.000	349559.7	11.0	22	.000

Two-way mixed effects model where people effects are random and measures effects are fixed.

- a. Type A intraclass correlation coefficients using an absolute agreement definition.
- b. The estimator is the same, whether the interaction effect is present or not.
- c. This estimate is computed assuming the interaction effect is absent, because it is not estimable otherwise.

Case Processing Summary

		N	%
Cases	Valid	12	100.0
	Excluded ^a	0	.0
	Total	12	100.0

a. Listwise deletion based on all variables in the procedure.

Reliability Statistics

Cronbach's Alpha	Cronbach's Alpha Based on Standardized Items	N of Items
1.000	1.000	3

Inter-Item Correlation Matrix

	Ag-Sn-Cs1	Ag-Sn-Cs2	Ag-Sn-Cs3
Ag-Sn-Cs1	1.000	1.000	1.000
Ag-Sn-Cs2	1.000	1.000	1.000
Ag-Sn-Cs3	1.000	1.000	1.000

Inter-Item Covariance Matrix

	Ag-Sn-Cs1	Ag-Sn-Cs2	Ag-Sn-Cs3
Ag-Sn-Cs1	2.421	2.425	2.426
Ag-Sn-Cs2	2.425	2.428	2.429
Ag-Sn-Cs3	2.426	2.429	2.430

Summary Item Statistics

	Mean	Minimum	Maximum	Range	Maximum / Minimum	Variance	N of Items
Inter-Item Covariances	2.427	2.425	2.429	.005	1.002	.000	3
Inter-Item Correlations	1.000	1.000	1.000	.000	1.000	.000	3

Intraclass Correlation Coefficient

	Intraclass Correlation ^a	95% Confidence Interval		F Test with True Value 0			
		Lower Bound	Upper Bound	Value	df1	df2	Sig
Single Measures	1.000 ^b	1.000	1.000	347323.0	11.0	22	.000
Average Measures	1.000 ^c	1.000	1.000	347323.0	11.0	22	.000

Two-way mixed effects model where people effects are random and measures effects are fixed.

- a. Type A intraclass correlation coefficients using an absolute agreement definition.
- b. The estimator is the same, whether the interaction effect is present or not.
- c. This estimate is computed assuming the interaction effect is absent, because it is not estimable otherwise.

Case Processing Summary

		N	%
Cases	Valid	12	100.0
	Excluded ^a	0	.0
	Total	12	100.0

a. Listwise deletion based on all variables in the procedure.

Reliability Statistics

Cronbach's Alpha	Cronbach's Alpha Based on Standardized Items	N of Items
1.000	1.000	3

Inter-Item Correlation Matrix

	Sn-Cs-Ag1	Sn-Cs-Ag2	Sn-Cs-Ag3
Sn-Cs-Ag1	1.000	1.000	1.000
Sn-Cs-Ag2	1.000	1.000	1.000
Sn-Cs-Ag3	1.000	1.000	1.000

Inter-Item Covariance Matrix

	Sn-Cs-Ag1	Sn-Cs-Ag2	Sn-Cs-Ag3
Sn-Cs-Ag1	2.383	2.384	2.383
Sn-Cs-Ag2	2.384	2.385	2.384
Sn-Cs-Ag3	2.383	2.384	2.384

Summary Item Statistics

	Mean	Minimum	Maximum	Range	Maximum / Minimum	Variance	N of Items
Inter-Item Covariances	2.384	2.383	2.384	.001	1.000	.000	3
Inter-Item Correlations	1.000	1.000	1.000	.000	1.000	.000	3

Intraclass Correlation Coefficient

	Intraclass Correlation ^a	95% Confidence Interval		F Test with True Value 0			
		Lower Bound	Upper Bound	Value	df1	df2	Sig
Single Measures	1.000 ^b	1.000	1.000	410438.0	11.0	22	.000
Average Measures	1.000 ^c	1.000	1.000	410438.0	11.0	22	.000

Two-way mixed effects model where people effects are random and measures effects are fixed.

- a. Type A intraclass correlation coefficients using an absolute agreement definition.
- b. The estimator is the same, whether the interaction effect is present or not.
- c. This estimate is computed assuming the interaction effect is absent, because it is not estimable otherwise.

Case Processing Summary

		N	%
Cases	Valid	12	100.0
	Excluded ^a	0	.0
	Total	12	100.0

a. Listwise deletion based on all variables in the procedure.

Reliability Statistics

Cronbach's Alpha	Cronbach's Alpha Based on Standardized Items	N of Items
1.000	1.000	3

Inter-Item Correlation Matrix

	Cs-Ag-Sn1	Cs-Ag-Sn2	Cs-Ag-Sn3
Cs-Ag-Sn1	1.000	1.000	1.000
Cs-Ag-Sn2	1.000	1.000	1.000
Cs-Ag-Sn3	1.000	1.000	1.000

Inter-Item Covariance Matrix

	Cs-Ag-Sn1	Cs-Ag-Sn2	Cs-Ag-Sn3
Cs-Ag-Sn1	.066	.065	.065
Cs-Ag-Sn2	.065	.065	.065
Cs-Ag-Sn3	.065	.065	.065

Summary Item Statistics

	Mean	Minimum	Maximum	Range	Maximum / Minimum	Variance	N of Items
Inter-Item Covariances	.065	.065	.065	.000	1.008	.000	3
Inter-Item Correlations	1.000	1.000	1.000	.000	1.000	.000	3

Intraclass Correlation Coefficient

	Intraclass Correlation ^a	95% Confidence Interval		F Test with True Value 0			
		Lower Bound	Upper Bound	Value	df1	df2	Sig
Single Measures	1.000 ^b	.999	1.000	9676.150	11.0	22	.000
Average Measures	1.000 ^c	1.000	1.000	9676.150	11.0	22	.000

Two-way mixed effects model where people effects are random and measures effects are fixed.

- a. Type A intraclass correlation coefficients using an absolute agreement definition.
- b. The estimator is the same, whether the interaction effect is present or not.
- c. This estimate is computed assuming the interaction effect is absent, because it is not estimable otherwise.